

---

---

# Containment Emergency Sump Performance

Technical Findings Related to  
Unresolved Safety Issue A-43

---

---

## U.S. Nuclear Regulatory Commission

Office of Nuclear Reactor Regulation

A. W. Serkiz, Task Manager



## NOTICE

### Availability of Reference Materials Cited in NRC Publications

Most documents cited in NRC publications will be available from one of the following sources:

1. The NRC Public Document Room, 1717 H Street, N.W.  
Washington, DC 20555
2. The NRC/GPO Sales Program, U.S. Nuclear Regulatory Commission,  
Washington, DC 20555
3. The National Technical Information Service, Springfield, VA 22161

Although the listing that follows represents the majority of documents cited in NRC publications, it is not intended to be exhaustive.

Referenced documents available for inspection and copying for a fee from the NRC Public Document Room include NRC correspondence and internal NRC memoranda; NRC Office of Inspection and Enforcement bulletins, circulars, information notices, inspection and investigation notices; Licensee Event Reports; vendor reports and correspondence; Commission papers; and applicant and licensee documents and correspondence.

The following documents in the NUREG series are available for purchase from the NRC/GPO Sales Program: formal NRC staff and contractor reports, NRC-sponsored conference proceedings, and NRC booklets and brochures. Also available are Regulatory Guides, NRC regulations in the *Code of Federal Regulations*, and *Nuclear Regulatory Commission Issuances*.

Documents available from the National Technical Information Service include NUREG series reports and technical reports prepared by other federal agencies and reports prepared by the Atomic Energy Commission, forerunner agency to the Nuclear Regulatory Commission.

Documents available from public and special technical libraries include all open literature items, such as books, journal and periodical articles, and transactions. *Federal Register* notices, federal and state legislation, and congressional reports can usually be obtained from these libraries.

Documents such as theses, dissertations, foreign reports and translations, and non-NRC conference proceedings are available for purchase from the organization sponsoring the publication cited.

Single copies of NRC draft reports are available free upon written request to the Division of Technical Information and Document Control, U.S. Nuclear Regulatory Commission, Washington, DC 20555.

Copies of industry codes and standards used in a substantive manner in the NRC regulatory process are maintained at the NRC Library, 7920 Norfolk Avenue, Bethesda, Maryland, and are available there for reference use by the public. Codes and standards are usually copyrighted and may be purchased from the originating organization or, if they are American National Standards, from the American National Standards Institute, 1430 Broadway, New York, NY 10018.

---

# Containment Emergency Sump Performance

Technical Findings Related to  
Unresolved Safety Issue A-43

---

Manuscript Completed: March 1983  
Date Published: April 1983

A. W. Serkiz, Task Manager

**Division of Safety Technology  
Office of Nuclear Reactor Regulation  
U.S. Nuclear Regulatory Commission  
Washington, D.C. 20555**



## ABSTRACT

This report summarizes key technical findings related to the Unresolved Safety Issue A-43, Containment Emergency Sump Performance, and provides recommendations for resolution of attendant safety issues. The key safety questions relate to: (a) effects of insulation debris on sump performance; (b) sump hydraulic performance as determined by design features, submergence, and plant induced effects; and (c) recirculation pump performance wherein air and/or particulate ingestion can occur.

The technical findings presented in this report provide information relevant to the design and performance evaluation of the containment emergency sump. These findings have been derived from extensive experimental measurements, generic plant studies and assessment of pumps utilized for long-term cooling. These results indicate a less severe post-LOCA situation than previously hypothesized (e.g., low levels of air ingestion over a wide range of sump designs and flow conditions, a debris hazard situation that is not widespread, and pump designs that can accommodate low levels of air ingestion). Therefore, these findings provide a technical basis for the development of changes proposed to the Standard Review Plan and Regulatory Guide 1.82.



# TABLE OF CONTENTS

	PAGE
Abstract-----	iii
Foreword-----	xi
Acknowledgments-----	xiii
1.0 INTRODUCTION-----	1
1.1 Safety Significance-----	1
1.2 Background-----	
1.3 Technical Issue-----	2
1.4 Summary of Recommendations-----	2
2.0 KEY FINDINGS SUMMARY-----	5
2.1 Pump Performance-----	5
2.2 Effects of Debris on Sump Performance-----	6
2.3 Sump Hydraulic Performance Findings-----	7
3.0 TECHNICAL FINDINGS-----	10
3.1 Introduction-----	10
3.2 Performance of Residual Heat Removal and Containment Spray System Pumps -- Technical Findings-----	11
3.2.1 Characteristics of RHR and CSS Pumps-----	11
3.2.2 Effects of Air or Particulate Ingestion, Cavitation, and Swirl on Pump Performance---	13
3.2.3 Calculation of Pump Inlet Conditions-----	25
3.3 Debris Assessment-----	28
3.3.1 Plant Insulation Survey Findings-----	28
3.3.2 Calculational Methods for Assessing Debris Hazards-----	33
3.3.3 Application of Methodology to 5 Sample Plants-----	41
3.3.4 Experimental Studies On Debris-----	43
3.4 Sump Hydraulic Performance-----	49
3.4.1 Envelope Analysis-----	52
3.4.2 General Sump Performance (All Tests)-----	58
3.4.3 Sump Performance During Accident Conditions (Perturbed Flow)-----	58

TABLE OF CONTENTS (Cont'd)

	PAGE
3.4.4 Geometric and Design Effects (Unperturbed Flow Tests)-----	59
3.4.5 Design or Operational Items of Special Concern in ECCS Sumps-----	59
4.0 INDEPENDENT PROGRAM REVIEWS-----	63
4.1 Sump Performance Review-----	63
4.2 Insulation Debris Effects Review-----	64
5.0 SUMMARY OF SUMP PERFORMANCE FINDINGS-----	69
5.1 General Overview-----	69
5.2 Sump Hydraulic Performance-----	69
5.3 Debris Assessments-----	78
5.4 Pump Performance Under Adverse Conditions-----	80
5.5 Combined Effects-----	83
REFERENCES-----	85
APPENDIX A--PLANT SUMP DESIGN AND CONTAINMENT LAYOUTS-----	A-1
APPENDIX B--A PROCEDURE FOR ESTIMATING DEBRIS GENERATION, TRANSPORT, AND SUMP BLOCKAGE POTENTIAL-----	B-1
APPENDIX C--INSULATION DEBRIS FORMATION UNDER JET FLOW CONDITIONS-----	C-1

## LIST OF FIGURES

	PAGE
3.1      Assembly schematic of centrifugal pump typical of those used for RHR or CSS service-----	14
3.2a     Performance and cavitation curves for RHR and CSS pumps. Head versus flow rate data normalized by individual best efficiency point values. NPSH required data normalized by best efficiency point head-----	15
3.2b     Performance and cavitation curves for CSS pumps. head vs. flow rate data normalized by individual best efficiency point values. NPSH required data normalized by best efficiency point head-----	16
3.3      Typical head degradation curves due to cavitation at four flow rates ( $Q_1$ to $Q_4$ )-----	18
3.4      Reduction in NPSH requirements as a function of liquid temperature-----	19
3.5      Head degradation under air ingesting conditions as a function of inlet void fraction (percent by volume)-----	21
3.6      Effect of air ingestion on NPSH requirements for a centrifugal pump-----	22
3.7      Schematic of Suction Systems for Centrifugal Pump-----	26
3.8      Outline of methods-----	35
3.9      Approach flow perturbations and screen blockage schemes-----	51
3.10     Break and drain flow impingement-----	53
3.11     Void fraction (percent of volume) as a function of Froude number; horizontal outlet configuration--	54
3.12     Surface vortex type as a function of Froude number; horizontal outlet configuration-----	55
3.13     Swirl as a function of Froude number; horizontal outlet configuration-----	55
3.14     Void fraction data for various Froude numbers; vertical outlet configuration-----	56

LIST OF FIGURES (Cont'd)

		PAGE
3.15	Surface vortex type as a function of Froude number; vertical outlet configuration-----	57
3.16	Swirl as a function of Froude number; vertical outlet configuration-----	57
5.1	Technical considerations relevant to containment emergency sump performance-----	70
5.2	Flow chart for calculation of pump inlet conditions-----	81
5.3	Combined technical considerations for sump performance-----	84

## LIST OF TABLES

		PAGE
3.1	RHR and CSS pump data-----	12
3.2	Reactor plants selected for insulation survey-----	29
3.3	Types and percentages of insulation used within the primary coolant system shield wall in plants surveyed-----	31
3.4	Reactor plants selected for detailed investigation of insulation debris generation potential-----	42
3.5	Summary table for 5 plant sample calculations-----	44
3.6	Summary of findings-----	46
5.1	Zero air ingestion hydraulics design findings-----	72
5.2	Hydraulics design findings-----	73
5.3	Geometric design envelope findings-----	74
5.4	Additional considerations related to sump size and placement -----	75
5.5	Screen, grate, and cover plate design findings-----	76
5.6	Findings for selected vortex suppression devices----	77
5.7	Debris assessment considerations-----	79



## FOREWORD

NUREG-0897 is being issued for public comment. It provides a concise and self-contained reference which summarizes technical findings relevant to the unresolved Safety Issue A-43, "Containment Emergency Sump Performance." NUREG-0897 is not a substitute for the requirements set forth in General Design Criteria 16, 35, 36, 37, 38, 40 and 50 in Appendix A to 10CFR50, nor a substitute for requirements set forth in NRC's Standard Review Plan or Regulatory Guides. The information contained herein is of a technical nature which can be used as background relevant to the proposed revisions to SRP Section 6.2.2 and Regulatory Guide 1.82.

## ACKNOWLEDGMENTS

The technical findings relevant to the Unresolved Safety Issue A-43, Containment Emergency Sump Performance, set forth in this report are the result of the combined efforts of staff at the Nuclear Regulatory Commission, the Department of Energy, Sandia National Laboratories (SNL), Alden Research Laboratory (ARL), Burns & Roe (B&R), Inc. and Creare, Inc. The following persons deserve special mention for their participation and contributions:

W. Butler, NRC/DSI	G. Otey, SNL
D. Dalghren, SNL	N. Padmanabhan, ARL
G. Hecker, ARL	P. Strom, SNL
D. Jaffee, NRC/DL	W. Swift, Creare
M. Krein, SNL	G. Weigand, SNL
A. Millunzi, DOE	M. Wester, SNL
P. Norian, NRC/DST	J. Wysocki, B&R
F. Orr, NRC/DSI	

In addition, acknowledgment is given to persons whose efforts are referenced herein; and to those persons who participated in "peer" reviews of results obtained and the application of such results. Particular acknowledgment is given to Gilbert Weigand who played a major role in maintaining technical quality and continuity throughout these efforts, and to George Hecker for his keen insight and questioning regarding the application of results obtained.

## 1.0 INTRODUCTION

### 1.1 Safety Significance

Following a loss-of-coolant accident (LOCA) in a pressurized water reactor (PWR), water discharged from the break will collect on the containment floor and within the containment emergency sump. Although the emergency core cooling systems (ECCS) and containment spray systems (CSS) initially draw water from the refueling water storage tank (RWST), long-term core cooling is affected by realignment of these ECCS pumps to the containment emergency sump. Thus, successful long-term recirculation depends upon the sump providing adequate, debris-free water to the recirculation pumps for extended periods of time. Moreover, the flow conditions through the sump and associated piping must not result in pressure losses or air entrainment that would inhibit proper pump operation. Without a proper sump design, long-term cooling could be significantly impaired.

### 1.2 Background

The importance of the ECCS sump and safety considerations associated with its design were early considerations in containment design. Net positive suction head (NPSH) requirements, operational verification, and sump design requirements are issues that have evolved and are currently contained in the following Regulatory Guides (RG):

- RG 1.1 -- Net Positive Suction Head for Emergency Core Cooling and Containment Heat Removal Systems Pumps, 1970.
- RG 1.79 -- Preoperational Testing of Emergency Core Cooling Systems for PWRs, 1974.
- RG 1.82 -- Sumps for Emergency Cooling and Containment Spray Systems, 1974.

Review of these Regulatory Guides reveals that the concerns of the Nuclear Regulatory Commission (NRC) staff regarding emergency sump performance were evolutionary in nature. Initially, staff concerns were addressed through in-plant tests (per RG 1.79) with a transition to containment and sump model tests in the mid-1970s. At that time, considerable emphasis was placed on "adequate" sump hydraulic performance during these model tests, and vortex formation was identified as the key determinant. The main concern was that formation of an air-core vortex would result in unacceptable levels of air ingestion and, subsequently, in severely degraded pump performance.

There was also concern about sump damage or blockage of the flow as a result of LOCA generated insulation debris, missiles etc. These concerns led to the formulation of some of the guidelines set forth in RG 1.82 (cover plates, debris screen, < 50 percent screen blockage, etc.).

In 1979, as a result of continued staff concern for safe operation of ECCS sumps, the Commission designated the issue as Unresolved Safety Issue (USI) A-43, "Containment Emergency Sump Performance." To assist in its resolution, the Department of Energy (DOE) provided funding for construction of a full-scale test facility at the Alden Research Laboratory (ARL) of Worcester Polytechnic Institute (WPI) (Reference 1). At about the same time, Task Action Plan (TAP) A-43 was developed to address all aspects of this safety issue.

### 1.3 Technical Issue

The principal concern is summarized in the following question:

In the recirculation mode following a LOCA, will the pumps receive water sufficiently free of debris and air and at sufficient pressure to satisfy NPSH requirements so that pump performance is not impaired?

This concern can be divided into three areas for technical consideration: sump design, insulation debris effects, and pump performance. The three areas are not independent, and certain combinations of effects must be considered as well.

This report presents the technical findings derived from extensive, full-scale experimental measurements, generic plant calculations, and residual heat removal (RHR) and CSS pump performance assessments. These technical findings provide a basis for resolving USI A-43.

### 1.4 Summary of Technical Findings

The following key determinations are derived from the technical findings contained in Section 3.



1. The hydraulic performance of containment emergency sumps should be based primarily on level of air ingestion into the sump suction inlet(s). Visual observations cannot be used to quantify the amount of air ingestion occurring. However, observations of sump surface vortex activity, principally the lack thereof, can be used to infer the absence of air ingestion.
2. Relative to acceptable levels of air ingestion, two options are available: a) 0 percent air ingestion, and b)  $\leq 2$  percent air ingestion, provided NPSH requirements at the pump inlet are satisfied. For sumps with marginal flow conditions or designs, vortex suppressors can reduce air ingestion to zero.
3. The sump design information, contained in Section 3.2, can be used to evaluate hydraulic design and performance. If the sump operational envelope falls outside of the A-43 experimental envelope, or recommended sump geometric features, additional analyses or data may be needed for support of proposed design.
4. The general sump design information set forth in RG 1.82, "Sumps for Emergency Core Cooling and Containment Spray Systems," such as use of screens and trash racks should be maintained. However, the currently specific 50 percent screen blockage can lead to non-conservative results. Finding 5 (below) addresses the question of screen blockage in a more rigorous manner.
5. The insulation debris evaluation methods, described in Section 3.3, provide a conservative means to determine quantities of debris that would be generated by a LOCA, the resulting screen blockage, and the attendant pressure drop.
6. Plant insulation surveys have shown that a variety of insulations have been employed in plants and in large quantities. Nonencapsulated insulations (particularly mineral wool and fibrous types) have been shown through plant specific calculations (see Section 3.3) to have the potential to result in total screen blockage following a LOCA. Plant specific studies have shown a strong plant layout and type of insulation dependence due to debris migration to the sump.



7. Recirculation pump operation can be assessed using the findings and methods provided in Section 3.2. Low levels of air ingestion ( $\leq 2$  percent) will not degrade pumping capability. However, as noted in Item 2, non-zero air entrainment conditions identified at the sump suction inlets should be evaluated for NPSH effects. Ingestion of small particles will not pose a pumping problem; however, pump seal systems warrant review from the viewpoint of possible clogging. Pumps that use water lubricated bearings or pumped fluid for bearing coolant warrant review because of the possible effects of debris on bearing operation.
8. BWRs need not be reviewed in as much detail as PWRs for determination of long-term recirculation capabilities. For the sake of completeness, some BWR-RHR suction configurations (representative of Mark I, Mark II and Mark III designs) were tested to determine air ingestion characteristics. The results reveal low levels of air ingestion (see Section 3.4); this data set can be used to evaluate BWR designs. The limited BWR insulation survey that was conducted revealed a high utilization of reflective metallic insulation and, therefore, debris effects are not believed to be significant.

## 2.0 KEY FINDINGS SUMMARY

### 2.1 Pump Performance

Sustained operation of RHR and CSS pumps in the recirculating mode presents two principal areas of concern:

- Possible degradation of the hydraulic performance of the pump (inability of pumps to maintain sufficient recirculation flow as a result of sump screen blockage, cavitation effects, or air ingestion).
- Possible degradation of pump performance over the long- or short-term due to mechanical problems (material erosion due to particulates or severe cavitation, shaft or bearing failure due to unbalanced loads, and shaft or impeller seizure due to particulates).

Pumps used in RHR and CSS systems are primarily single stage centrifugal designs of low specific speed. CSS pumps are generally rated at flows of about 1500 gpm, heads of 400 feet, and require about 20 feet of NPSH at their inlet; RHR pumps are generally rated at about 3000 gpm, heads of 300 feet, and require about 20 feet NPSH at maximum flow. Rating points and submergence requirements for the pumps are plant specific. Pump materials are generally highly resistant to erosion, corrosion, and cavitation damage.

Test results show that under normal flow conditions and in the absence of cavitation effects, performance is only slightly degraded when air ingestion is less than 2 percent. This value would be a conservative estimate for acceptable performance. For higher amounts of air ingestion, pump performance is dependent on many variables, but air ingestion in excess of 15 percent almost completely degrades the performance of pumps of this type.

Submergence or net positive suction head requirements (NPSHR) for RHR and CSS pumps (routinely determined by manufacturers' tests) are established by a percent degradation in pump output pressure. (Individual specifications determine that NPSH required be set according to a 1 percent or 3 percent criterion.) No standard exists for the percent degradation criterion, nor for the margin between NPSH available and that required in setting RHR and CSS pump submergence. Air ingestion affects NPSHR. Test data on the combined effects of air ingestion and cavitation are limited, but the combined effects of both increase the NPSH required. A value of 3 percent degradation criterion in pump output pressure for the combined effects of air ingestion and cavitation appears to be a realistic value.

The types and quantities of debris which are likely to reach the pump should not impair long term hydraulic performance. In pumps with mechanical shaft seals, accumulated quantities of soft or abrasive debris in the seal flow passages may result in clogging or excessive wear; both of which may lead to increased seal leakage. Catastrophic failure of a shaft seal as a result of debris ingestion is considered unlikely. In the event of complete failure of shaft seals, the pump leakage would be restricted by the throttle or safety bushing incorporated in these seals. Debris may cause failure of water lubricated bearings. These systems should be evaluated on a case by case basis.

## 2.2 Effects of Debris on Sump Performance

The safety issues related to debris effects on sump performance concern screen blockage and attendant potential loss of pump suction pressure.

Results of the insulation debris studies are summarized below.

- Types of insulations used vary from plant to plant, with newer plants generally using reflective metallic insulation that is not likely to cause blockage problems. Types of insulation used in the 19 plants surveyed in this study are shown in Table 3.3.
- Detailed methods were developed for determining the quantities, sources, and transport mechanisms of debris that could be generated during a LOCA and for assessing the consequences of the blockage of sump inlets that might result (see Figure 3.8).
- The methods developed for debris assessment were evaluated by application to 5 selected plants to establish variability due to plant design, type(s) of insulation employed and sump design. Table 3.5 summarizes the calculated results as a function of break location and plant selected. Screen blockages greater than 5 percent were calculated, with 2 of the plant calculations resulting in 100 percent screen blockage. For the Salem plant, low flow velocities, large screen area, sump design and location resulted in low pressure losses through the blocked screen. Therefore, NPSH requirements were not impacted. For the Maine Yankee plant, large quantities of nonencapsulated mineral wool were calculated to be transported to a small sump screen area. In this case, a 100 percent screen blockage with high pressure drop was predicted. Although conservative assumptions have been embodied into these analyses methods, the variabilities

due to plant design and types of insulations employed illustrate the need for plant specific evaluations.

- Mirror (reflective type) insulations do not appear to pose screen blockage problems. Velocities required for migration of such insulation is relatively high.
- Low density insulations, having a closed cell structure, will float and are not likely to impede flow through the pump screens except where the screens are not totally submerged.
- Low density hygroscopic insulation having equilibrium densities greater than water require a plant specific assessment of screen blockage effects.
- Non-encapsulated insulation (particularly mineral fiber, fiberglass, or mineral wool blanket) require a plant specific evaluation to determine the potential for sump screen blockage. (Section 3.3, Section 5.3, and Appendix B provide a conservative method for assessing screen blockage effects.) Some debris will not be collected on sump screens by virtue of its size and shape distribution.

### 2.3 Sump Hydraulic Performance Findings

Data obtained from full-scale sump tests provide a sound base for assessing pump hydraulic performance. Both side-suction and bottom-suction designs were tested over a wide range of design parameters, and the effects of elevated water temperatures were assessed. Scaling experiments (1:4, 1:2, 1:1) were also conducted to provide a means for assessing the validity of previous scaled model tests. The effectiveness of certain vortex suppression devices was also evaluated. For completeness, plant specific and LOCA-introduced effects (condenser drain flow, break flow impingement, large swirl and sump circulation effects, and sump screen blockage) were evaluated experimentally at full scale. Results of this test program are summarized below.

- The broad data base from the sump studies resulted in the development of envelope curves for reliably quantifying the expected upper-bound for the hydraulic performance of any given sump whose essential features fall approximately within the flow and geometric ranges tested.
- Vortices are unstable, randomly formed, and, for cases where air ingestion occurs, cannot be used to quantify air ingestion levels, suction inlet losses, or intake pipe fluid swirl. The full-scale tests show that for water submergences greater than 8 feet, and inlet water velocities of less than 7 ft/sec, significant vortex activity disappears.



- Based on void fraction measurements, air ingestion was found to be less than 2 percent in most cases; only highly perturbed flow conditions associated with large screen blockage and/or deliberately induced approach water swirl at low submergences and high flow resulted in high levels of air ingestion. (These tests revealed the importance of measuring void fraction and demonstrated the ineffectiveness of visual observations of vortices as a means of quantitatively evaluating air entrainment.)
- Swirl angles in suction pipes were generally found to have decreased to about  $4^\circ$  at 14 pipe diameters from inlets; angles of up to  $7^\circ$  at 15 pipe diameters from inlets were observed in tests at low submergence with induced flow perturbations.
- Hydraulic grade line measurements for all experiments revealed that the sump loss coefficient was insensitive to sump design variation. Loss coefficients are basically a function of intake geometry, and the measured values are consistent with those obtained from standard hydraulic handbooks.
- High temperature testing (up to  $165^\circ\text{F}$ ) revealed water temperature (or previously hypothesized Reynolds number effects) had no measurable effect on surface vortexing, air ingestion, pipe swirl, or loss coefficient.
- Vortex suppressor testing revealed that cage-type and submerged grid-type designs generally (a) reduce surface vortexing from a full air-core vortex to surface swirl only; (b) reduced air ingestion to or near zero; (c) reduced pipe swirl to less than  $5^\circ$ ; and (d) had no significant effect on loss coefficient.
- There were no major differences in the hydraulic performance of vertical outlet sumps and horizontal outlet sumps of the same geometry and flow conditions.
- Comparison of the different scale model results showed that scale modeling down to 1:4 scale, using Froude number similitude, adequately predicted the performance variables (void fraction, vortex type, swirl, and loss coefficient) of full-scale tests. Tests on 1:4, 1:2, and 1:1 scale versions of the same sump under comparable operating conditions showed no significant scale effects in the modeling of air-withdrawal due to surface vortices or in free surface vortex behavior. Additionally, swirl and inlet losses were accurately predicted by model tests providing specified Reynolds number criteria were maintained.



- A parametric assessment of nonuniform approach flow into the sump due to specific structural features did not reveal any significant adverse effects.
- Drain flow impingement on the sump water surface resulted in extensive turbulence that tended to reduce vortexing and did not lead to increased air ingestion.
- Break flow impingement tests resulted in findings similar to those for drain flow; significant air entrainment did not occur.
- Screen blockage tests, in most instances, did not reveal significant increases in air ingestion or subsequent degradation in the hydraulic performance of the sump. There were some cases where certain screen blockage schemes, up to 75 percent screen area blocked, resulted in significant air ingestion (see Figures 3.11 and 3.14). However, in each case, the use of a vortex suppressor eliminated the air-core vortex and reduced the air ingestion to zero or negligible levels. Thus, the effectiveness of vortex suppressors (even submerged floor grating designs) has been demonstrated.

The full-scale test program has resulted in an extensive data base that has broad applicability and can be used in lieu of model tests, or in-plant tests (provided the sump design falls within the experimental envelope investigated).

### 3.0 TECHNICAL FINDINGS

#### 3.1 Introduction

Prior to the development of a plan for the resolution of Unresolved Safety Issue A-43, the following key safety questions were identified:

1. What are the performance capabilities of pumps used in containment recirculation systems, and how tolerant are such pumps to air entrainment, cavitation and the potential ingestion of debris and particulates that may pass through screens?
2. Were a LOCA to occur, would the amount and type of debris generated from containment insulation (and its subsequent transport within containment) cause significant sump screen blockage and, if so, would such blockage be of sufficient magnitude to reduce NPSH available below NPSH required?
3. Can geometric and hydraulic sump system designs be established for which acceptable sump performance can be assured?

It was recognized that resolution of USI A-43 depended upon successful responses to these questions. This effort was undertaken in three parallel tasks, each designed to respond to one of the key safety questions.

The first question was addressed through an evaluation of the general physical and performance characteristics of RHR and CSS pumps used in existing plants. Conditions likely to cause degraded performance or damage to pumps were identified, and the effects of such conditions on pump performance were evaluated. This effort was undertaken by Create, Inc., and the results are reported in Reference 2.

The second question was addressed in three parts: (a) a survey was conducted of 19 power reactor plants concerning the quantity, types, and location of insulation used within containment; (b) detailed methods were developed for determining the quantities and sources of debris that could be generated during a LOCA. This information, used in conjunction with the development of criteria for the initiation and continuation of debris movement, allowed estimates to be made of the quantities and character of insulation debris that could potentially be transported to sump screens. (c) Computational methods were also developed that can provide estimates of head losses as a result of such debris buildup on sump screens. This work was undertaken by Burns and Roe, Inc., and is reported in References 3, 4, and 5. Experimental determinations were made of these parameters

(debris generation by jets, velocity requirements for the onset and continuation of debris migration, the phenomena of debris buildup on sump screens and associated head losses) at Alden Research Laboratory. Results of these efforts are reported in References 6 and 7.

The third key safety question was addressed in an investigation of the behavior of ECCS sumps under diverse flow conditions that might occur during a LOCA. The test program was designed to cover a broad range of geometric and flow variables representative of emergency sump designs. This work was undertaken jointly by Alden Research Laboratory, of Worcester Polytechnic Institute, and Sandia National Laboratories, and is reported in Reference 9, 21, 22, and 23.

### 3.2 Performance of Residual Heat Removal and Containment Spray System Pumps -- Technical Findings

This section summarizes the general physical and performance characteristics of RHR and CSS pumps used in a sample of existing plants. All plants in the sample are PWRs. Effects likely to cause degraded performance or damage are identified, and results from an analysis of these effects on RHR and CSS pump performance are presented.

#### 3.2.1 Characteristics of RHR and CSS Pumps in PWRs

A study of pumps used in 12 operating nuclear plants has shown that although individual pump details are plant specific, the pumps used in RHR and CSS services are similar in type, mechanical construction, and performance.

Similarities in the types of pumps are shown in Table 3.1, which lists the manufacturer, model number, and rated conditions for each of the pumps utilized in the plants surveyed. The column labeled "Specific Speed" provides a parameter conventionally used by pump manufacturers to specify hydraulic characteristics and, hence, the overall design configuration of a pump. As the table shows, all pumps are in the specific speed range of 800-1600 with specific speed defined as  $N_s = (\text{Speed}) (\text{Volumetric Flow})^{1/2} / (\text{Head})^{3/4}$ . Thus, all are relatively high head, centrifugal pumps with nearly radial impellers.

4 The class of pumps used for RHR and CSS service have similarities in mechanical construction:

Table 3.1

RHR and CSS Pump Data

Plant	-----Manufacturer*/Model-----		-----Rated Conditions-----			
	RHR	CSS	(RPM) Speed	(FT) Head	(GPM) Flow	Specific Speed
Arkansas Unit #2	I-R 6x23 WD		1800	350	3100	1238
		I-R 8x20 WD	1800	525	2200	851
Calvert Cliffs 1&2	I-R 8x21 AL		1780	360	3000	1205
		B&W 6x8x11 HSMJ	3580	375	1350	1544
Crystal River #3	W 8HN-184		1780	350	3000	1205
		W6HND-134	3550	450	1500	1407
GINNA	Pac 6" SVC		1770	280	1560	1016
Haddom Neck	Pac 8" LX		1770	300	2200	1152
		Pac 8" LX	1770	300	2200	1152
Kewaunee	B-J 6x10x18 VDSM		1770	260	2000	1222
		I-B 4x11 AN	3550	475	1300	1257
McGuire 1&2	I-R 8x20 WD		1780	375	3000	1144
		I-R 8x20 WD	1780	380	3400	1205
Midland #2	B&W 10x12x21 ASMK		1780	370	3000	1156
		B&W 6x8x135 MK	3550	387	1300	1467
Millstone Unit 2	I-R (No Model #)		1770	350	3000	1198
		G3736-4x6-13DV	3560	477	1400	1370
Oconee #3	I-R 8x21 AL		1780	360	3000	1180
		I-R 4x11 A	3550	460	1490	1380
Prairie Island	B-J 6x10x18 VDSM		1770	285	2000	1141
		I-R 4x11 AN	3550	500	1300	1210
Prairie Island 1&2	B-J 6x10x18 VDSM	I-R 4x11 AN	1780	280	2000	1156
			3550	5100	1300	1210
Salem #1	I-R 8x20W		1780	350	3000	1205
		G 3415 8x10-22	1780	450	2600	929

\*Pac -- Pacific

I-R -- Ingersoll-Rand

W -- Worthington

G -- Gould

B&amp;W -- Babcock &amp; Wilcox

B-J -- Byron Jackson

Specific Speed is defined as  $N_s = \text{Speed (Flow)}^{1/2} / (\text{Head})^{3/4}$ 

In this definition: Speed is in rpm, flow in gpm and head in ft.



- Impellers and casings are usually austenitic stainless steel -- highly resistant to damage by cavitation, corrosion and erosion.
- Impellers are shrouded, with wear rings to minimize leakage.
- Shaft seals are the mechanical type.
- Bearings are grease or oil lubricated ball-type.

A pump assembly typical of pumps used for RHR and CSS service is shown in cross-section in Figure 3.1.

Similarities in the performance of pumps used in RHR and CSS service are shown in Figure 3.2. Performance and cavitation data from each of the pumps listed in Table 3.1 have been plotted for comparison. Performance data are given in terms of normalized head vs. normalized flow rate where the best-efficiency-point head and flow are used for the reference values. Cavitation data are given in terms of NPSH required.

### 3.2.2 Effects of Cavitation, Air or Particulate Ingestion, and Swirl on Pump Performance

Several items have been identified as potential causes of long- or short-term degradation of CSS and RHR pumps:

- Cavitation -- may cause head degradation and damage to impellers
- Air ingestion -- may cause head degradation
- Particulate ingestion -- may cause damage to internal parts
- Swirl at the pump inlet -- may cause head degradation

All of these effects also have the potential for inducing hydraulic or mechanical unbalanced loads.

### Cavitation

Net positive suction head is defined as the total pressure at the pump inlet above vapor pressure at the liquid temperature, expressed in terms of liquid head (pressure/specific weight), and is equivalent to the amount of subcooling at the pump inlet. If the NPSH available at the pump is less than the NPSH required, some degree of cavitation is assured and some degradation of performance and perhaps material erosion is likely.

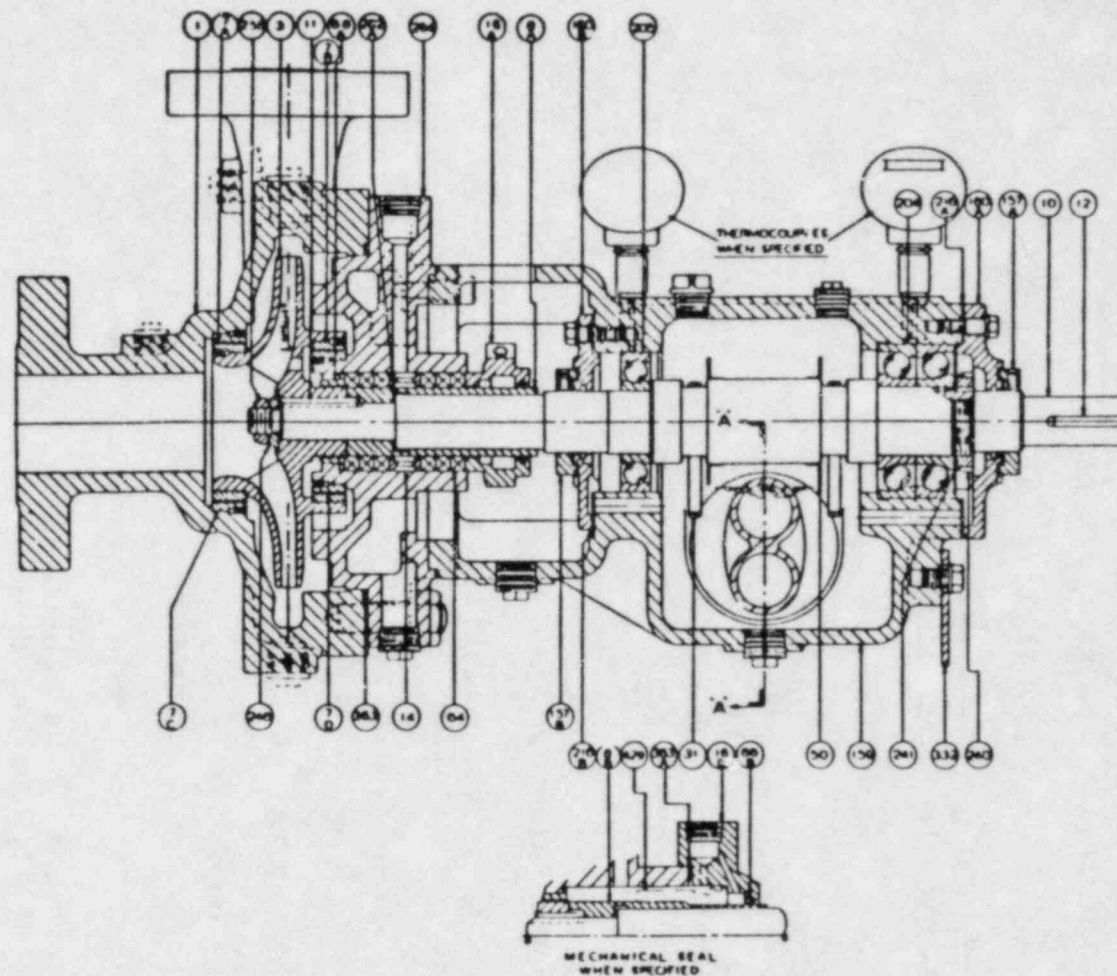


Figure 3.1. ASSEMBLY SCHEMATIC OF CENTRIFUGAL PUMP  
TYPICAL OF THOSE USED FOR RHR OR CSS SERVICE

# RHR Pumps

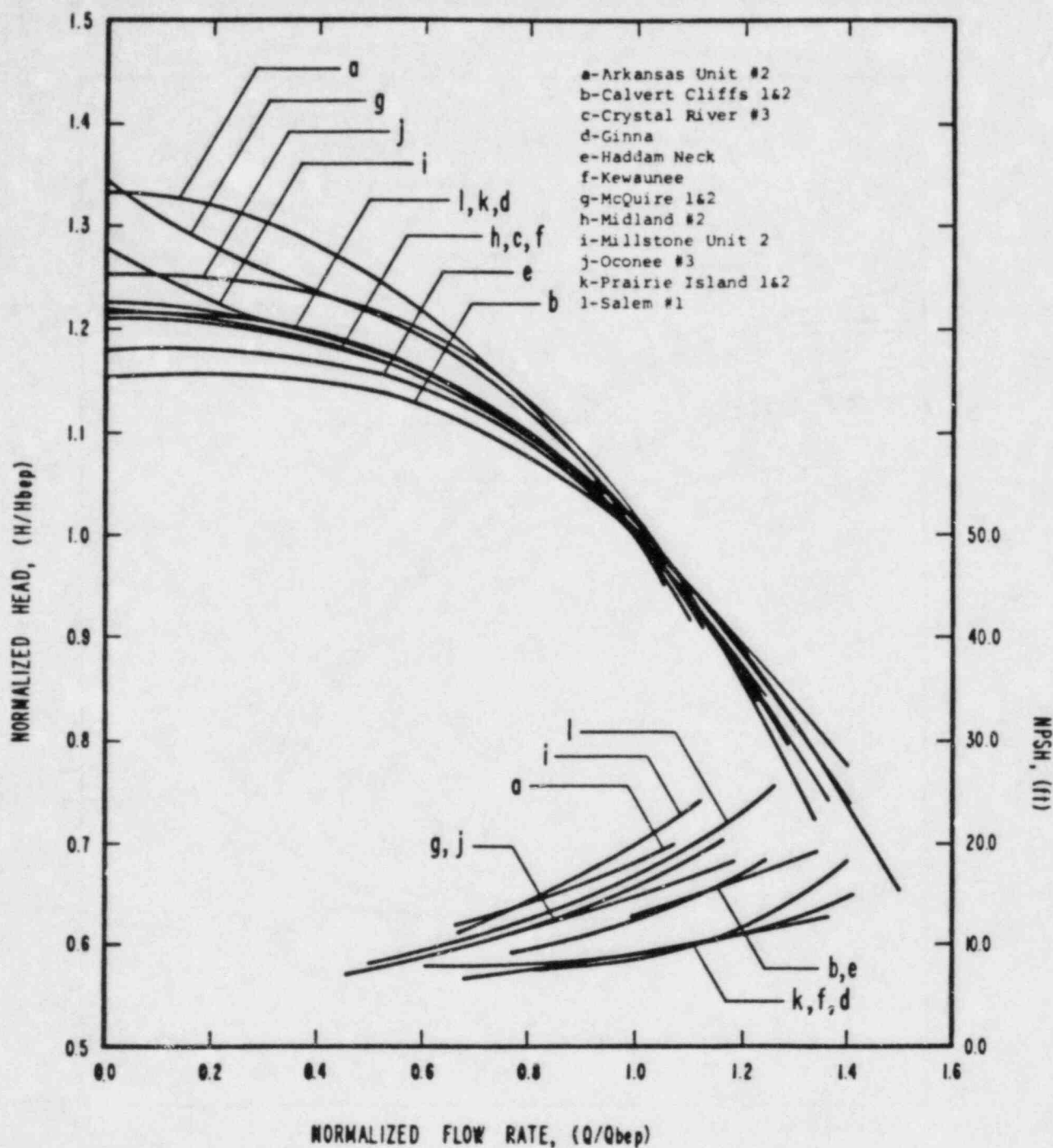


Figure 3.2a. Performance and Cavitation Curves for RHR Pumps. Head vs. Flow Rate Data Normalized by Individual Best Efficiency Point Values.

# CSS Pumps

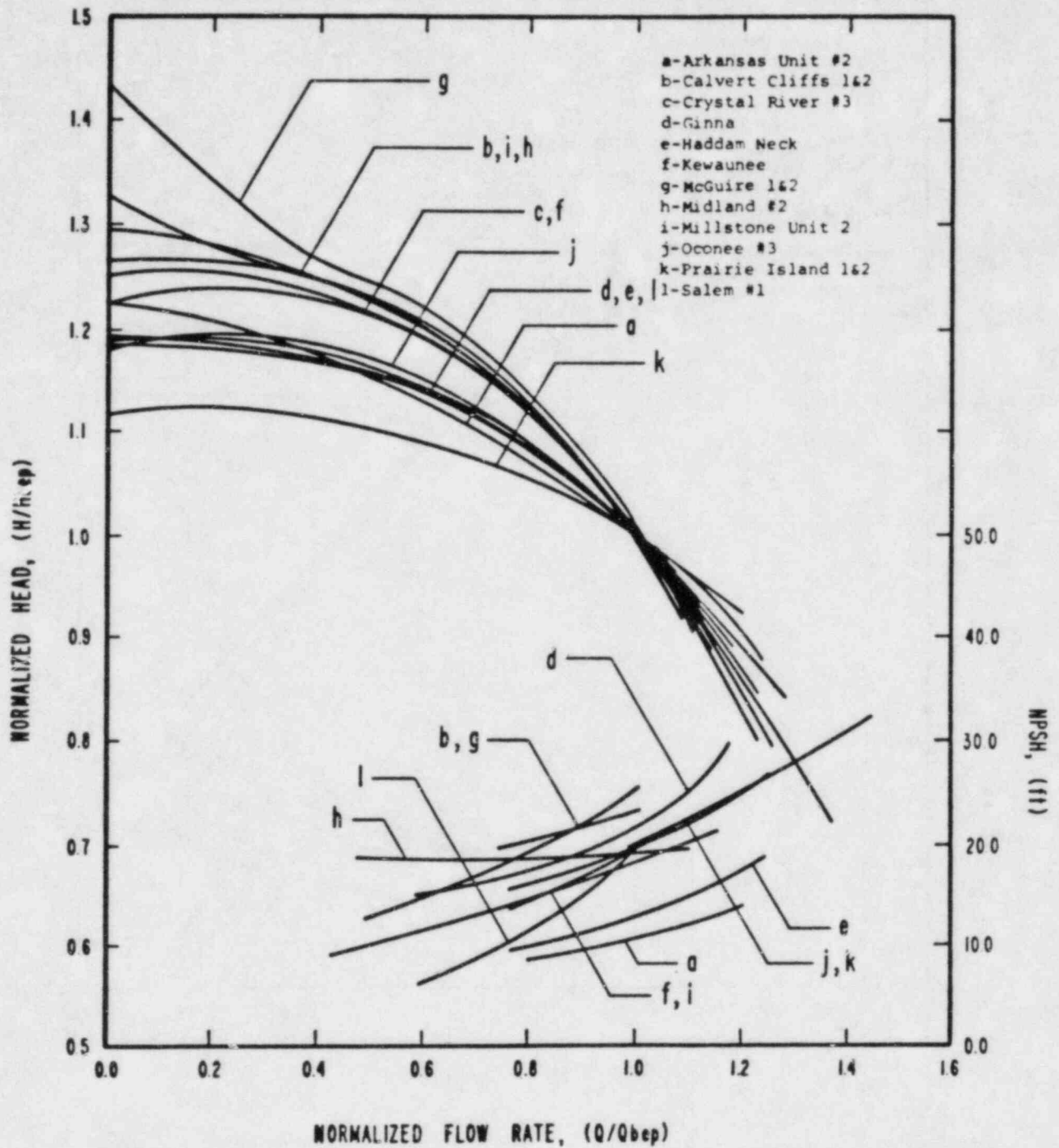


Figure 3.2b. Performance and Cavitation Curves for CSS Pumps. Head vs. Flow Rate Data Normalized by Individual Best Efficiency Point Values.



There is no fixed standard for identifying the NPSH required for a given pump. Unless stipulated by specifications, manufacturers have used some percentage (1 percent or 3 percent) in head degradation as the criterion for establishing the NPSH required at some flow condition. These are empirically established values for which very rapid degradation occurs and severe erosion is likely to occur. Figure 3.3 illustrates the changes in pump performance at several flow rates as a function of net positive suction head. (The curves are typical of those obtained by pump manufacturers to define the NPSH required for their pumps.) As NPSH is reduced for each flow rate shown (Q1-Q4), a point is reached below the 3 percent limit at which substantial degradation begins. Fluid system designers may choose to apply some margin to the NPSH requirements for a pump when designing RHR and CSS systems, but currently no standard margin between NPSH required and NPSH available has been established by NRC regulations.

Some conservatism may be introduced in the calculation of NPSH following guidelines established in RG 1.1 where no credit is allowed for increased containment pressure. However RG 1.1 does not address sub-atmospheric conditions in containment with respect to NPSH.

Cavitation behavior of pumps changes at elevated liquid temperatures. Figure 3.4 from the Hydraulic Institute Standards (Reference 10), shows that as liquid temperatures increase, less NPSH is required by the pump. As a result, increases in liquid temperature have two effects on NPSH: (1) the vapor pressure increases, which reduces NPSH available; (2) the NPSH required is reduced by an amount given in Figure 3.4.

The austenitic stainless steels specified for impellers and casings in RHR and CSS pumps are highly resistant to erosion damage caused by cavitation. Erosion rates for extended operation are not significant as long as the NPSH available exceeds the NPSH requirement of the pump.

### Air Ingestion

The key findings derived for RHR and CSS pumps with respect to air ingestion are based primarily on data from carefully conducted tests in air/water mixtures on pumps of a scale and specific speed range comparable to RHR and CSS pumps.\* Test

---

\*All relevant test data were gathered through reviews of technical papers and interviews with pump manufacturers. Manufacturers' test data on air/water performance of pumps are sparse, applying primarily to the development of commercial pumps for the paper industry. Although these pumps are similar to those used for RHR and CSS service, test methods and results are generally poorly documented. Therefore, manufacturers' data

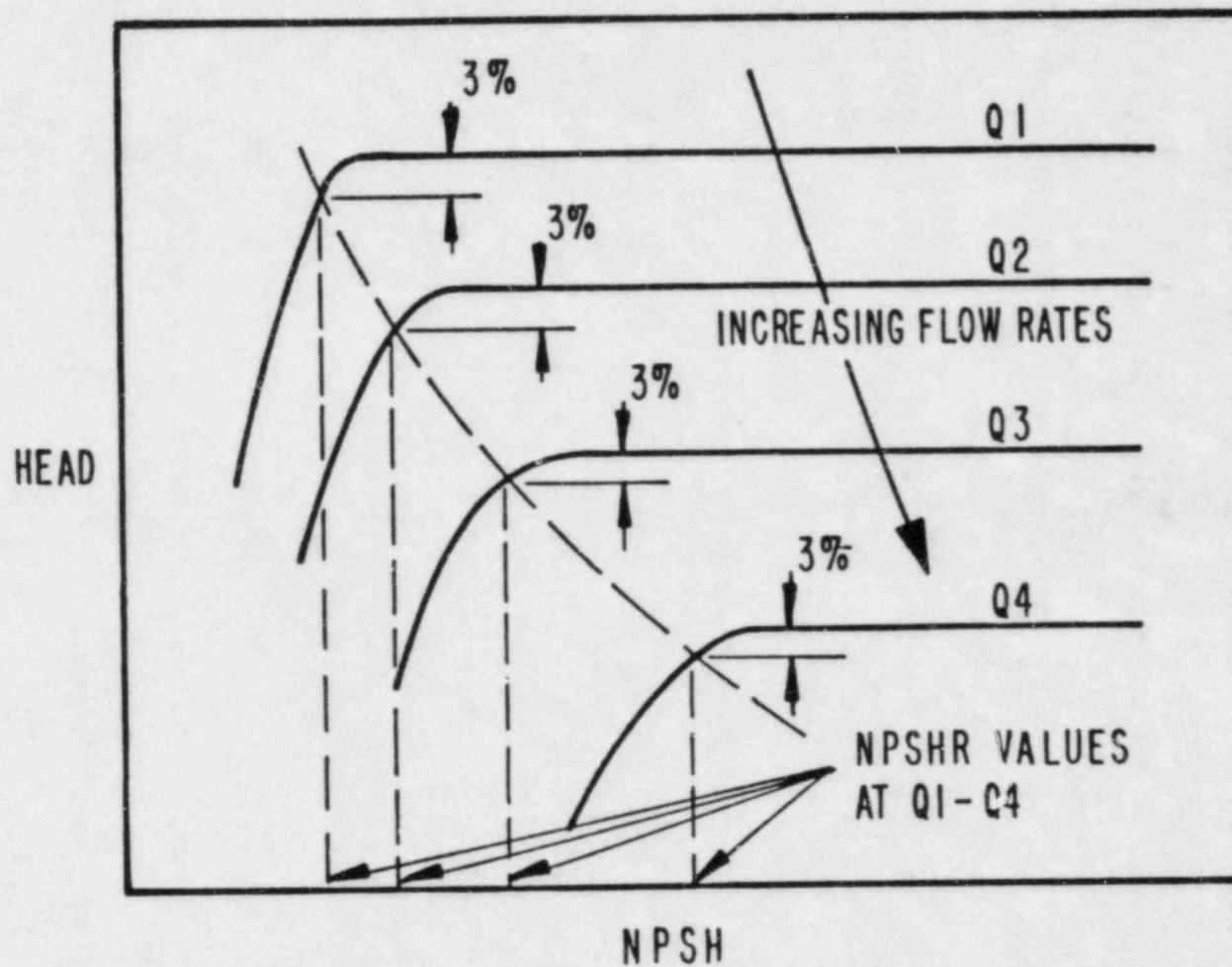


Figure 3.3 TYPICAL HEAD DEGRADATION CURVES DUE TO CAVITATION AT FOUR FLOW RATES (Q1, Q2, Q3 AND Q4)

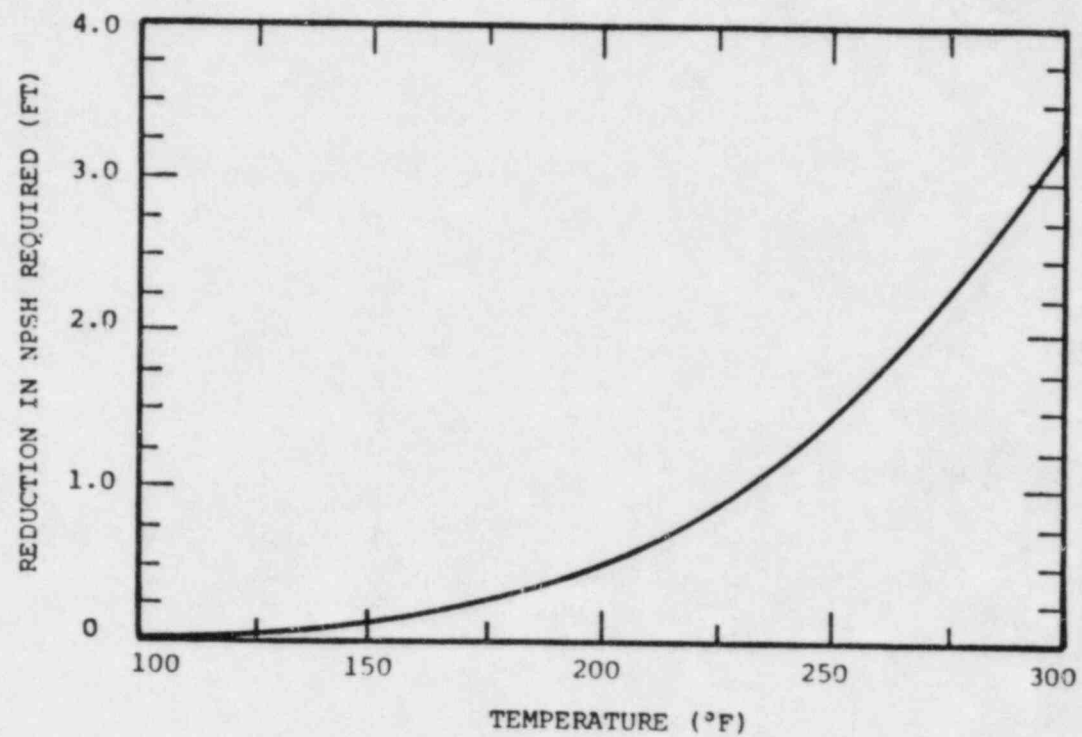


Figure 3.4. REDUCTION IN PUMP NPSH REQUIREMENTS AS A FUNCTION OF LIQUID TEMPERATURE (REFERENCE 12).

data from independent programs on different pumps have been plotted in Figure 3.5 to illustrate the degradation in head at different levels of air ingestion (percent by volume) at several operating points. Performance degradation is indicated by the ratio of the two-phase (air/water) pressure rise to the single-phase (water) pressure rise.

Figure 3.5 shows that for low levels of air ingestion, the degradation in pump head follows the curve (dashed line) predicted by the change in average fluid density due to the air content. Above 2 percent void fraction, the data depart from this theoretical line and the rate of degradation increases.

Above void fractions of about 15 percent, pump performance is almost totally degraded. The degradation process between 2 and 15 percent void fraction is dependent on operating conditions, pump design, and other unidentified variables. (These findings closely approximate the guidelines empirically established by pump manufacturers: at air ingestion levels of less than 3 percent, degradation is generally not a concern; for air ingestion levels of approximately 5 percent, performance is pump and site dependent; for an ingestion greater than 15 percent, the performance of most centrifugal pumps is fully degraded.)

For CSS or RHR pump operation at very low flow rates (< about 25 percent of best efficiency point) even small quantities of air may accumulate resulting in air "binding" and complete degradation of pump performance.

#### Combined Effects of Cavitation and Air Ingestion

Few data on the combined effects of cavitation and air ingestion are available. Figure 3.6, using test results from Reference 11, shows that as air ingestion rates increase, the

---

have not been used to establish the air/water performance characteristics of pumps in this report. (Manufacturers' data and testimonials do, however, corroborate published data.) Only sources of information meeting the following criteria were used:

- \*Subject pumps must be low specific speed ( $N_s = 800-2000$ )
- \*Subject pumps must be of "reasonable" design -- pumps having efficiencies of >60 percent and impellers >6" diameter.
- \*Reasonable care must have been used in experimental

techniques and in the documentation of results.

Test results meeting these criteria were then reduced to common, normalizing parameters and plotted for comparison.



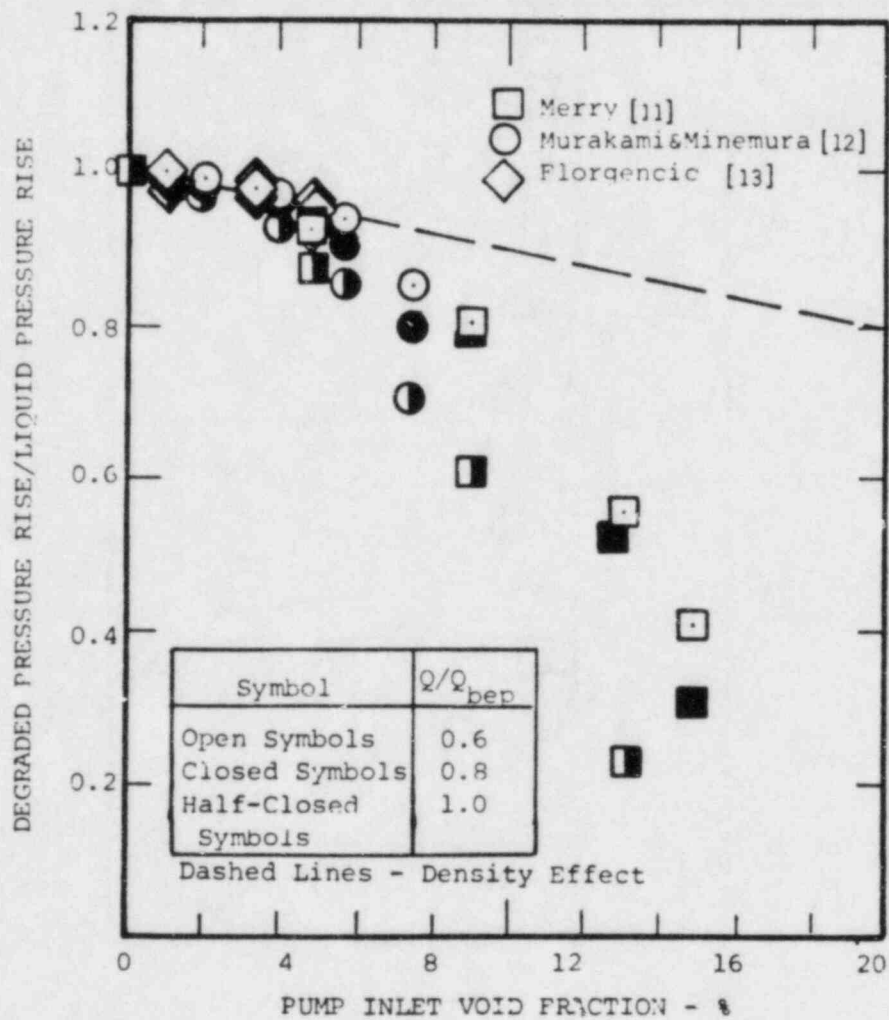


**Figure 3.5.** HEAD DEGRADATION UNDER AIR INGESTING CONDITIONS AS A FUNCTION OF INLET VOID FRACTION (% OF TOTAL FLOW RATE BY VOLUME).

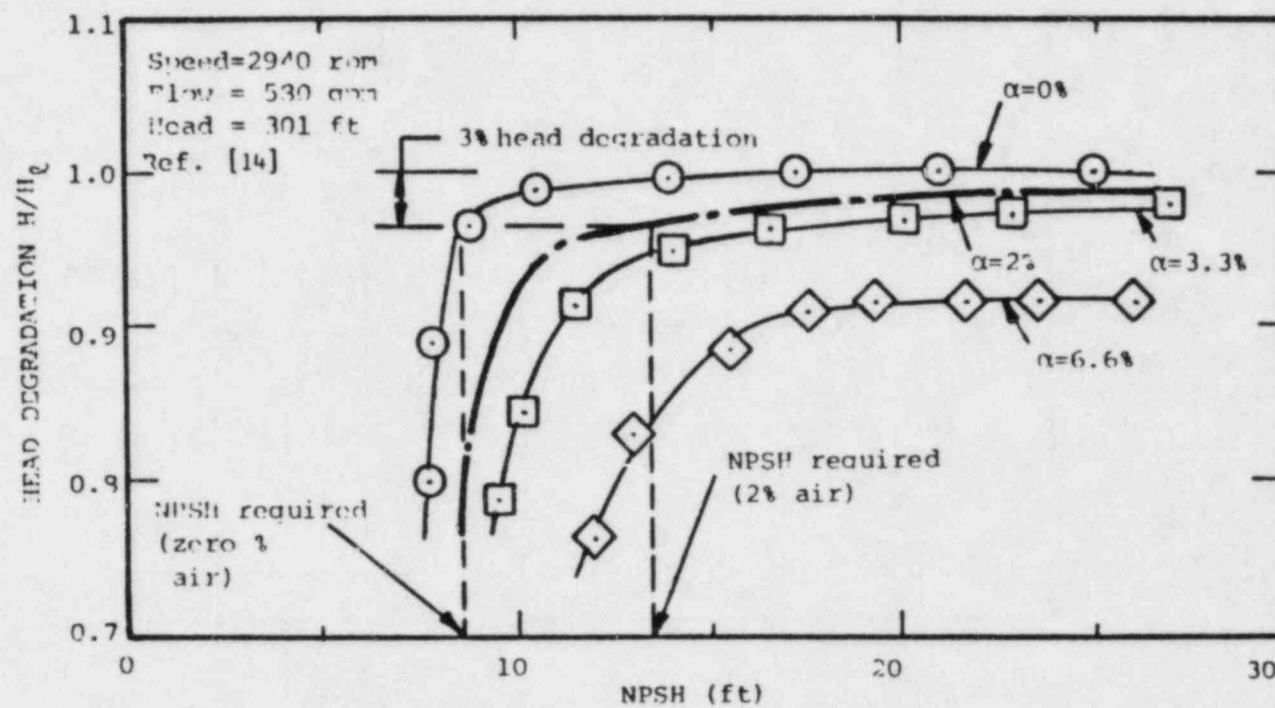


Figure 3.6. EFFECT OF AIR INGESTION ON NPSH REQUIREMENTS FOR A CENTRIFUGAL PUMP.

NPSH requirement for a pump also increases. The curves for this particular pump show that air ingestion levels of about 2 percent results in a 50 percent increase in the NPSH required (allowed head degradation based upon 3 percent degradation from the liquid head performance).

### Particulate Ingestion

The assessment of pump performance under particulate ingesting conditions is based on estimates of the type and concentrations of debris likely to be transported through the screens to the pump inlet. In the absence of comprehensive test data to quantify types and concentrations of debris which will reach the pumps it has been estimated that concentrations of fine, abrasive precipitated hydroxides are of the order of 0.1 percent by mass and concentrations of fibrous debris are of the order of 1 percent by volume.\* The effects of particulates in these quantities has been assessed on the basis of known behavior of this type pump under similar operating circumstances.

Ingestion of particulates through pumps is not likely to cause performance degradation for the quantities and types of debris estimated above. Due to the presence of upstream screens, particulates likely to reach the pumps should be small enough to pass directly through the minimum cross-section passages of the pumps. Because of generally low pipe velocities on the pump suction side, particulates reaching the pumps should be of near neutral buoyancy and, therefore, behave like the pump fluid.

Manufacturers tests and experience with these types of pumps have shown that abrasive slurry mixtures up to concentrations of 1 percent by mass should cause no serious degradation in performance. Similarly, tests on pumps of similar construction to evaluate the capability of pumps of this type to handle fibrous paper stock have shown that quantities up to 4 percent should cause no appreciable degradation.

A major concern in the effects of particulates on performance and operability of the pumps has been the effects of fibrous or other debris (such as paint chips) on pump seal and bearings systems. It is possible that porting within cyclone separators

---

\*The concentration for abrasive  $AlO(H)$  was obtained from Reference 16 where 3000 pounds of precipitate was estimated to develop in 30 days and recirculate with 3.7 million pounds of water (Reference 16). The 1 percent by volume concentration of fibrous debris is based on the quantity of fibrous insulation reaching the sump screens from Maine Yankee plant (Table 3.6) mixing with 200,000 gallons from RWST and being recirculated through the pumps.

and in the flush ports for mechanical shaft seals or water lubricated bearings may become clogged with debris.

In such an event, seal or bearing failure is likely. In the PWR plants which were reviewed, pumps used oil or permanent lubricated bearings and mechanical shaft seals. For these configurations, the seals may be subject to failure due to clogging, but the bearings are not. The construction of mechanical face seals used in these pumps is such that complete pump degradation or failure is not likely even in the event of seal failure. For situations where the pumps incorporate water lubricated bearings (in some BWRs) loss of lubricant due to clogging of passages is likely to cause bearing failure.

### Swirl

The effects of swirl due to sump vortices on pump performance are negligible if the pumps are located at significant distances from sumps. Tests discussed in Section 3.4 of this report indicate that swirl angles in the suction pipe 14 pipe-diameters from the outlet of the sump were typically  $4^\circ$  (swirl will decay with distance in a pipe). RHR and CSS pumps are generally preceded by valves, elbows, and piping with characteristic lengths on the order of 40 or more pipe diameters; this system of piping components is more likely to determine the flow distributions (swirl) at the pump inlet than is the swirl caused by sump hydraulics. For pumps with inlet bells directly in the sumps, vortices and accompanying swirl in the inlet bell can cause severe problems, due to asymmetric hydraulic loads in the impeller. This configuration should be avoided.



### 3.2.3 Calculation of Pump Inlet Conditions

Given the findings noted above, the following steps outline the resulting calculational procedure for assessing the inlet conditions to the pump. The procedure follows routine calculation methods used for estimation NPSH available, except that steps are also incorporated which allow for air ingestion effects. Figure 3.7 shows a schematic of the pump suction system with appropriate nomenclature.

1. Determine the hydrostatic water pressure (gage),  $P_{sg}$ , at the sump suction inlet centerline, accounting for temperature dependency and minimum water level.
2. Based on the sump hydraulic assessment, determine the potential level of air ingestion at the sump suction pipe  $\alpha_s$ , as discussed in Section 5.2.
3. Calculate the pressure losses in the suction pipe between the sump and the pump inlet flange. Pressure losses are calculated for each suction piping element (i.e., inlet loss, elbow loss, valves, pipe friction) using the average velocity through each element  $V_i$ , and a loss coefficient,  $K_i$ , for each element. The total pressure losses are then:

$$P_l = (\gamma/144) \sum K_i V_i^2 / 2g$$

where  $\gamma$  is the specific weight of water (lb/ft<sup>3</sup>) and 144 is the conversion from psf to psi.

The loss coefficients are defined as:

$$K_i = \frac{h_{li}}{V_i^2 / 2g}$$

where:  $h_{li}$  is the head loss in ft of water in element  $i$ ,

$g$  is the acceleration due to gravity, and

$V_i$  is the average velocity in element  $i$  in fps.

Loss coefficients can be found in standard hydraulic data references such as found in Reference 10.

4. Calculate the absolute static pressure at the pump inlet  $P_p$ .

$$P_p = P_{sa} - P_l + P_h - P_d$$

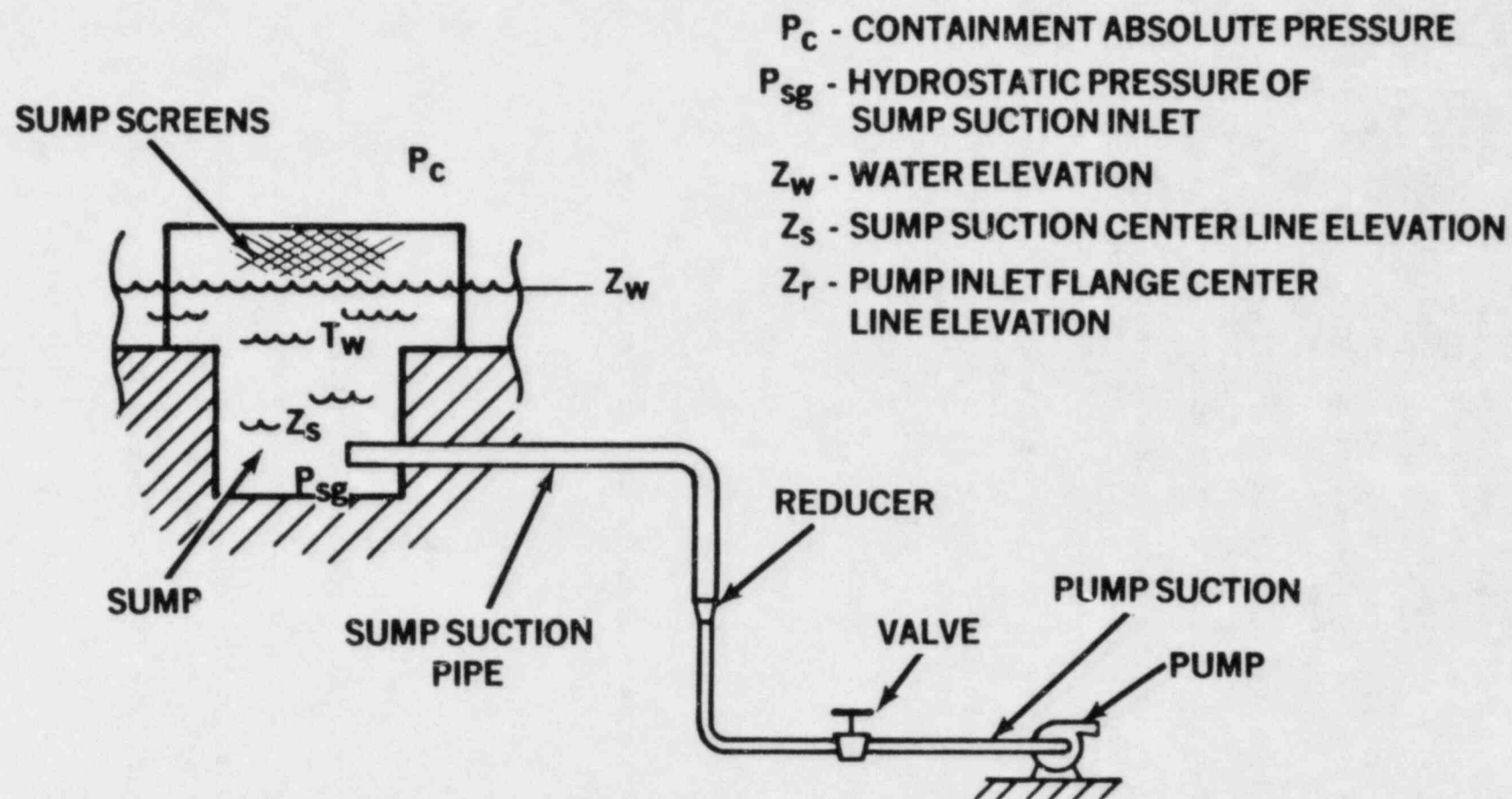


Figure 3.7. Schematic of Suction Systems for Centrifugal Pump

where:  $P_{sa}$  is the total absolute pressure at the sump suction pipe centerline which is the sum of the hydrostatic pressure,  $P_{sg}$ , and the containment absolute pressure,  $P_c$ , (determined in accordance with RG 1.1 and 1.82 for NPSH determination).

$P_f$  is the suction loss determined in Step 3.

$P_h$  is the hydrostatic pressure due to the elevation difference between the sump suction pipe centerline,  $Z_s$ , and the pump inlet flange centerline,  $Z_p$ .

$$P_h = (\gamma / 144) (Z_s - Z_p)$$

$P_d$  is the dynamic pressure at the pump inlet flange using the average velocity at the pump suction flange,  $V_p$ .

$$P_d = \frac{\gamma V_p^2}{144 \cdot 2g}$$

The value for  $P_p$  will be used to correct the volumetric flow rate of air at the sump suction pipe for density changes. If air ingestion is zero, Steps 4, 5 and 6 can be ignored.

5. Calculate the corrected air volume flow rate at the pump inlet,  $\alpha_p$ , based on perfect gas, isothermal process:

$$\alpha_p = (P_{sa}/P_p) \alpha_s$$

6. If  $\alpha_p$  is greater than 2 percent, inlet conditions are not acceptable.
7. Calculate NPSH at the pump inlet flange, taking into account requirements of RG 1.1 and 1.82.

$$NPSH = (P_c + P_{sg} - P_f + P_h - P_{vp}) (144/\gamma)$$

where  $P_{vp}$  is the vapor pressure of the water at evaluation temperature.

8. If air ingestion,  $\alpha_p$ , is not zero, NPSH required from the pump manufacturer's curves must be modified to account for air ingestion.

$$\beta = 0.50 (\alpha_p) + 1.0$$

where  $\alpha_p$  is the air ingestion level percent by volume at the pump inlet flange. Then:

$$\text{NPSH required (air/water)} = \beta \times (\text{NSPH required for water})$$

9. If NPSH from Step 7 is greater than NPSH required from Step 8, pump inlet conditions should be satisfactory.

### 3.3 Debris Assessment

The safety concerns related to LOCA generation of debris resulting from the breakup of thermal insulation, and the potential for sump screen blockage were addressed generically as follows:

1. A survey of nineteen reactor power plants was conducted to identify insulation types used, quantities and distribution, methods of attachment, components and piping insulated, variability of plant layouts, sump designs and location.
2. A calculational procedure was developed for estimating quantities of insulation which the pipe break jet might destroy or dislodge, for estimating debris migration during the recirculation mode and for estimating the degree of screen blockage that might occur. A series of engineering models were established and concise review methods were developed.
3. The debris calculational methods described in 2, above, were then applied to five PWRs to determine the influence of various types of insulations and plant layout effects (i.e., sump location versus break location). In addition, the calculational methods and results obtained were subjected to external, independent technical review (i.e., peer panel reviews).
4. Experiments were conducted to establish the onset of insulation debris generation from typical mineral wool and fiberglass insulations, their buoyancy and migration characteristics, and the potential of such insulations and their debris to create screen blockage.

The results are summarized in the following subsections.

#### 3.3.1 Plant Insulation Survey Findings

Table 3.2 lists the plants surveyed.

The results of these insulation surveys are summarized in Table 3.3, wherein tabulations of the respective insulations are made for the respective plants and comparison of the



TABLE 3.2

Reactor Plants Selected for Insulation Survey

<u>Plant and Location</u>	<u>Reactor</u>	<u>Rating</u>	<u>Start-Up Date</u>	<u>Utility</u>	<u>Architect/Engineer</u>
Oconee Unit 3 Seneca, SC	B&W-PWR	860 MWe	1974	Duke Power Co.	Duke Power Co.
Crystal River Unit 3 Red Level, FL	B&W-PWR	825 MWe	1977	Florida Power Corp.	Gilbert
Midland Unit 2 Midland, MI	B&W-PWR	805 MWe	1983*	Consumers Power Co.	Bechtel
Haddam Neck Haddam Neck, CT	W-PWR	575 MWe	1968	Connecticut Yankee Atomic Power Co.	Stone & Webster
Robert E. Ginna Ontario, NY	W-PWR	490 MWe	1970	Rochester Gas & Electric Corp.	Gilbert
H. B. Robinson Hartsville, SC	W-PWR	665 MWe	1971	Carolina Power & Light Co.	Ebasco
Prairie Island 1 & 2 Red Wing, MN	W-PWR	520 MWe	1973 <sup>¶</sup>	Northern States Power Co.	Fluor Power Services
Kewaunee Carlton, WI	W-PWR	535 MWe	1974	Wisconsin Public Services Corp.	Fluor Power Services
Salem Unit 1 Salem, NJ	W-PWR	1090 MWe	1977	Public Service Electric & Gas Co.	Public Service Electric & Gas Co.
McGuire Units 1 & 2** Gowans Ford, NC	W-PWR	1180 MWe	1981*	Duke Power Co.	Duke Power Co.

\*Estimated dates

<sup>¶</sup>Unit 2 start-up date is 1974  
 Source: Nuclear News, August 1981

 \*\*Unit 2 estimated start-up date is 1983  
 Source: Nuclear News, February 1981

TABLE 3.2 (Continued)

<u>Plant and Location</u>	<u>Reactor</u>	<u>Rating</u>	<u>Start-Up Date</u>	<u>Utility</u>	<u>Architect/Engineer</u>
Sequoyah Unit 2 Daisy, TN	W-PWR	1148 MWe	1982*	Tennessee Valley Authority	Tennessee Valley Authority
Maine Yankee Wiscasset, ME	CE-PWR	790 MWe	1972	Maine Yankee Atomic Power Co.	Stone and Webster
Millestone Unit 2 Waterford, CT	CE-PWR	870 MWe	1975	Northeast Utilities	Bechtel
St. Lucie Unit 1 Hutchinson Island, FL	CE-PWR	777 MWe	1976	Florida Power & Light Co.	Ebasco
Calvert Cliffs Units 1 & 2 Lusby, MD	CE-PWR	850 MWe	1975**	Baltimore Gas & Electric Co.	Bechtel
Arkansas Unit 2 Russellville, AR	CE-PWR	858 MWe	1980	Arkansas Power & Light Co.	Bechtel
Waterford Unit 3 Taft, LA	CE-PWR	1165 MWe	1983*	Louisiana Power & Light Co.	Ebasco
Cooper Brownsville, NB	GE-BWR I	778 MWe	1974	Nebraska Public Power District	Burns and Roe
WPPSS Unit 2 Hanford, WA	GE-BWR II	1150 MWe	1983*	Washington Public Power Supply System	Burns and Roe

\*Estimated dates

\*\*Unit 2 start-up date is 1977

Source: Nuclear News, August 1981

TABLE 3.3

Types and Percentages of Insulation Used Within the Primary Coolant  
System Shield Wall in Plants Surveyed

Plant	-----Types of Insulation and Percentage*-----					
	Reflective Metallic	Totally Encapsulated	Mineral Fiber/Wool Blanket	Calcium Silicate Block	Unibestos Block	Fiberglass
Oconee Unit 3	98	--	--	--	--	2
Crystal River Unit 3	94	5	1	--	--	--
Midland Unit 2	78	--	--	--	--	22
Haddam Neck	3	--	--	--	95 <sup>¶</sup>	1
Robert E. Ginna	--	--	5	80	10	--
H. B. Robinson	--	--	--	15	85	--
Prairie Island Units 1 & 2	98	--	--	--	--	2
Kewaunee	61	--	--	--	39	--
Salem Unit 1	39	8	53**	--	--	--
McGuire Units 1 & 2	100	--	--	--	--	--
Sequoyah Unit 2	100	--	--	--	--	--
Maine Yankee	13	--	48	25	13	1
Millstone Unit 2	25	35	5	30	--	--
St. Lucie Unit 1	10	--	--	90	--	--
Calvert Cliffs Units 1 & 2	41	59	--	--	--	--
Arkansas Unit 2	46	53	--	--	--	1
Waterford Unit 3	15	85	--	--	--	--
Cooper	30	70	--	--	--	--
WPPSS Unit 2	100	--	--	--	--	--

\*Tolerance is  $\pm$  20 percent

\*\*Both totally and semi-encapsulated Cerablanket is used, however, inside containment only totally encapsulated is employed.

<sup>¶</sup>Unibestos is currently being replaced by Calcium Silicate. However, both types of insulation have the same sump blockage characteristics.

respective amounts of insulations used in a particular plant is provided on a percentage basis. Additional detailed information for each plant surveyed has been assembled into reference data packages and has been published as NUREG/CR-2403 and NUREG/CR-2403, Supplement No. 1 (References 3 and 4). These reports detail the types and amounts of insulation employed, their location in containment, components insulated, material characteristics, methods of installation, etc. In addition, the plant sump designs and screen details are provided in simplified drawings for ease of reference. Appendix A of this report illustrates the plant specific sump designs and plant layouts; the variability plant-to-plant is quite evident. Plant design information was obtained for plants representative of the 4 U.S. light water reactor vendors and the selected sample consisted of plants designed by 8 U.S. architect-engineering firms. New and old plants were surveyed.

The types of insulation employed in nuclear power plants are as follows:

1. Reflective metallic insulation, generally constructed from stainless steel, although aluminum internal foils have also been used.
2. Totally encapsulated insulation panels which utilize more effective thermal insulators (e.g., mineral wool fiber, fiberglass, calcium silicate, etc.). The principal point of distinction is that the encapsulation material (i.e., stainless steel) provides a container that is resistant to break jet forces and promotes the maintenance of the insulation in large blocks.
3. Nonencapsulated insulations (e.g., mineral wool, fiber wool, calcium silicate blocks, fiberglass blankets, unibestos block, etc.) which, if directly impacted by the break jet and subsequently immersed in the steam-water environment within containment, can be viewed to pose screen blockage problems and must be evaluated.

The plant variability and selection/utilization variability noted above preclude a singular generic debris assessment. Rather, the prevalent situations lead to the necessity of developing logical and consistent debris calculational methods for assessment and quantification of debris generated and screen blockage severity. The following subsection outlines calculational methods and models for systematically performing debris calculations. Past evaluations have relied to a great extent on R.G. 1.82 which addresses an assumed acceptable limit of 50 percent screen blockage, but does not require an engineering



estimate of the amounts of insulation debris which a LOCA might generate, nor an assessment of the attendant sump screen blockage.

### 3.3.2 Calculational Methods for Assessing Debris Hazards

The calculational methods described herein were developed by Burns & Roe, Inc., engineering staff and are applicable for analyzing the diversity of plant layouts, sump locations, insulation types and piping runs typified by the plant surveys conducted (see Section 3.3.1 and Appendix A).

These calculational methods (which are described in greater detail in Reference 5 and Appendices B and C) provide an analysis tool which allows a systematic estimation of the quantities of debris generated. The assumption is made at the outset that the postulated pipe ruptures are those defined in NRC's Standard Review Plan (NUREG-0800), Section 3.6.2, and use is made of the break jet models provided in References 17 and 24. In the treatment given here, the jet model in Reference 17 has been modified to provide more conservatism in the results. In addition, jet impingement effects are calculated\*, short-term transport due to blowdown forces and long-term transport due to the flow of recirculated water are estimated as is the screen blockage by debris.

As can be expected, plant layout, types of insulation employed, and quantities thereof are the controlling inputs. Since the majority of postulated rupture locations (PRLs) are located within the crane wall region, and attention to that portion of the plant is required. Reflective metallic insulations will sink and transport will be along the plant flows. Low density insulation (if non-hygroscopic) will float and migrate to the screens--but will not cause blockage if water levels are high enough. Nonencapsulated insulations will be subjected to direct high temperature, high pressure water and steam jets. Destruction, dispersion and displacement will likely occur. Encapsulated insulation sections will tend to maintain a geometric structural shape which is large, and although migration could occur, a densely packed (or blocked) screen situation is less likely. The insulation material of primary concern is the nonencapsulated, or free (due to jet breakup) fibrous insulation as characterized by mineral wool, fiber glass, wool blanket materials. It has been demonstrated

---

\*In recent NRC supported research of two-phase jet phenomena and jet loads (References 18, 19, and 24) stagnation pressure in two-phase jets and pressure loading on two-dimensional targets were investigated. This research has shown that the target load depends upon the thermodynamic conditions immediately upstream of the break and the distance to the target. For highly subcooled vessel conditions a potential exists for extremely high pressures (greater than 2000 psia for PWRs) on targets within several diameters of the break.

(References 7, 14, 15, and 25) experimentally that free fibers and shreds can migrate (at near neutral buoyancy) to the screens where they can adhere and form layers sufficiently thick to result in significant screen blockages with high attendant pressure drops.

These methods for sequential evaluation are outlined in Figure 3.8, Sheets 1, 2, 3 and 4, in which the respective steps described below are identified.

STEP 1 -- Identification of the number, orientation, and location of the PRL to be analyzed. These postulated pipe ruptures are defined in the NRC Standard Review Plan, Section 3.6.2, which provides guidance for selecting the number, orientation, and location of the postulated ruptures within containment.\* In general, PRLs are selected for analysis as follows:

1. All PRLs which are identified in the Final Safety Analysis Report (FSAR)
2. From PRLs identified, select breaks that are:
  - a) located in large diameter, high energy lines
  - b) oriented toward principal sources of insulation (steam generators, coolant pumps, pressurizers, hot legs, cold legs, cross-over piping, etc.).
3. Four or five breaks are selected for further analysis by noting jet travel direction for unrestrained or restrained pipes and breaks are selected that project insulation toward the sump area. (Breaks dislodging the greatest amount of insulation that will be transported toward the sump should be selected without regard for initial transport direction).

STEP 2 -- Estimation of the amount of insulation debris that might be generated by postulated pipe rupture. Debris is generated by three mechanisms:

1. Jet Impingement -- generates debris by subjecting the insulation to a high velocity, high differential pressure field that strips the insulation from the target.

---

\*For plants that have already filed FSARs, the design basis break locations inside containment have been tabulated and may be found in FSAR's, Section 3.6.2, for plants filing FSARs under the revised format. Information for FSAR plants that filed prior to the revised format effective date may be found in Accident Analysis (Chapter 15), Design of Structures, Components, Equipment and Systems (Chapter 3), and Engineered Safety Features (Chapter 6 or an Appendix).

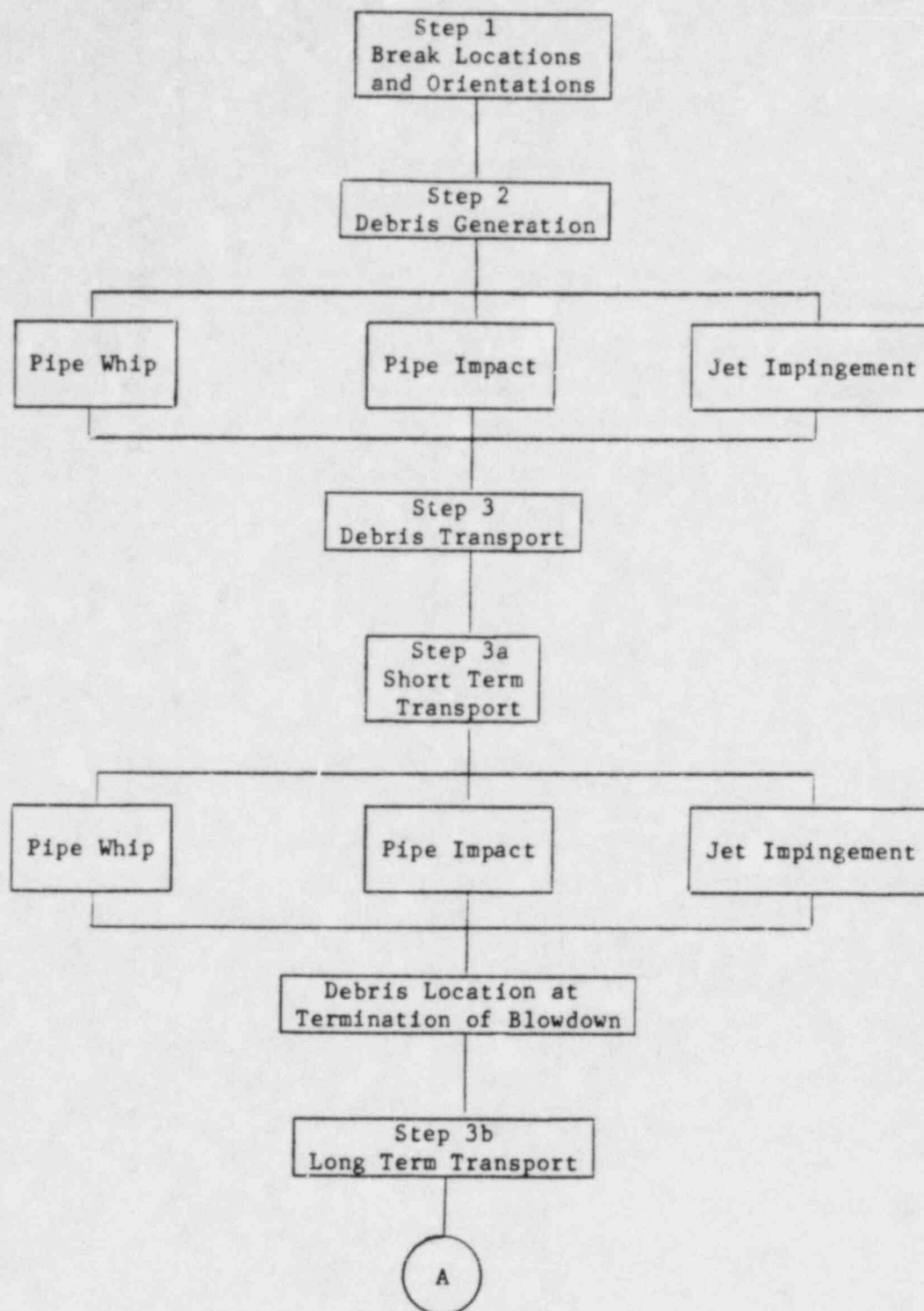


Figure 3.8 - Sheet 1  
Outline of Methods

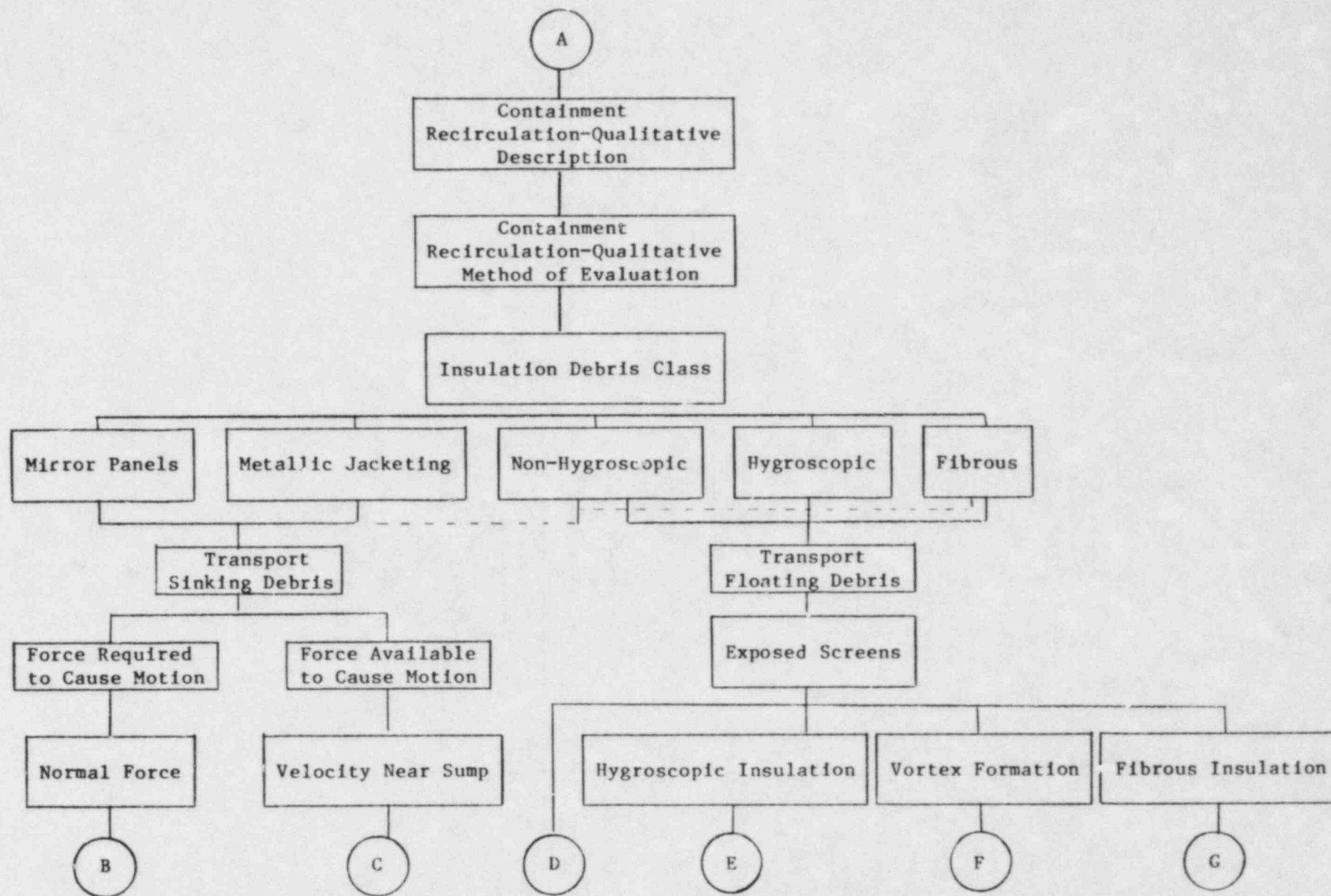


Figure 3.8 - Sheet 2  
Outline of Methods



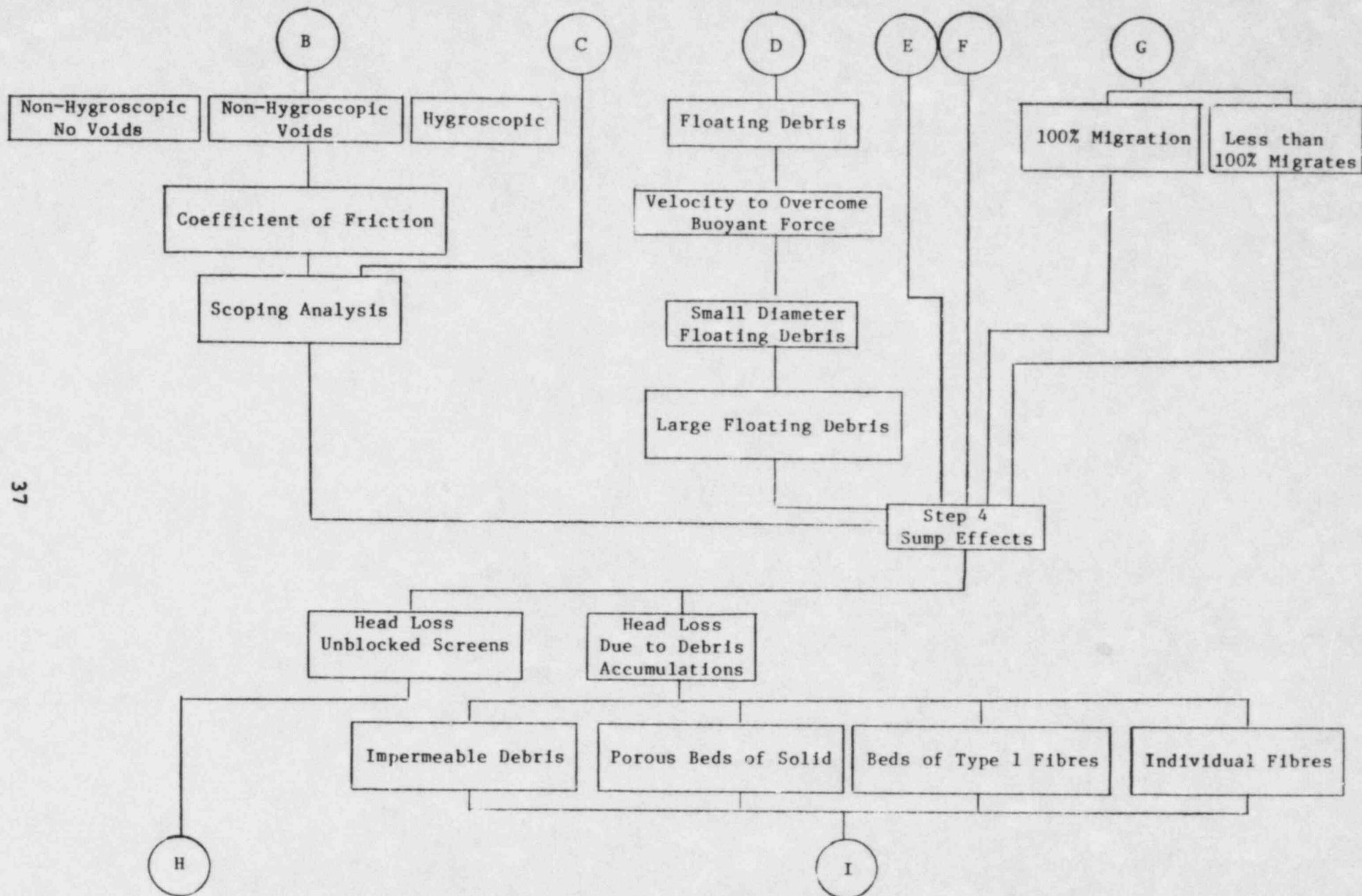


Figure 3.8 - Sheet 3  
Outline of Methods

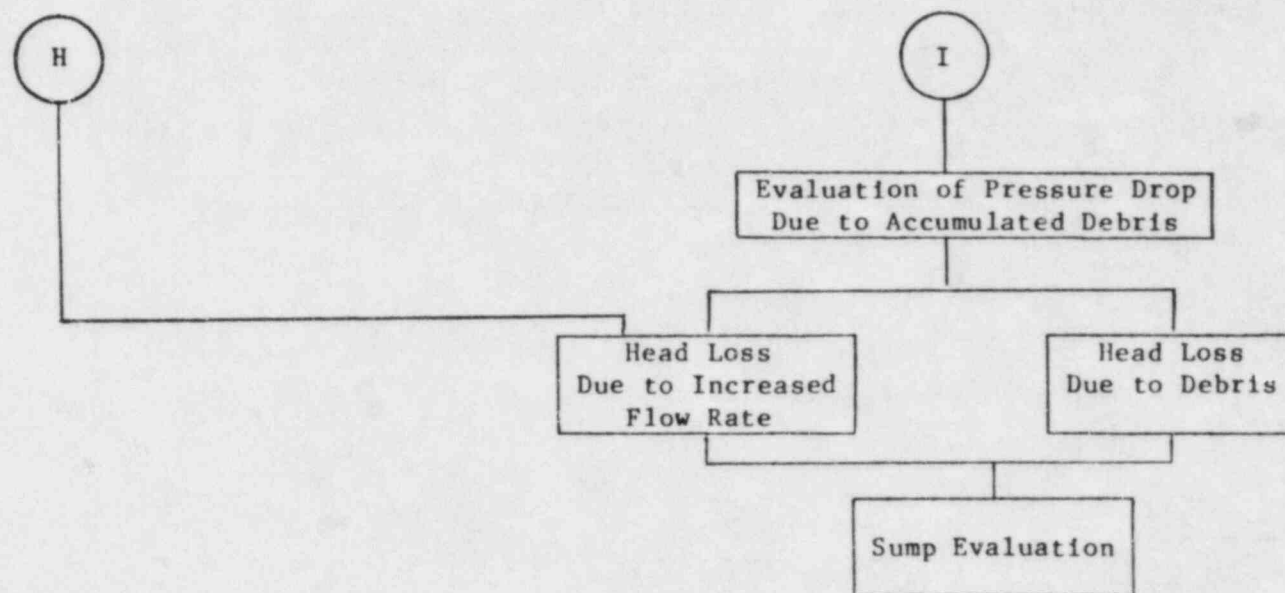


Figure 3.8 - Sheet 4  
Outline of Methods

This is the principal debris generation mechanism (i.e., 90 percent of debris generated).

2. Pipe Whip -generates insulation debris due to the motion of unrestrained piping segments.
3. Pipe Impact -- generates additional insulation debris by the impact of unrestrained piping segments with insulated structures, components, or other piping systems.

Specific methods for calculating the amount of debris generated by each mechanism are given in Reference 5 and Appendices B and C. Methods for calculating the magnitude of jet thrust, jet impingement forces, stagnation pressure as a function of distance, and other hydrodynamic effects were adapted from Standard Review Plan, Section 3.6.2, and engineering handbooks.

STEP 3 -- Calculation of short-term and long-term transport of insulation debris.

1. Short term transport -- debris motion caused by pipe whip, pipe impact, jet impingement mechanisms -- terminates at the end of the blowdown transient.

Velocities of debris caused by pipe whip and pipe impact are assumed to cause motion in a straight line that continues until impact with walls or other obstructions. Debris then drops vertically to floors, grates, or other structures.

Debris generated and entrained into the jet by jet impingement will not stop upon impact with obstructing structures, but will change direction. Consequently, debris can pass through doorways or other openings not directly in line with pipe breaks. The jet force at an obstruction is determined using the stagnation pressure equation (Reference 5).

2. Long-term transport -- begins with activation of the containment recirculation system. Fluid velocity, debris density, debris size, and effects of coolant on debris integrity are analyzed to determine if long-term transport could occur. For debris transport, the migration patterns of dislodged insulation within containment are established. Insulation debris may be typed either as Sinking (mirror panels, metallic jacketing or hygroscopic insulation with equilibrium densities greater than that of water) or Floating (non-hygroscopic, hygroscopic, fibrous).

Sinking Debris -- will be transported to the sump if the water velocity is sufficient to overcome drag force. The analysis considers the hydrodynamic forces needed to move debris on the containment floor to the sump inlet, and determines the local velocities that exist within containment. Experimental studies allow estimates of those velocities required to transport insulation debris to sump screens.

Floating Debris -- is assumed to migrate to the sump. The possibility of sump blockage is determined by evaluating the local velocity required to overcome the buoyant force of the debris and comparing this value to the local velocity existing at the sump. The floating debris model is valid also for predicting the behavior near sump intakes of floating fibrous insulation. Suspended fibrous debris is assumed to migrate to the sump. The effect of blockage is determined by evaluating the pressure drop across the resulting debris mat formed on the sump screen.

STEP 4 -- Determination of Screen Blockage and Attendant Pressure Drops. The results of Steps 1 through 3 can now be used to estimate the extent of screen blockage that might occur due to debris migration. These debris migration models can be used to estimate screen blockages in terms of the quantities of debris transported and screen blockage patterns can be deduced. Attendant pressure drop is the critical parameter for determining effects on required pump NPSH. Careful consideration should be given to head losses for blocked screens. In the calculation of blockage by fibrous debris, the equivalent insulation blockage thickness ( $t_i$ ), should be calculated as:

$$t_i = \frac{\text{Volume of debris transported}}{\text{Available Screen Area}} \quad .$$

Pressure drop calculations, using the above relationship, have been made on two selected examples where blockage has been calculated to be total (Salem Unit 1 and Maine Yankee). Such calculations, provided in Reference 5, have made use of the methods and assumptions present in the referenced report. In the estimation of pressure drops at sump screens due to fibrous insulation debris, the methods provided in Reference 5 and Appendices B and C are applicable. However, the pressure drop versus insulation debris thickness information developed experimentally should be used in calculations of sump acceptability (Reference 7).



These four steps of the debris analysis provide a conservative method for evaluating the potential for generation of insulation debris in a power reactor station, the potential for blockage of the sump screens due to LOCA-generated insulation debris, and for assessing the impact of insulation debris on sustained operation of the containment recirculation system. They provide a set of methods for assessing the potential safety hazard of insulation debris and can be used to aid in assessing debris effects (screen blockage) in any reactor primary containment.

### 3.3.3 Application of Methods to 5 Sample Plants

The methods described in the previous section were applied to 5 plants selected from the 19 originally surveyed. Sample calculations were performed to prove the methods and to identify any problem areas for plant or insulation types. Plants of varying design with different insulation inventories were selected. Table 3.4 summarizes these plants by type, owner, location, size, and architect/engineer. Tables 3.2 and 3.3 summarize the types of insulation present in each plant. The tables show that a broad spectrum of insulation types, both singly and in combinations, were found to be in use.

Table 3.5 describes the location of the emergency sump, summarizes the location of the various types of insulation in the plant, and provides an assessment of the migration potential of debris generated as a result of a pipe break, as derived from the development provided in Reference 5.

Table 3.6 summarizes, for each plant, the PRLs, the quantities of debris generated, the quantities of debris transported to the sump screens, unblocked screen areas, blocked screen areas, and the percentages of sump inlet areas that are blocked; the table concludes with a qualitative indication of the severity of the potential sump blockage. The estimates provided in this summary derive from Reference 5.

Although the estimated quantities of debris and attendant screen blockages show a high variability, the findings are quite revealing. Large quantities of debris are estimated to be produced. This results from the conservative assumption that all jet-targeted insulation is stripped and conservative assumptions as to transport to the sump. In addition, calculated screen blockages vary due to sump screen area variability. Screen blockages in excess of 50 percent (see the Sequoyah #2 results) have been calculated. However, the screen pressure drop at Sequoyah has been determined to be negligible, since Sequoyah utilizes all reflective metallic insulation. Plants having large screen areas (i.e., Salem

TABLE 3.4

Reactor Plants Selected for Detailed Investigation  
of Insulation Debris Generation Potential

<u>Plant and Location</u>	<u>Reactor</u>	<u>Rating</u>	<u>Start-Up Date</u>	<u>Utility</u>	<u>Architect/Engineer</u>
Maine Yankee Wiscasset, ME	CE-PWR	790 MWe	1972	Maine Yankee Atomic Power Co.	Stone and Webster
Arkansas Unit 2 Russellville, AR	CE-PWR	858 MWe	1980	Arkansas Power & Light Co.	Bechtel
Salem Unit 1 Salem, NJ	W-PWR	1090 MWe	1977	Public Service Electric & Gas Co.	Public Service Electric & Gas Co.
Sequoyah Unit 2 Daisy, TN	W-PWR	1148 MWe	1982*	Tennessee Valley Authority	Tennessee Valley Authority
Prairie Island Unit 1 Redwing, MN	W-PWR	520 MWe	1973	Northern States Power Co.	Fluor Power Services

\*Estimated date

Unit 1 with a 936 ft<sup>2</sup> screen) can tolerate large quantities of transported debris. On the other hand, plants with smaller screens and fibrous, nonencapsulated insulation targeted by principal pipe breaks (such as Maine Yankee) have been identified as having a potential for unacceptable pressure drops.

Plant and insulation effects are evident. The methods given above, however, can be used to evaluate plants for the degree of screen blockage that various insulations can pose. The methods have been tested against a broad spectrum of plants and evaluated independently (see Section 4.2). The results point out the deficiency of the 50 percent screen blockage guidance set forth in RG 1.82, which has been used in the past at times without the benefit of plant specific debris evaluations and attendant loss in required NPSH. These calculations also show that the answers the analysis method provides can vary over a wide range of blockages; plant dependent features dominate the blockage calculations.

#### 3.3.4 Experimental Studies on Debris

Following the studies conducted by Burns and Roe, experimental work was carried out at Alden Research Laboratory to examine in a preliminary way the generation, buoyancy, and transport characteristics, as well as the potential for sump blockage of typical as-fabricated insulation and insulation debris. These experimental studies are reported in References 6 and 7.

#### Susceptability of Fibrous Insulation to Debris Formation

Experiments have been reported to study the onset of failure of as-fabricated fibrous insulation due to jet impingement. These tests were conducted using incompressible water jets at ambient temperature for various stagnation pressures and for two angles of jet impingement: normal to the insulation surface and 45° to the insulation surface. These tests demonstrated that the stagnation pressure was the preliminary scaling variable with regard to the forces applied to an insulation panel (sometimes referred to as insulation pillows). The experiments studied the stagnation pressure to determine the level required for damage to the cover fabrics and failure of the insulation panel (fibrous insulation release). Tests were conducted using three types of insulation panels: Type 1 was made of mineral wool enclosed in a Mylar coated asbestos cover, Types 2 and 3 were made of fiberglass insulation covered with silicone glass cloth and fiberglass cloth, respectively. The insulation that was the most susceptible to failure was the Type 1 insulating panels. Visible damage occurred at stagnation pressures of about 10 psig (90° impact) and 15 psig (45° impact); failure of the pillow occurred at stagnation pressures of about 35 psig (90° impact) and 30 psig (45° impact). Visible damage was defined as the pressure at which the first signs of structural failure occurred, e.g., fraying of the fibers in the covering, etc. Failure of the insulation panel was defined as the pressure where there was a release of fibrous insulation from the as-fabricated insulation panel. In both instances the insulation

TABLE 3.5

Summary Table for 5 Plant Sample Calculations

Plant and Reactor Manufacturer	Type of Insulation Utilized	Location of Emergency Sump	Final Assessment of Migration Potential of Debris Generated as a Result of a Pipe Break
Maine Yankee (CE) (Combustion Engineering)	Reactor vessel uses reflective metallic insulation. Pressurizer, reactor coolant pumps, and steam generators use calcium silicate molded block jacketed insulation for nonremovable sections and mineral fiber/wool for the removable sections. Primary coolant piping uses removable mineral fiber/wool blankets. Main steam, feedwater, residual heat removal, and chemical and volume control system piping use calcium silicate or unibestos molded block insulation. Component cooling lines use fiberglass jacketed antisweat insulation.	Outside the reactor coolant system shield wall below basement floor.	Plant calculations show that for some of the postulated breaks total screen blockage can occur due to the transport of unencapsulated fibrous insulation. Since the sump screen area is small (108 ft <sup>2</sup> ), the calculated pressure drop (6.3 psi) is excessive. Further investigation is necessary to confirm the fibrous bed pressure drop correlation employed.
Arkansas Unit 2 (CE)	Reactor coolant piping, reactor vessel bottom head of steam generator, and pressurizer use reflective metallic insulation. Feedwater pressurizer safety relief valve, and balance of steam generator blowdown use totally encapsulated calcium silicate or expanded perlite molded block insulation. Main steam piping uses calcium silicate or expanded perlite block with stainless steel jacketing. Chilled water piping uses fiberglass with stainless steel jacketing.	Outside the reactor coolant system shield wall below basement floor.	Total debris is large (76,800 Ft <sup>2</sup> ) but is incapable of either migrating to the sump (reflective metallic) or being drawn into the screens (calcium silicate). Extensive blockage of the inboard screens occurs but outboard screens are more than adequate to pass the required flow without introducing excessive head losses.



TABLE 3.5 (Continued)

Plant and Reactor Manufacturer	Type of Insulation Utilized	Location of Emergency Sump	Final Assessment of Migration Potential of Debris Generated as a Result of a Pipe Break
Salem Unit 1 (W) (Westinghouse)	Reactor vessel, primary coolant piping, pressurizer, reactor coolant pumps, and bottom part of steam generator use reflective metallic insulation. Upper part of steam generator uses semi-encapsulated cerablanket insulation. Main steam, feedwater, residual heat removal, safety injection, and chemical and volume control system piping use totally encapsulated cerablanket. Service water and component cooling-water piping use antisweat insulation.	Outside the reactor coolant system shield wall below basement floor. Water drains into emergency sump through trenches in the floor in addition to directly from annular space outside of shield wall.	Postulated breaks resulted in large quantities of debris. Calculations indicate total screen blockage to occur. Calculations showed that large quantities of debris would be generated by postulated breaks. They further showed the potential for total screen blockage. However, this plant design has large debris intercept areas, in addition to the local sump screen. This, when coupled with the low recirculation velocities within containment, results in a low blocked screen $\Delta P$ which does result in insufficient NPSH.
Sequoyah Unit 2 (W)	All piping and equipment within the shielded crane wall area use reflective metallic insulation.	Inside the crane shield wall below containment floor.	While a large percentage of the sump intake area was blocked (approximately 74%), the remaining screen area is capable of passing the required recirculation flow without excessive head loss. Pump NPSH requirements are not impaired.
Prairie Island Unit 1 (W)	Mirror insulation is used on reactor vessel, steam generator, reactor coolant pump, pressurizer, excess letdown heat exchanger, regenerative heat exchanger, surge line, high pressure safety injection loop, primary coolant piping, steam generator blowdown lines, pressurizer spray piping, chemical and volume control piping, accumulator, low pressure safety injection, feedwater, main steam, auxiliary feedwater, residual heat removal, steam generator supports. Fiberglass insulation is used on main steam and feedwater hangers and restraints.	Outside reactor coolant shield wall, below basement floor.	The quantity of insulation debris generated is large ( $>3000 \text{ Ft}^2$ ) but is unable to migrate to the sump since reflective metallic is extensively employed. The quantity of fibrous insulation generated is not sufficient to block a sump intake area large enough to cause excessive pressure drop.

TABLE 3.6

Summary of Findings

Plant	Break	Debris* Generated	Debris* At Sump	Total* Sump Screen Area	Blocked* Sump Screen Area	Percent Blockage	Note
Salem Unit 1	Hot Leg	2692	1197	1078**	1078**	100	1
	Cold Leg	4737	2290	1078**	1078**	100	1
	Main Steam	----	0	1078**	0	0	2
	Feedwater	----	0	1078**	0	0	2
Arkansas Unit 2	Main Steam	7161	6517	287	95	33	3
	Feedwater 1	278	0	287	189	66	4
	Feedwater 2	97	---	---	---	---	5
Maine Yankee	Main Steam	3314	---	108	---	---	6
	Hot Leg 1	1071	---	108	---	---	6
	Hot Leg 2	1642	---	108	---	---	6
	Crossover 1	1642	---	108	---	---	6
	Crossover 2	1596	394	108	108	100	7
	Cold Leg	431	---	108	---	---	6
	Emerg. Feed.	215	---	108	---	---	6
Sequoyah Unit 2	Feedwater	248	15	41	15	37	8
	Hot Leg	2840	27	41	27	66	9
	Coolant Pump	1009	15	41	15	37	8
	Hot Leg	2840	27	41	27	66	9
	S.G. No. 4	528	20	41	20	49	9
	S.G. No. 1	3257	15	41	15	37	8
	Loop Closure	5632	15	41	15	37	8
Prairie Island Unit 1	Main Steam	4316	39	60	39	65	8
	Feedwater	1299	0	60	0	0	10
	Hot Leg	4131	39	60	39	65	8
	Cold Leg	1221	0	60	0	0	10
	Crossover	5009	39	60	39	65	8

\*Units of ft<sup>2</sup>

\*\*Total debris intercept area available in this plant to accept LOCA-generated debris.  
The sump screen area at the sum is 68 ft<sup>2</sup>.

NOTES:

1. As insulation is fibrous, uniform deposition is assumed (i.e., 100% of sump screens are blocked). Pressure drop is insufficient to adversely affect NPSH.
2. No debris reaches the sump region due to gratings as shown in Figure A-24.
3. Entire inboard screen blocked; outboard screen has sufficient unblocked area.
4. Entire outboard screen blocked; inboard screen has sufficient unblocked area.
5. Scoping analysis -- Feedwater 1 was more severe.
6. These cases are parts of a scoping analysis. Cold leg failure was most limiting.
7. Screen blockage is calculated to be total. Calculated pressure drop across fibrous debris bed is sufficient to offset any available NPSH margin, subject to assumption of total sump screen blockage with no credit for debris capture in transport.
8. Blockage acceptable from pressure drop standpoint.
9. Blockage as percentage of screen area is high, but pressure drop is acceptable.
10. Insulation does not reach sump.

panel was subjected for a period of five minutes to an impact from a two inch diameter, incompressible water jet at a constant stagnation pressure,  $P_0$ . In Reference 6 the recommended value of stagnation pressure for fibrous insulation panel failure was 20 psig. Additional experimental details are given in Reference 6.

Analytical studies (References 18, 19, and 24) of two-phase jets suggest that the extrapolation of results obtained from single-phase incompressible fluid studies to two-phase LOCA (loss-of coolant accident) conditions may not be conservative. This stems from: (1) a potentially important mechanism for debris generation by a LOCA jet may be stress to covering fibers resulting from fluid flow tangential to the insulation surface at high velocities and (2) the potential for the area affected by two-phase jet expansion to extend to an angle greater than  $90^\circ$  ( $90^\circ$  is assumed in the analytical treatment provided herein). Further discussion is provided in Appendix C.

#### Buoyancy, Transport, and Head loss of Fibrous Insulations

Buoyancy, transport, and head loss experiments were conducted with three types of as-fabricated and fragmented fibrous insulations the three types of as-fabricated insulation panels were:

- Type 1: 4" mineral wool or refractory mineral fiber core mineral (6 lb. density) covered with Uniroyal #6555 asbestos cloth coated with 1/2 mil. Mylar.
- Type 2: 4" Burlglass 1200, or 4 layers of 1" thick Filomat D (fiberglass) core material, inner covering of knitted stainless steel mesh, outer covering of Alpha Maritex silicone aluminum cloth, product #2619.
- Type 3: Same insulation core materials as Type 2. Inner and outer covering of 18 ounce Alpha Maritex cloth, product #7371.

The Buoyancy Tests revealed that:

- a) In general, the time needed for both mineral wool and fiberglass insulation to sink was found to be less at higher water temperatures.
- b) Mineral wool does not readily absorb water and can remain afloat for several days.
- c) Fiberglass insulation readily absorbs water, particularly hot water, and sinks rapidly (from 20 seconds to 30 seconds in  $120^\circ\text{F}$  water).
- d) Undamaged fiberglass pillows of type 3 (and possibly also of type 2) can trap air inside their covers and remain afloat for several days.



- e) Based on the observed sinking rates, it may be concluded that mineral wool pillows and some undamaged fiberglass pillows (those that trap air inside their cover) will remain afloat after activation of the containment recirculation system (approximately twenty minutes after beginning of LOCA). Those floating pillows will be readily transported to the sink before activation of the recirculation system and will move only if the water velocity exceeds the reported incipient transport velocities.
- f) The reflective metallic insulation sample tested sank immediately and the closed cell (foam glass) insulation sample floated indefinitely.

The Transportation Tests revealed that:

- a) Water velocities needed to initiate the motion of insulation are on the order of 0.2 ft/sec for individual shreds, 0.5 to 0.7 ft/sec for individual small pieces (up to 4 inches on the side), and 0.9 to 1.5 ft/sec for individual large pieces (up to 2 ft on the side).
- b) Whole sunken pillows require flow velocities of 1.1 ft/sec for type 1 (mineral wool) and 1.6 to 2.4 ft/sec for type 2 and 3 (fiberglass) to flip vertically on to the screen.
- c) Whole floating pillows require a water velocity in excess of 2.3 ft/sec to flip vertically against the screen.
- d) Insulation pillows broken up in finite size sunken fragments tend to congregate near the bottom of the screen if there is no turbulence generator, and depending on the water depth, unblocked space can remain near the top of the screens. With turbulence generators (vertical posts 2 ft upstream of the screen), some insulation fragments get lifted from the bottom and collect higher on the screen.
- e) Insulation shreds, once in motion, tend to become suspended in the water column and collect over the entire screen area.
- f) The reflective metallic insulation sample tested required a flow velocity of 2.6 ft/sec to start and keep moving.

The Head Loss tests revealed that:

- a) The measured head loss across a vertical screen in a flume due to blockage by insulation released upstream varies from 7 to 10 times the approach velocity head,  $V^2/2g$ , for whole sunken pillows, from 13 to 36 times the approach velocity head for opened or broken up pillows and in excess of 240 times the approach velocity head for shredded pillows. These results correspond to a 50% screen blockage with the undamaged pillows. Opened pillows with separated,



fragmented or shredded insulation layers, however, have enough area to block the entire screen. The screen was entirely (but not uniformly) covered only in the test with the shredded insulation. In the other tests, open space remained on the screen.

For these conditions, the maximum measured head loss of 240 times the approach velocity head (for shredded pillows) would give screen head losses of 0.15 ft to 0.60 ft for approach velocities of 0.2 ft/sec to 0.4 ft/sec.

- b) Measured head losses through beds of accumulated fragments or shreds of mineral wool or fiberglass insulation were observed to vary nonlinearly with approach velocity and bed thickness.

For mineral wool fragments the larger head losses were observed for the larger fragments tested (3 x 2 to 4 x 1/8 inch). For an insulation thickness of 1 inch, the maximum head loss was 0.4 ft at 0.2 ft/sec and 1.4 ft at 0.4 ft/sec.

For fiberglass insulation fragments and shreds, the larger head losses were observed for the shreds. For an insulation thickness of 1 inch, the maximum head loss was 1.2 ft at 0.2 ft/sec and 6 ft at 0.4 ft/sec.

- c) The head loss through as-fabricated insulation material is higher, by a factor of up to 10, than that for accumulated fragments. For example, with water at 105 to 120°F and an approach velocity of 0.2 ft/sec, the head loss through 2 inches of undisturbed mineral wool is about 3.5 ft and the head loss through 1 inch of undisturbed fiberglass is about 20 ft. These head losses are for insulation samples sealed to the walls and the head loss would be less if leakage occurred around the sample.
- d) In addition to the variables of insulation thickness and approach flow velocity, the actual head loss which may be expected across a sump screen is seen to depend critically on the manner of screen blockage. If some unblocked screen area remains, or if water can flow between pieces of insulation, the head loss would be small, whereas, if the entire screen area is uniformly covered with mats of undisturbed insulation or accumulated fibers, the head loss can be many feet.
- e) Best-fit expressions for the head loss through fibrous insulation were derived and reported in Reference 7.

### 3.4 Sump Hydraulic Performance

To investigate the behavior of ECCS sumps under flow conditions that might occur during a LOCA, a test program was designed to cover a broad range of geometric features and flow variables representative of containment emergency sump designs.

Because some of the hydraulic phenomena of concern, particularly air ingestion, could involve scale effects if tested at reduced scale, a full-scale experimental facility was used. Three broad areas of interest for ECCS sump design were investigated:

- Fundamental behavior of the sump with reasonably uniform approach flow conditions
- Changes in the fundamental behavior of the sump as a result of potential accident conditions -- screen blockage, break and drain flow, obstructions, nonuniform approach flow, etc., -- that could cause degraded performance in the recirculation system
- Design and operational items of special concern in ECCS sumps.

The test program was designed to allow information from initial tests to be used to plan or redirect later tests; hence, the tests were not necessarily conducted in the order listed below. Although the experimental program was modified, and tests were added on several occasions, tests used in the investigation may be divided into 7 series:

Factorial Tests -- A fractional factorial matrix of tests was used to study primary sump flow and geometric variables. The factorial matrix provided a wide range of parameter variations and a method for effectively testing a large number of variables and determining their interdependencies.

Secondary Geometric Variable Sensitivity Tests -- The effects on sump performance of secondary geometric variables and design parameters of special concern in ECCS sumps were tested by holding all sump variables constant except one, for which several values were tested.

Severe Flow Perturbations Tests -- The behaviors of selected sump geometries subjected to approach flow perturbations were investigated. Major flow disturbances considered were screen blockage (up to 75 percent), nonuniform approach velocity distribution, break-flow and drain-flow impingement, start-up transients, and obstructions as illustrated in Figures 3.9 and 3.10.

Vortex Suppression Tests -- The effectiveness of several types of vortex suppressors and inlet configurations were evaluated.

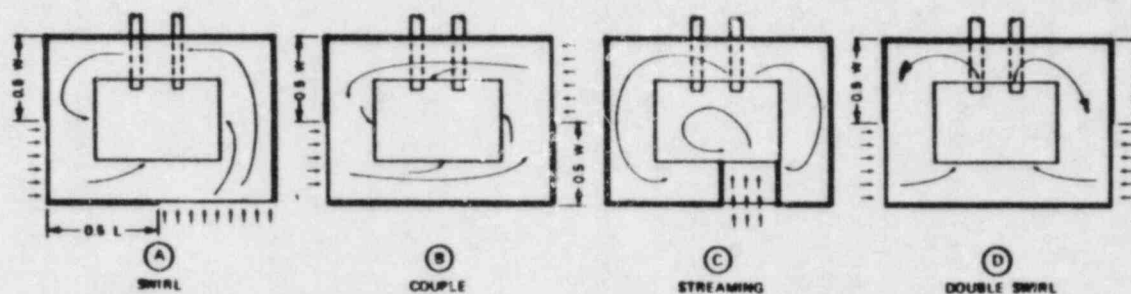
Scale Tests -- Scaling effects in geometrically scaled models using Froude number similitude and pipe velocity similitude were tested.

Boiling Water Reactor (BWR) Suction Pipe Inlet Tests -- The hydraulic performance of BWR suction pipe geometries typical of Mark I, II, and III designs was evaluated.

# **NON-UNIFORM FLOW AND SCREEN BLOCKAGE SCHEMES**

**NON-UNIFORM FLOW  
(FLOW DISTRIBUTOR BLOCKAGE)**

W = 30 FT  
L = 60 FT



**\*SCREEN BLOCKAGE**

W = SUMP WIDTH  
L = SUMP LENGTH

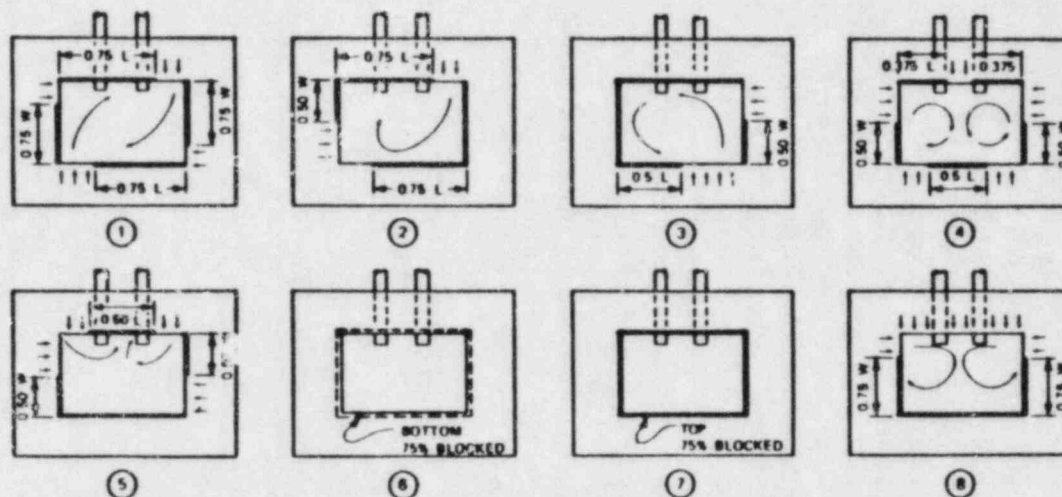


Figure 3.9. Approach Flow Perturbations and Screen Blockage Schemes.

Data resulting from the sump performance studies were analyzed using two approaches: (1) functional correlations of the dependent variables in which the correlations were the result of response-surface regression analysis or nondimensional empirical data fitting, and (2) bounding envelope analyses in which boundary curves indicate the maximum response of the data for each of the hydraulic performance parameters as a function of the sump flow variables (the Froude number in particular). Due to the extremely small values of the dependent variables and to the complex time-varying nature of the three-dimensional flows in the sump, the functional correlations approach showed no consistent, generally applicable, correlation between the dependent and independent variables; hence, the hydraulic performance of a particular sump under given flow and submergence conditions could not be reliably predicted using this approach. However, the broad data base resulting from the sump studies made possible the use of envelope analyses for reliably predicting the expected upper-bound for the hydraulic performance (void fraction, vortex type, swirl angle, and inlet loss coefficient) of any given sump whose essential features fall approximately within the flow and geometric ranges tested.

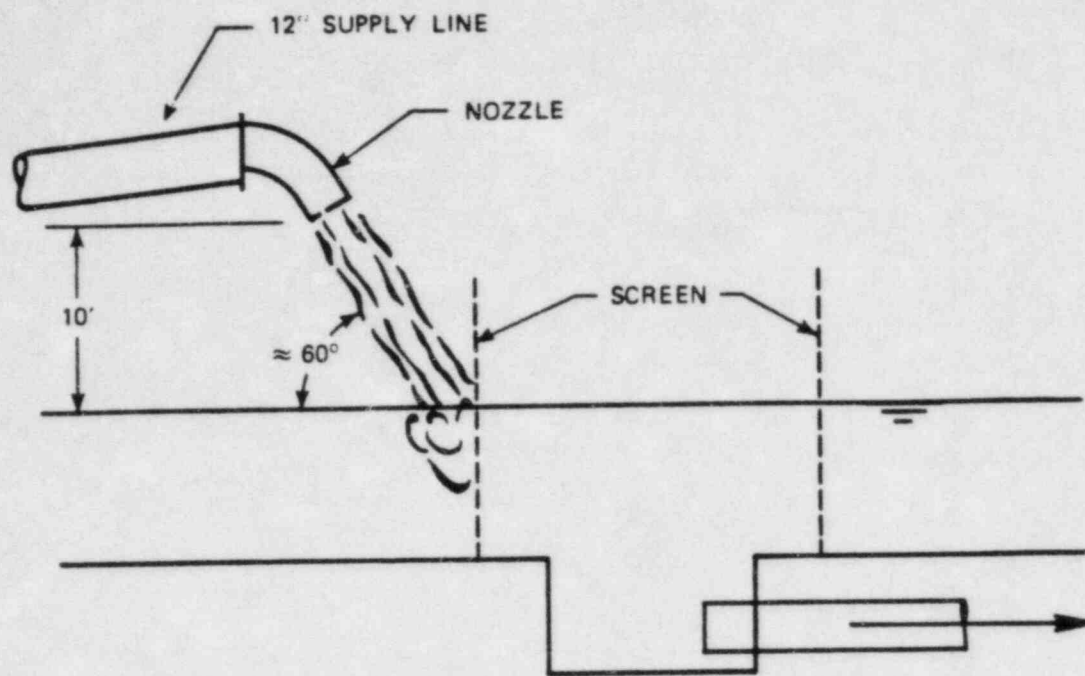
The ability to describe the performance of ECCS sumps, with or without flow perturbations, using bounding envelope curves is the most significant result of the test program. The application of an envelope analysis to test data resulting from all the sump performance tests is discussed in the following subsection of this report. Findings of the sump performance tests are described in greater detail in subsequent sections.

#### 3.4.1 Envelope Analysis

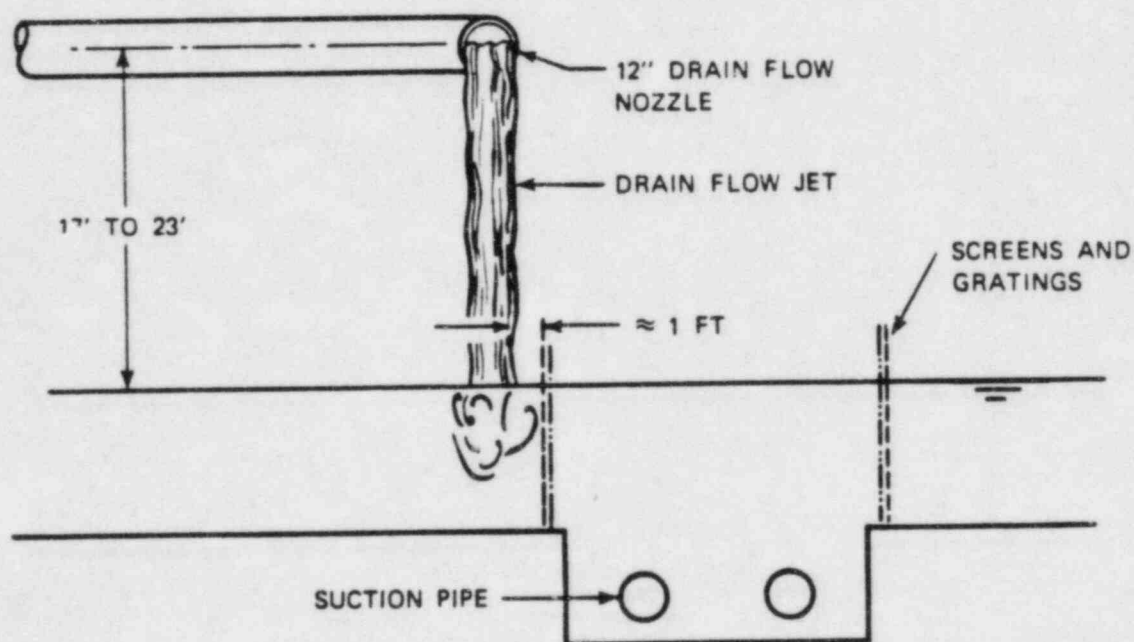
The sump performance test program generated a data base covering a broad range of ECCS geometric variables, flow conditions (including potential accident conditions), and design options (horizontal or vertical inlets, single or dual pipes, etc.). An envelope analysis applied to this broad range of data resulted in boundary curves that describe the maximum expected air ingestion, surface vortex activity, swirl, and sump head loss as a function of key sump flow variables (Froude number, velocity, etc.).

Figures 3.11, 3.12, and 3.13 show typical envelope analysis curves for air ingestion, surface vortex activity, and swirl in sumps with dual, horizontal outlets. Figures 3.14, 3.15, and 3.16 show typical envelope analysis curves for air ingestion, surface vortex activity, and swirl in sumps with dual, vertical outlets.





a. Break Flow Jet Impingement



b. Drain Flow Jet Impingement

Figure 3.10. Break and Drain Flow Impingement.

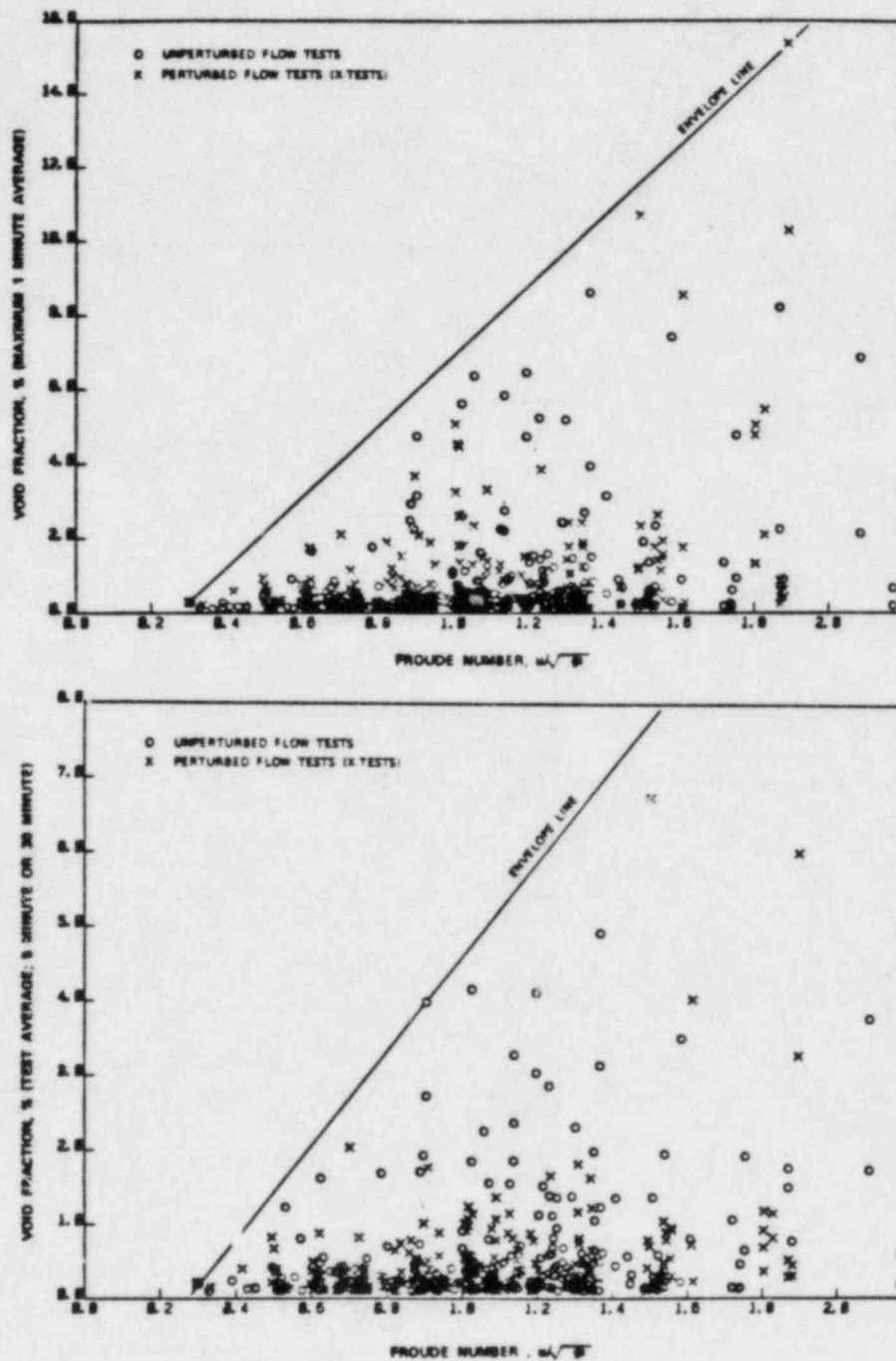


Figure 3.11. Void Fraction (% by Volume) as a Function of Froude Number; Horizontal Outlet Configuration. Only data points indicating nonzero void fraction are plotted.

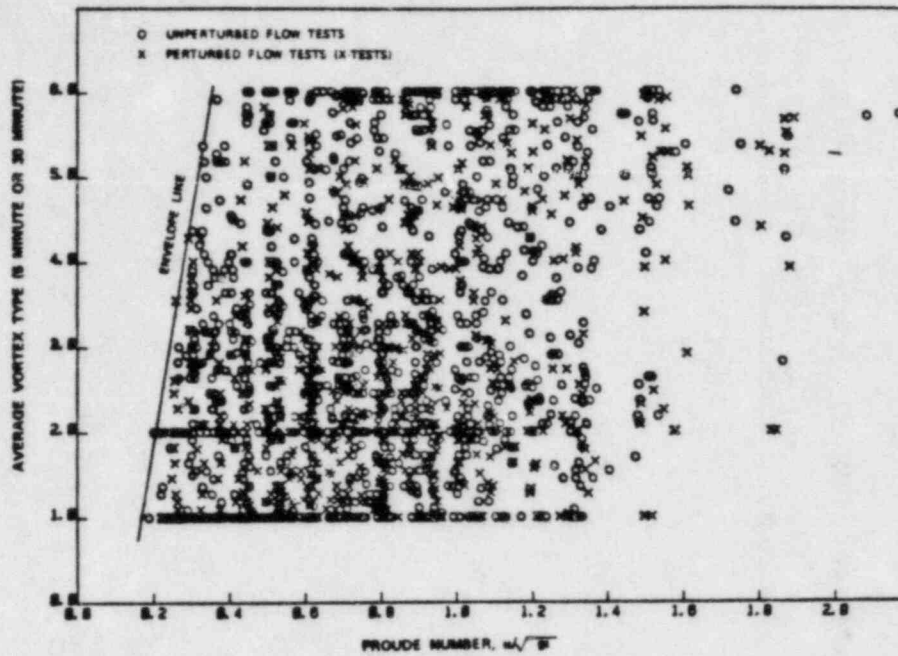


Figure 3.12. Surface Vortex Type as a Function of Froude Number; Horizontal Outlet Configuration.

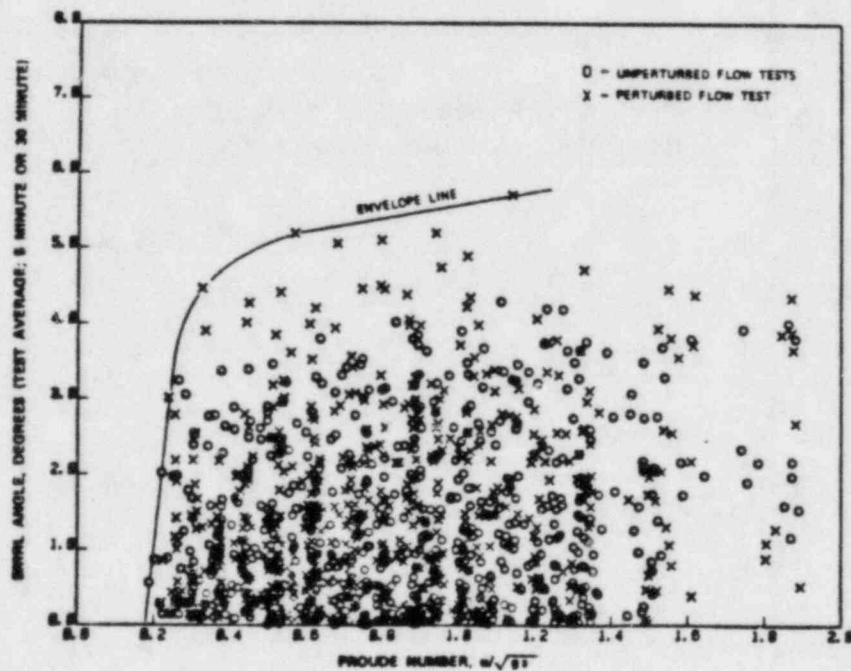


Figure 3.13. Swirl as a Function Froude Number; Horizontal Outlet Configuration.

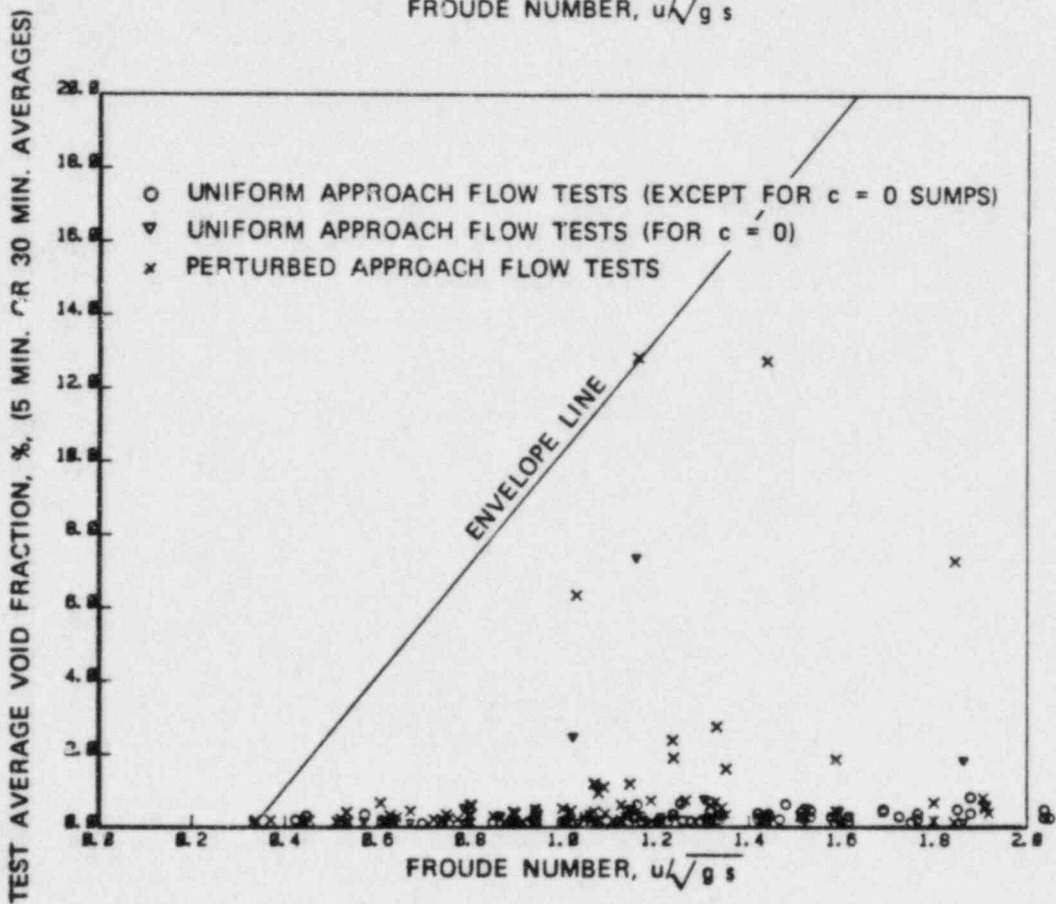
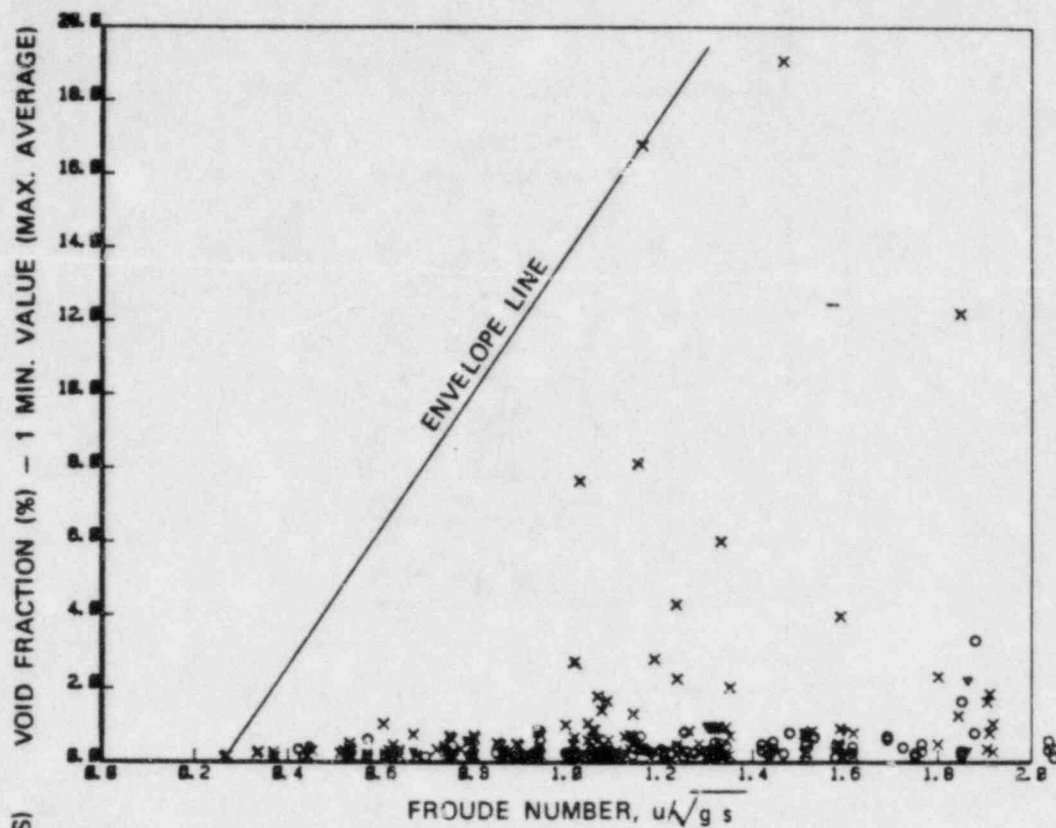


Figure 3.14. Void Fraction Data for Various Froude Numbers; Vertical Outlet Configuration. Only data for nonzero void fraction plotted.



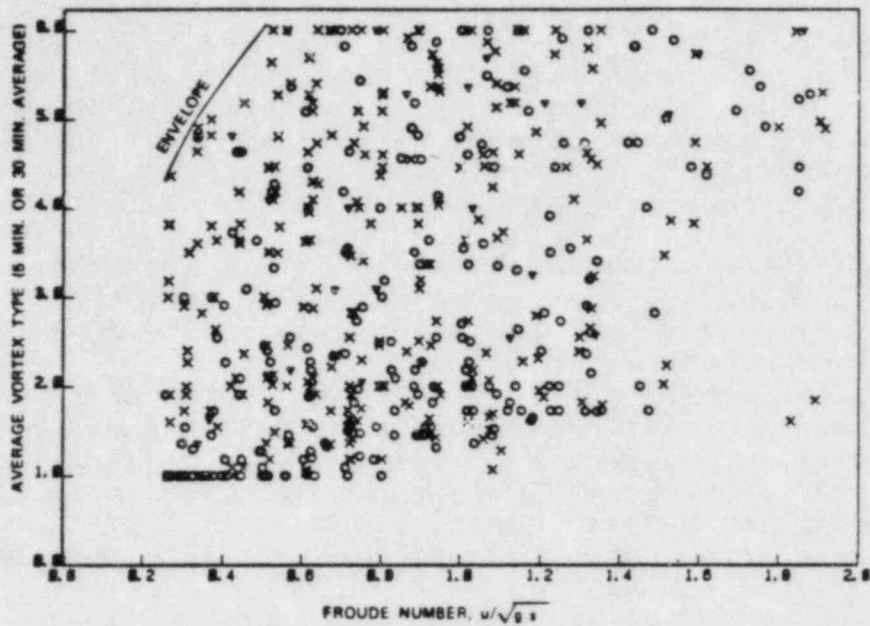


Figure 3.15. Surface Vortex Type as a Function of Froude number; Vertical Outlet Configuration.

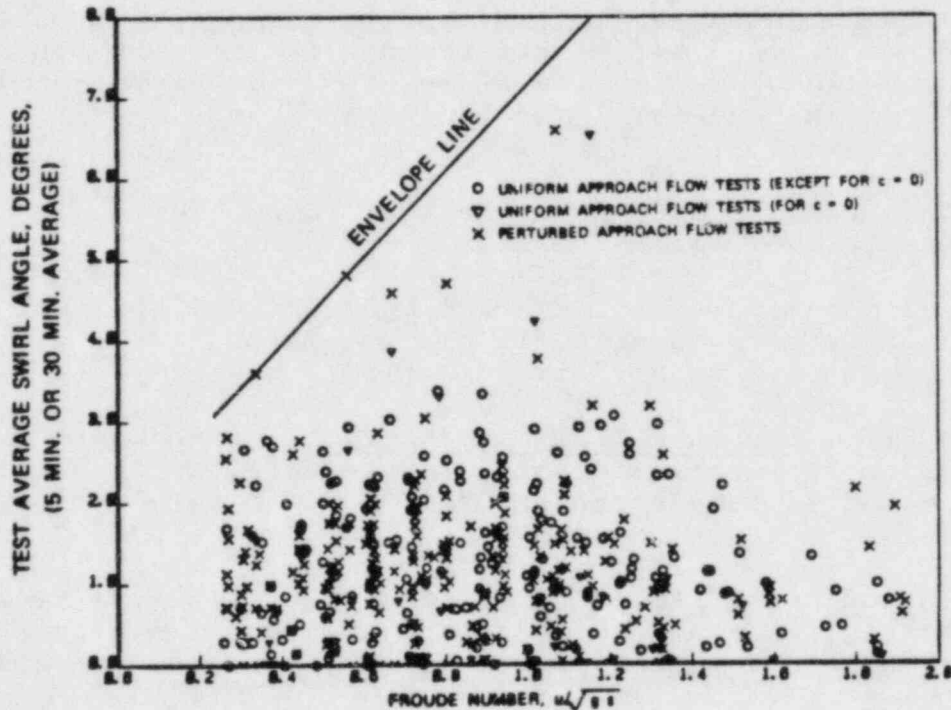


Figure 3.16. Swirl as a Function of Froude Number; Vertical Outlet Configuration.

### 3.4.2 General Sump Performance (All Tests)

Free Surface Vortices -- Vortex size and type resulting from a given geometric flow condition are difficult to predict and are not reliable indicators of sump performance. Performance parameters -- void fraction, pressure loss coefficient, and swirl angle -- are not well correlated with observed vortex formations.

Air Ingestion -- Measured levels of air ingestion, even with air core vortices, were generally less than 2 percent. Maximum values of air ingestion with deliberately induced swirl and blockage conditions were less than 7 percent for horizontal inlets and 12 percent for vertical inlets; these high levels always occurred for high flow and low submergence ( $F$  generally greater than 1.0). For submergences of 8 feet or higher, none of the configurations tested indicated air-drawing vortices ingesting more than 1 percent over the entire flow range even with severe flow perturbations.

Swirl (measured 14 diameters from suction inlet) -- Flow swirl within the intake pipes, with or without flow perturbations, was very low. In almost all cases, the swirl angle was less than  $4^\circ$ , an acceptable value for RHR and CSS pumps. The maximum value for severely perturbed flows was about  $8^\circ$  and occurred during the screen blockage test series.

Sump Head Losses -- Suction pipe intake pressure loss coefficient for most of the tests, with and without flow perturbations, was in the range of  $0.8 \pm 0.2$  and agreed with recommended hydraulic handbook values.

### 3.4.3. Sump Performance During Accident Conditions (Perturbed Flow)

Screen Blockage -- Screen blockages up to 75 percent of the sump screen resulted in air ingestion levels similar to those noted under "Air Ingestion" above.

Nonuniform Approach Flow Distributions -- Nonuniform approach flows, particularly streaming flow, generally increased surface vortexing and the associated void fraction.

Drain and Break Flow -- Drain and breakflow effects were generally found not to cause any additional air-ingestion. They reduced vortexing severities by surface wave action.

Obstructions -- Obstructions ( $\phi$  2 ft or less in cross-section) had no influence on vortexing, air withdrawals, swirl, or inlet losses.

Transients -- Under transient, start-up conditions, momentary vortices were strong, but no air-core vortices giving withdrawals exceeding 5 percent void fraction (1 minute average) were observed.

#### 3.4.4 Geometric and Design Effects (Unperturbed Flow Tests)

In general, no consistent trends applicable for the entire range of tests were observed in the data between the hydraulic response of the sump (air withdrawal, swirl, etc.) and secondary geometric parameters. However, for some ranges of flow and submergences, the following observations are applicable:

- Greater depth from containment floor to the pipe center-line reduces surface vortexing and swirl.
- Lower approach flow depths with higher approach velocities may cause increased turbulence levels serving to dissipate surface vortexing.
- There is no advantage in extending the suction pipe beyond 1 pipe diameter from the wall.
- Suction pipe inlets located with less distance to the sump wall and greater pipe spacing reduces vortexing and swirl.

#### 3.4.5 Design or Operational Items of Special Concern in ECCS Sumps

Vertical Outlets -- Comparison of vertical outlet data to corresponding horizontal outlet data showed some, but no major differences, in hydraulic performance of vertical outlet sumps and horizontal outlet sumps of the same geometry and flow conditions: average vortex types agreed within  $\pm 1$ ; air withdrawals were somewhat higher for vertical outlet sumps, usually within 1 percent (30 minute averages) and 4 percent (1 and 5 minute averages); swirl angles differed only within  $\pm 1$  degree. As in the case with horizontal outlets where sump performance was best with pipe projections close to the wall, vertical pipe outlets with perturbations performed best when placed close to the wall rather than at the center of the sump.

Cover Plate -- A solid top cover plate over the sump was effective in suppressing vortices as long as the cover plate was submerged and proper venting of air from underneath was provided. No air-drawing vortices were observed for the submerged cover plate tests, and no significant changes in swirl or loss coefficients occurred.

Elevated Water Temperature --Changing water temperature over the range from 40°F to 167°F had no significant effect on horizontal outlet sump performance parameters.

### Vortex Suppressors

Cage shaped vortex suppressors made of floor grating to form cubes 3 and 4 ft on a side, and single layer horizontal floor grating over the entire sump area, were both found to be effective in suppressing vortices and reducing air-ingestion to zero. These suppressors were tested using 12-inch outlet pipes, and with the water levels ranging from 0.5 to 6.5 ft above the top of the suppressors. Adverse screen blockages were used in conjunction with sump configurations which produced considerable air-ingestion and strong vortexing without the suppressors; thus, suppressors' effectiveness were tested when hydraulic conditions were least desirable. The suppressors also reduced pipe swirl and did not cause any significant increase in inlet losses. Both the cage shaped grating suppressors as well as the horizontal floor grates were made of standard 1.5 inch floor grates.

Tests on a cage shaped suppressor less than 3 ft on a side indicated the existence of air-core vortices for certain ranges of flows and submergences, even though air-withdrawals were found reduced to insignificant levels.

Either properly sized cage shaped suppressors made of floor grating, or floor grating over the entire sump area, may therefore be used to reduce air-ingestion to zero in cases where the sump design and/or approach flow creates otherwise undesirable vortexing and air-ingestion.

### Single Outlets

Two sump configurations (4 ft x 4 ft and 7 ft x 5 ft in plan, both 4.5 ft deep; 12 inch outlets) were tested under unperturbed (uniform) and perturbed approach flows with screen blockages up to 75 percent of the screen area. For both the configurations, unperturbed flow tests indicated air-withdrawals were always less than 1 percent by volume for the entire range of tested flows and submergences ( $F = 0.3$  to  $1.6$ ). Even with perturbed flows, zero or near zero air-withdrawals were measured in both sumps for Froude numbers less than 0.8, suggesting insignificant vortexing problems. For Froude numbers above 0.8, a few tests indicated significantly high air-withdrawal (up to 17.4 percent air by volume; 1 minute average) especially for the smaller sized sump. Measured swirl values in the pipes were insignificant for both the tested sumps, being in the range of 2 to 3 degrees even with flow perturbations. The inlet loss coefficients for both sump configurations were in the expected ranges for such protruding outlets,  $0.8 \pm 0.2$ .



### Dual-Outlet Sumps With Solid Partition Walls

Four dual-outlet sump configurations (one 20 ft x 10 ft sump with 24 inch diameter outlets and three 8 ft x 10 ft sumps with 24 inch, 12 inch and 6 inch outlets, respectively) were tested with solid partition walls in the sumps between the pipe outlets and with only one outlet operational. None of the tests indicated any significant increases in vortexing, air-withdrawals, swirl, or inlet losses compared to dual pipe operation without partition walls. Thus, providing a partition wall in a sump should not cause any additional problems when only one pipe is operating.

### Bellmouths at Pipe Entrance

Limited tests on a sump configuration were conducted with and without a bellmouth attachment to the 12 inch outlets. Adding bellmouths at the pipe entrances did not show any significant changes in the vortex types, air-withdrawals, and pipe swirl compared to those which otherwise existed under the same hydraulic conditions. Up to about 40 percent reduction in inlet losses was noticed with the addition of a bellmouth.

### BWR Suction Pipe Inlets

The hydraulic performance of three representative BWR Residual Heat Removal System suction inlet configurations; namely, Mark I, Mark II, and Mark III designs, were investigated over a Froude number range of from about 0.2 to 1.1 under both unperturbed (uniform) and perturbed approach flow conditions. Zero air-withdrawal was measured for both configurations at Froude numbers equal to or less than 0.8 under all tests approach flows. At a Froude number above 0.8, under perturbed approach flows, the Mark I design (single inlet with conical strainer) allowed air-core vortices drawing up to 4 percent air by volume (1 minute average), while the Mark II and Mark III design (which had a "tee" inlet with conical strainers on each end) showed air-withdrawals only up to 0.5 percent by volume (1 minute average). Swirl levels in the pipe were found to be about 0 to 3 degrees for the Mark I design and 2 to 7 degrees for Mark II and Mark III design. The inlet loss coefficient, including entrance and strainer losses (and "tee losses," if applicable), was determined to be about 1.0 for Mark I design and 1.7 for Mark II and Mark III designs, expressed in terms of suction pipe velocity head.

### Scale Model Tests

To evaluate the use of reduced scale hydraulic models to determine the performance of containment emergency sumps and to investigate, in particular, possible scale effects in modeling the hydraulic phenomenon of concern, a test program involving

two reduced scale models (1:2 and 1:4) of a full size sump (1:1) was undertaken (Reference 22).

The test results show that the hydraulic models predicted the hydraulic performance of the full sized sump; namely, vortexing, air-ingestion from free surface vortices, pipe flow swirl, and the inlet loss coefficient. No scale effects on vortexing or air-withdrawals were apparent within the tested range for both models. However, an accurate prediction of pipe flow swirl and inlet loss coefficient was found to require that the approach flow Reynolds number and the pipe Reynolds number be above certain limits.

Based on these results, it is concluded that properly designed and operated reduced scale hydraulic models of geometric scales 1:4 or larger could be used to properly evaluate the hydraulic performance of a sump design. Evaluations of sump hydraulic model studies conducted in the past can be derived from this series of tests.

#### Pump Overspeed Tests

Two 8 x 10 x 4.5 ft sumps (one with horizontal outlets; one with vertical outlets) were tested at higher flow rates to simulate pump overspeed or run-out (to Froude number = 1.6) conditions. No strong air-core vortices were observed with air-withdrawals greater than 1 percent (1 min or 30 min averages).

Maximum recorded pipe swirl angle was  $0.9^\circ$  (at 14.5 pipe diameters from entrance); inlet loss coefficients averaged 0.8 (Reference 23).

#### 4.0 INDEPENDENT PROGRAM REVIEWS

Program reviews were conducted before and during key phases of the work reported in Chapter 3. These reviews were performed for the purpose of soliciting comments and technical concerns about the program's direction and goals from experts not connected with the implementation and execution of TAP A-43. The reviewers were selected from among the foremost authorities in each of the areas reviewed. Two reviews were held; they were

- sump hydraulic performance
- insulation debris calculational methods effects

##### 4.1 Sump Performance Review

The review consisted of two panel meetings.\* The primary purpose of the first meeting, held March 17, 1981, was to introduce in detail the program plan and initial test results. The second meeting, held June 4, 1981, was primarily for reviewer response and comment.† Additionally, at both meetings the reviewers were provided with preliminary program redirections, and were requested to comment on results to date and give an analysis of the proposed future program plan. Overall, the reviewers approved of the program, the experimental test plan, its conduct, and data analysis. They concluded that the program and its directions were appropriate for resolving the sump performance issues.

In direct response to reviewer comments, the temperature tests were performed immediately following the first 25 configurations, and, therefore, earlier in the program than originally planned.

---

\*Meetings were held on March 17, 1981, at Germantown, Maryland, and June 4, 1981, at Alden Research Laboratory of WPI, Holden, Massachusetts. Review attendees and their affiliations were as given below: P. Tullis/Utah State University; D. Simons/Simons, Li and Associates; R. Gardiner/Western Canada Hydraulic Laboratories; D. Canup/Duke Power Company; W. Butler/U.S. Nuclear Regulatory Commission; S. Vigander/Tennessee Valley Authority (TVA); J. Kennedy/University of Iowa; R. Letendre/Combustion Engineering, Inc. R. Letendre did not attend the meeting of June 4, 1981.

†Formal written response and comments were requested at the close of the second meeting. These responses are available through the Office of Light Water Safety Research, Department of Energy, Washington, DC.



Divergent opinions emerged during the review concerning the potential for pump performance degradation when the fluid temperature was near saturation. Some concerns were expressed regarding the possibility of degraded pump performance due to cavitation or the release of dissolved air into the water in the suction lines leading to the pumps. Other opinions suggested that pump performance should be satisfactory at coolant temperatures near saturation, because the solubility of air in water is low near saturation and, provided cavitation were not occurring in the pump, any voids would collapse due to the static pressure increase with depth in the sump. These collapsing bubbles would then form a turbulent environment and inhibit surface vortex activity. The pump issues raised by the reviewers, although not pertinent to the sump hydraulics program, are a part of USI A-43 and have been addressed and resolved (see Section 3.2).

The experimental research program did not examine the effects on sump systems of temperatures near saturation. Temperature effects were examined to the limits of the capacity of the experimental facility (about 165°F). However, up to that limit, no temperature effects on sump system performance were detected.

An area of general peer review group agreement was that sump system performance, with respect to air entrainment, could be improved in most sump configurations by the addition of a vortex suppression device(s). One reviewer, however, commented that such a device(s) might be removed during some phase of reactor operations and not be replaced. Such a possibility, in his judgment, was sufficient justification for an experimental research program that would allow the development of adequate sump design guidelines that were based upon justifiable physical criteria (in the absence of vortex suppressors). The results of the studies provided in Section 3.4 confirm the usefulness of vortex suppressors in the improvement of sump system performance and, further, provide hydraulic results for developing acceptable sump design guidelines.

The adequacy of recirculation sump pumps for performing reliably when air/water mixtures are present and the long-term cooling function required of the ECCS were matters of some concern to the review group. These concerns have been resolved by the development of sump design guidelines which take into account pump performance specifications.

#### 4.2 Insulation Debris Effects Review

The purpose of this review was to determine the adequacy of methods (described in Section 3.2 and in detail in Reference 5) to conservatively estimate quantities of insulation debris that might be produced in containment, its transport and its potential for sump screen blockage.



The review was conducted in two phases. In the initial phase, a draft report describing the methods was provided to peer panel and other reviewers\* to solicit their comments.

Reviewers provided highly useful criticisms and comments with recommendations for improvements in the physical basis and rigor of the development.

As a consequence of the reviews, the draft document was modified to accommodate the comments of the reviewers. The modified document was then transmitted to the reviewers who were then requested to prepare comments for a formal peer panel review, the second phase of the review process.

Formal peer panel review took place at NRC Headquarters on March 31, 1982. Panelists Kennedy and Canup were unable to attend the meeting. A number of attendees, in addition to peer panel members, participated in the review.<sup>†</sup> Questions that were raised during the meeting and their disposition are given below:

1. It was observed that under some circumstances, the amount of debris generated with the potential to migrate to the sump could be greater than that estimated in the draft report. It was resolved by determining that the report would require the selection of those pipe break locations and jet targets that would generate the maximum of potentially transportable debris without regard to initial blowdown and transport direction.
2. Questions were raised about a) the applicability of the jet model used in the debris generation portion of the report, b) the assumption of uniform distribution of debris across the face of the jet and, c) the use of a 0.5 psi stagnation pressure cut-off for debris generation. Resolution of 2.a)

---

\*Peer panel reviewers were: R. Gardiner/Western Canada Hydraulic Laboratories; D. Simons/Simons, Li & Associates, Inc.; D. Canup/Duke Power Company; R. Mango/Combustion Engineering, Inc.; P. Tullis/Utah State University; J. Kennedy/University of Iowa; W. Butler/U.S. Nuclear Regulatory Commission; and S. Vigander/Tennessee Valley Authority. Other reviewers included G. Weigand/Sandia and R. Bosnak, G. Mazetis, and T. Speis/U.S. Nuclear Regulatory Commission. Their written review comments are available through The Division of Safety Technology, U.S. Nuclear Regulatory Commission, Washington, DC.

<sup>†</sup>Other attendees were: S. Hanauer/NRC; K. Kniel/NRC; C. Liang/NRC; P. Norian/NRC; F. Orr/NRC; A. Serkiz/NRC; J. Shapaker/NRC; G. Hecker/Alden Research Laboratory; E. Gahan/Burns and Roe; J. Wysacki/Burns and Roe; W. Swift/Creare, Inc.; P. Strom/Sandia; and G. Weigand/Sandia.

was arrived at by agreement that a modified Moody jet model (Reference 17) would be allowed to model the jet. It was agreed that the stripping of all insulation from plant and piping within the crane wall and within the jet represented a conservative treatment of insulation debris generation.

Discussions on Item 2.b) concluded that a definite probability existed that debris distribution across the face of the jet would not be uniform. It was agreed that a distribution of debris across the jet face would be provided that would represent the geometric distribution of insulation targeted by the jet in the containment. In addition, because of uncertainties in jet transport to walls, it was agreed that the quantities of debris estimated to exit through crane wall openings would be doubled over those quantities which would have been calculated in the draft report.

The use of a 0.5 psi stagnation pressure cut-off (Item 2.c)), for insulation damage was questioned by a number of reviewers. Technical views were put forward by a Sandia staff member on the expected performance of jets under LOCA conditions. He stated that centerline stagnation pressures above 15 psig could be expected for at least five diameters downstream of high energy, high pressure breaks. An AEC report (The Effects of Atomic Weapons, G. Glasstone, ed.) was cited by Burns and Roe as the origin of the cut-off estimate for debris generation. Alden Research Laboratory reported on preliminary experiments at ARL that have shown that little insulation damage occurred to fibrous insulation assemblies up to 6.5 psi water jet pressures. It was agreed that the 0.5 psi stagnation pressure represented a conservative treatment for the onset of insulation debris generation. It was further agreed that the assumption that all insulation within the jet cone would be transformed to insulation debris was conservative. The last assumption was chosen to represent the volume within which insulation debris would be generated under the treatment provided in Reference 5. The results of work performed subsequently on the issues are provided in Section 5.3 of this report.

3. Discussions were held on the physical accuracy of the model in representing pipe whip, pipe impact, the direction of motion of dislodged insulation and its trajectory. It was first pointed out that the quantities of insulation generated by this mechanism would amount to 10 percent or less of that generated by jet forces. It was further pointed out that the treatment in the report was designed to conservatively scope the problem, as opposed to providing detailed descriptions of system dynamics. It was agreed that the use of the treatment in the report would conservatively estimate the quantities of insulation debris produced by a minor contributor to debris production and, as such, was satisfactory.

4. Questions were raised on the treatment of long term transport following blowdown. These questions related to:

- a) recirculation flow velocities within containment,
- b) hydraulic lift provided to sunken debris,
- c) drawdown of floating debris onto less than fully submerged sump screens (ice-jam effect) and,
- d) transport mechanisms of sunken debris, such as tumbling and sliding.

In the resolution of 4. a), agreement was reached to account for obstructions in flow paths and subsequent flow expansion.

Agreement was reached on Item 4. b) horizontally oriented if lift were to be approximated by drag for horizontal debris, zero for vertically oriented debris and disregarded for tumbling debris.

Item 4. c), was recognized as a potentially important mechanism for screen blockage. It will be treated by established methods available in the literature.

Tumbling and other transport mechanisms, as noted under Item 4. d), could significantly affect the movement of debris towards screens. Panelists agreed to treatments which they considered to be conservative in dealing with debris movement via these mechanisms.

5. Arguments were raised that a period of debris transport intermediate to short term transport and long term transport (as defined here) might exist. It was postulated that transport during such an interim period might seriously affect potential sump blockage. Inasmuch as the report assumes that all floating debris reaches the sump, such an interim migration period would not affect the consequences of such transport. With respect to debris of density equal to or greater than unity and its transport, discussions brought out that the likelihood of a significant effect during such an interim period would be minor, flow patterns would show no preferential transport toward the sump and entrainment would be higher in the recirculation mode than in the interim period.
6. An issue that failed to be resolved was the behavior of fibrous insulation in its migration toward a sump and the potential for blockage by such material. As an issue, this problem has been indicated to exist at only a few plants and is, consequently, plant specific. Nevertheless, it was an open issue at the time of the meetings. Following the meetings,



experimental studies were conducted at Alden Research Laboratory to estimate stagnation pressures required for the onset of debris generation for nonencapsulated mineral wool and fiberglass insulations (Reference 6), the transport characteristics of such debris and the pressure losses at sump screens caused by the accumulation of fibrous debris on screens (Reference 7). These findings are reflected in the findings provided in Section 5.3 of this report.

All panelists, excepting S. Vigander of TVA, concluded that the use of the methods discussed would result in conservative estimates of sump screen blockage. Vigander commented that while he was of the opinion that the treatment would yield conservative, perhaps ultra-conservative, results, he could not with certainty arrive at that conclusion. He suggested that uncertainty analyses be conducted to establish the levels of conservatism (if any) that are provided in the development. Other panelists agreed that quantitative or qualitative error analyses would be desirable, although the needs for such analyses were deemed not to be immediate or pressing.



## 5.0 SUMMARY OF SUMP PERFORMANCE TECHNICAL FINDINGS

### 5.1 General Overview

The containment emergency sump should be evaluated to determine design adequacy for providing a reliable water source to the ECCS and CSS pumps during a post-LOCA period. Both sump hydraulic performance under adverse conditions, and potential LOCA-induced insulation debris effects require adequate technical assessment to assure that long-term recirculation can be maintained. Typical technical considerations are shown in Figure 5.1. Each major area of concern--pump performance, sump hydraulics, and debris generation potential--can be assessed separately, but the combined effects of all three areas should then be assessed to determine the overall effect on the NPSH requirements of the pumps. The sections below summarize technical findings and provide concise data sets.

### 5.2 Sump Hydraulic Performance

Full scale tests show that adequate sump hydraulic performance is principally a function of depth of water (the submergence level of the suction pipe) and the rate of pumping (suction inlet water velocity). These variables can be combined to form a dimensionless quantity defined as the Froude number:

$$\text{Froude number} = V/\sqrt{gs}$$

where

- V = suction pipe mean velocity,
- s = submergence (water depth from surface to suction pipe centerline), and
- g = acceleration due to gravity.

The extent of air withdrawn from the sump by ingestion is the principal parameter to be determined. Small amounts of air (i.e.,  $\leq 2$  percent by volume) can significantly degrade pumping capacity (References 11, 12, and 13).

Section 3.4 summarizes the results of full scale hydraulic tests. Figures 3.11 and 3.14 show typical void fraction data as a function of Froude number. References 9, 20, 21, 22 and 24, provide more detailed results from the test program at ARL. Generally, sump design acceptability should be based upon  $\leq 2$  percent air ingestion to assure adequate pump performance.

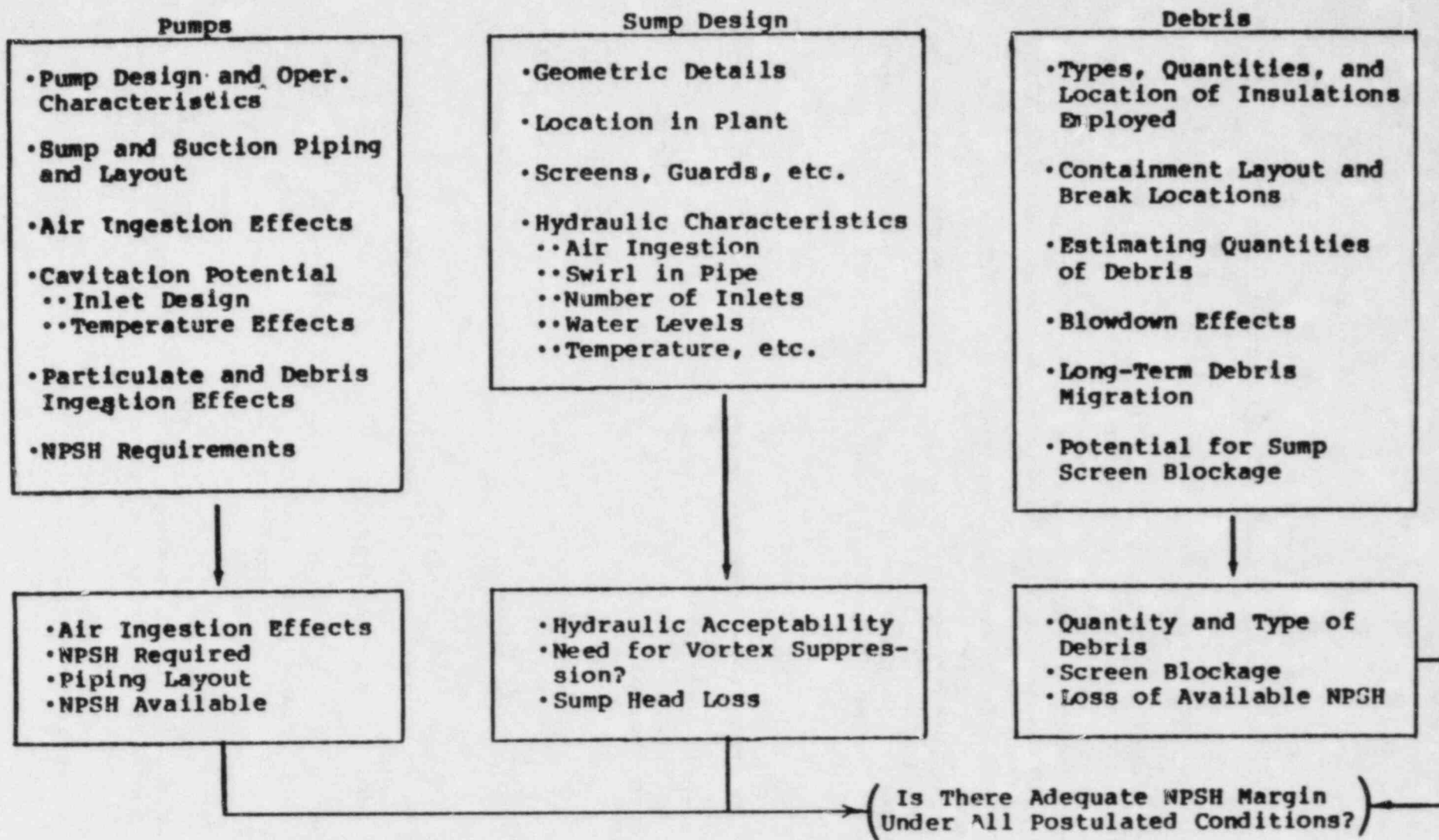


Figure 5.1. Technical Considerations Relevant to Containment Emergency Sump Performance

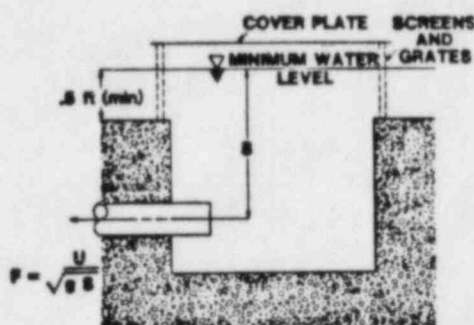
Sump hydraulic performance can, therefore, be assessed as follows:

1. Table 5.1 provides technical findings for sump designs where negligible (or zero) air ingestion would exist.
2. The adequacy of the sump geometric design and hydraulics performance based on air ingestion levels of  $< 2$  percent can be determined using Tables 5.2, 5.3, and 5.4.
3. Vortex suppressors provide a means to achieve zero air ingestion. Vortex suppression devices such as those shown in Table 5.6 have been shown to reduce air ingestion levels to essentially zero.
4. Table 5.5 provides additional information pertinent to screens and grates that would affect hydraulic performance.
5. Elevated water temperature has been shown to have negligible effect on sump hydraulic performance in full scale tests conducted at temperatures up to 165°F.

TABLE 5.1

Zero Air Ingestion  
Hydraulics Design Findings

Item	Horizontal Outlets	Vertical Outlets
Minimum Submergence, $s$ (ft)	10	10
Maximum Froude Number, $F$	0.25	0.25
Maximum Pipe Velocity, $U$ (ft/s)	4	4



Geometric Findings\*

Item	Horizontal Outlets**	Vertical Outlets**
Aspect Ratio	1 to 5	1 to 5
Minimum Perimeter	dual: 36 ft; single: 16 ft	dual: 36 ft; single: 16 ft
$(B-e_y)/d$	$\geq 3$	$\leq 1$
$c/d$	$\geq 1.5$	$\geq 0; \leq 1$
$e_y/d$	$\geq 0; \leq 1$	$\geq 1.5$
Minimum Screen Area	dual: 75 ft <sup>2</sup> ; single: 35 ft <sup>2</sup>	dual: 75 ft <sup>2</sup> ; single: 35 ft <sup>2</sup>

\*See Table 5.3 for definitions. The geometric findings were established using experimental results from References 9, 21, 22, and 23 and the variable ranges over which such data was taken.

\*\*dual = dual outlet design, single = single outlet design.



TABLE 5.2  
Hydraulics Design Findings

Item	Horizontal Outlets		Vertical Outlets	
	Dual	Single	Dual	Single
Minimum Submergence, $s$ (ft)	7.0	8.0	8.0	10
Maximum Froude Number, $F$	0.53	0.40	0.41	0.33
Maximum Pipe Velocity, $U$ (ft/s)	8.0	6.5	7.0	6.0
Maximum Screen Face Velocity (Blocked and minimum submergence) (ft/s)	3.0	3.0	3.0	3.0
Minimum Water Level (inside screens and grates)	Sufficient to cover 1.5 ft of open screen			
Maximum Approach Flow Velocity (ft/s)	0.36	0.36	0.36	0.36
Sump Loss Coefficient, $C_L$	1.2	1.2	1.2	1.2
<hr/>				
Air Withdrawal, $\alpha_s, \alpha_o$	-2.47	-4.75	-4.75	-9.35
$\alpha_s = \alpha_o + \alpha_1 \times F$ (% air by Volume)	$\alpha_1$	9.38	18.04	18.69
		35.95		

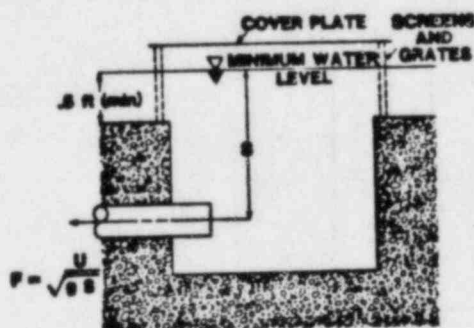


TABLE 5.3

## Geometric Design Envelope Findings

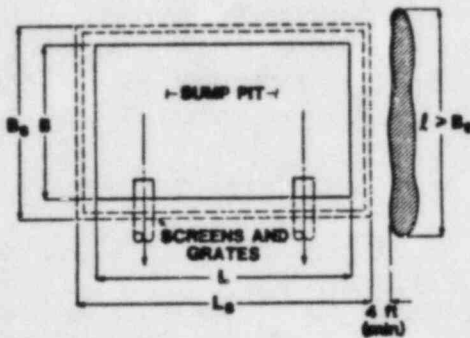
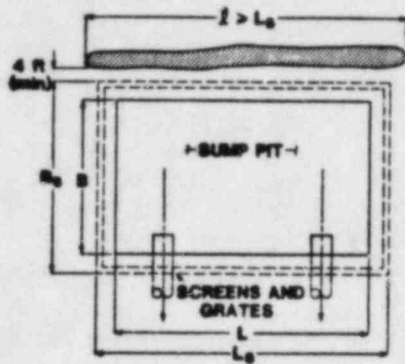
		Size and Placement		Inlet Position**						Screens & Grates
		Aspect Ratio	Min. Perimeter	$e_y/d$	$(B-e_y)/d$	$c/d$	$b/d$	$f/d$	$e_x/d$	Min. Screen Area (Plane face)
Horizontal Outlets	Dual	1 to 5	36 ft	$\geq 0$	$\geq 3$	$\geq 1.5$	$\geq 1$	$\geq 4$	1.5* or	75 ft <sup>2</sup>
	Single	1 to 5	16 ft	$\leq 1$				-	$> 1.5$	35 ft <sup>2</sup>
Vertical Outlets	Dual	1 to 5	36 ft	1.5* or	$\leq 1$	$\geq 0$	$\geq 1$	$\geq 4$	1.5* or	75 ft <sup>2</sup>
	Single	1 to 5	16 ft	$> 1.5$		$\leq 1$		-	$> 1.5$	35 ft <sup>2</sup>
Definitions		<p>ASPECT RATIO, <math>AR = L/B</math> MINIMUM PERIMETER, <math>P_{min} = 2(L + B)</math></p>								

\*\*Preferred location.

\*Dimensions are always measured to pipe centerline.

TABLE 5.4

Additional Considerations Related  
To Sump Size and Placement\*



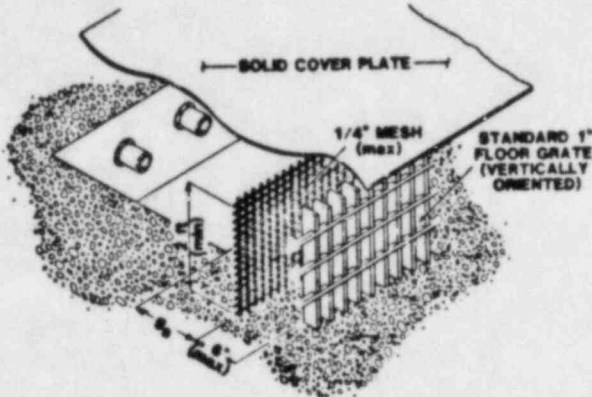
1. Aspect Ratio, see Table 5.1.
2. Minimum Sump Perimeter, see Table 5.1.
3. Sump clearance of 4 ft between the screens/grates and any wall or obstruction of length  $l$  equal to or greater than the adjacent screen/grates length ( $B_s$  or  $L_s$ ).
4. A solid wall or large obstruction may form the boundary of the sump on one side only, i.e., the sump must have three (3) sides open to the approach flow.

\*These additional considerations are provided to ensure that the experimental data boundaries (upon which Tables 5.2 and 5.3 are based) resulting from the experimental studies at Alden Research Laboratory are noted.

TABLE 5.5

Screen, Grate, and Cover Plate Design Findings\*

1. Minimum plane face screen area, see Table 5.2.
2. Minimum height of open screen should be 2 feet.



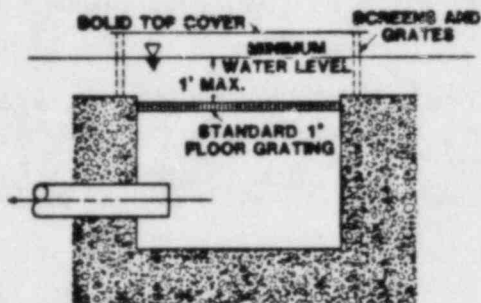
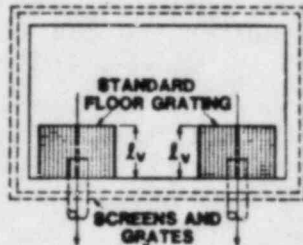
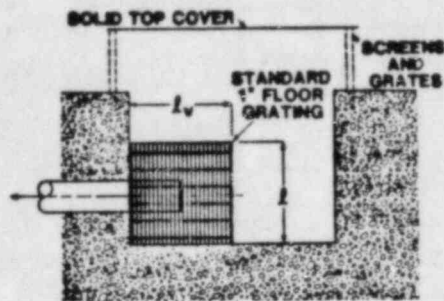
3. Distance from sump side to screens,  $g_s$ ;  $g_s$  may be any reasonable value.
4. Screens should be 1/4 inch mesh or finer.
5. Gratings should be vertically oriented 1 to 1-1/2 inch standard floor grate or equivalent.
6. The distance between the screens and grates shall be 6 inches or less.

7. A solid cover plate above the sump and extending to the screens and grates is required; the cover plate must be designed to ensure the release of air trapped below the plate (a cover plate located below the minimum water level is preferable).

\*These additional details are pertinent to the Alden Research Laboratory's full scale tests and were found to yield satisfactory sump hydraulic performance.



TABLE 5.6

Findings For Selected Vortex Suppression Devices\*

1. Cubic arrangement of standard 1-1/2 inch or deeper floor grating (or its equivalent) with a characteristic length,  $l_v$ , that is  $\geq 3$  pipe diameters; the top of the cube must be submerged a minimum of 6 inches below the minimum water level. Non-cubic designs, where  $l_v$  is  $\geq 3$  pipe diameters for the horizontal upper grate, satisfying the depth and distances to the water minimum water surface given for cubic designs are acceptable.

2. Standard 1-1/2 inch or deeper floor grating (or its equivalent) located horizontally over the entire sump and containment floor inside the screens and located between 3 inches and 12 inches below the minimum water level.

\*These types of vortex suppressors were tested at Alden Research Laboratory and have demonstrated the capability to reduce air ingestion to 0%, even under the most adverse conditions simulated.

### 5.3 Debris Assessments

Debris assessments should consider the initiating mechanisms (pipe break locations, orientations, and break jet energy content), evaluation of the amount of debris that might be generated, short- and long-term transport, the potential for sump screen blockage, and head loss that could degrade available NPSH. Table 5.7 outlines key considerations requiring evaluation. Evaluation of potential debris effects requires the following information:

1. Identification of major break locations (per SRP 3.5.2) and jet energy levels.
2. Types, quantities, methods of fabrication and installation, mechanical attachments, and hygroscopic characteristics of the insulation employed on primary and secondary system piping, reactor pressure vessel, and major components (e.g., steam generators, reactor coolant pumps, pressurizer, tanks, etc.) that can become targets of expanding jet(s) identified under Item (1).
3. Containment plan and elevation drawings showing high energy line piping runs, system components, and piping that are sources of insulation debris, structures and system equipment that become obstructions to debris transport, sump location(s), and drawings showing sump design details, including trash rack and screen details, as well as suction piping orientation.
4. Expected water levels during recirculation and RHR and CSS pump NPSH requirements versus flow rate.

Generic findings regarding debris that might be generated, transported and lodged against sump screens (and the plant specific dependence of these phenomena) are discussed in Section 3.3 and presented in detail in References 5, 6, and 7. The following paragraphs summarize the findings:

1. Break locations, type and size of breaks, and break jet targets are major factors to consider in the estimation of potential quantities of debris generated. The break-jet is a high energy two-phase expansion that is capable of shredding insulation and insulation coverings into small pieces or fibers by producing high impingement pressures and large jet loads. A discussion comparing two-phase jet phenomena with single-phase incompressible jet phenomena is given in Appendix C.
2. Mirror (reflective metallic insulations) and totally encapsulated insulations do not appear to pose screen blockage problems. However, if the sump location can be directly targeted by an expanding break jet, a close examination should be made of possible jet load damage to such insulations and their possible prompt transport to the sump.

TABLE 5.7

Debris Assessment Considerations\*

<u>CONSIDERATION</u>	<u>EVALUATE</u>
1) Debris Generator (Pipe Breaks & Location as identified in SRP Section 3.6.2)	<ul style="list-style-type: none"> <li>○ Major Pipe Breaks &amp; Location</li> <li>○ Pipe Whip &amp; Pipe Impact</li> <li>○ Break Jet Expansion Envelope (This is the <u>major</u> debris generator)</li> </ul>
2) Expanding Jets	<ul style="list-style-type: none"> <li>○ Jet Expansion Envelope</li> <li>○ Piping &amp; Plant Components Targeted (i.e., steam generators)</li> <li>○ Jet Forces on Insulation</li> <li>○ Insulation Which Can Be Destroyed or Dislodged by Blowdown Jets.</li> <li>○ Sump Structure (i.e., screen) Survivability Under Jet Loading</li> <li>○ Jet/Equipment Interaction</li> <li>○ Jet/Crane Wall Interaction</li> <li>○ Sump Location Relative to Expanding Break Jet</li> </ul>
3) Short-Term Debris Transport (transport by blowdown jet forces)	
4) Long-Term Debris Transport (transport to the sump during the recirculation phase)	<ul style="list-style-type: none"> <li>○ Containment Layout &amp; Sump Location</li> <li>○ Heavy (or "Sinking") Debris</li> <li>○ Floating Debris</li> <li>○ Neutral Buoyancy Debris</li> </ul>
5) Screen Blockage Effects (impairment of flow and/or NPSH margin)	<ul style="list-style-type: none"> <li>○ Screen Design</li> <li>○ Sump Location</li> <li>○ Water Level Under Post LOCA Conditions</li> <li>○ Flow Requirements</li> </ul>
<hr/>	
Key Elements for Assessment of Debris Effects	<ul style="list-style-type: none"> <li>○ Estimated Amount of Debris That Can Reach Sump</li> <li>○ Screen Blockage</li> <li>○ <math>\Delta P</math> Across Blocked Screens</li> </ul>

---

\*per debris estimation methods described in Section 3.3

3. Low density insulations, such as calcium silicate and unibestos, have closed cell structures and float. They are unlikely to impede flow through sump screens. Partially submerged screens should, however, be evaluated for pull-down of floating debris. Low density hygroscopic insulations that, upon being wetted, have equilibrium densities greater than water require plant specific determinations of screen blockage effects.
4. Nonencapsulated insulations (particularly mineral wool and fiberglass materials) have been shown to present the possibility for high screen blockages or large screen blockage effects (References 5, 7, 14, and 15). These materials, even if deposited in relatively small thickness layers onto sump screens (e.g., on the order of an inch or less), can result in high pressure drops. For plants employing reflective metallic, nonhygroscopic, and/or in particular fibrous, nonencapsulated insulations, the potential for screen blockage should be calculated using the methods provided in Appendix B, Estimating Debris Generation, Transport, and Sump Screen Blockage Potential. Appendix B, in Tables B.1 and B.2, gives short quick methods for assessing the potential for sump screen blockage, and also gives, in Figure B.1, an involved procedure for calculating the effects of insulation debris from detailed plant specific calculations. Both the short methods and the more involved methods were developed from information provided in References 5, 6, 7, 14, and 15. Where plant specific determinations of screen blockage effects are required, the methods provided in Reference 5 should be followed.

#### 5.4 Pump Performance Under Adverse Conditions

The pump industry historically has determined net positive suction head requirements for pumps on the basis of a percentage degradation in performance. The percentage is arbitrary, but generally 1 percent or 3 percent. A 2 percent limit on allowed air ingestion was selected here because data show that air ingestion levels exceeding 2 percent has the potential to produce significant head degradation. Either the 2 percent limit in air ingestion or the NPSH requirement to limit cavitation may be used independently when the two effects act independently. However, air ingestion levels less than 2 percent will affect NPSH requirements. In determining these combined effects, the effects of air ingestion on NPSH required must be taken into account.

A calculational method for assessing pump inlet conditions is shown in Figure 5.2. For a given sump design, the following procedure can be followed:



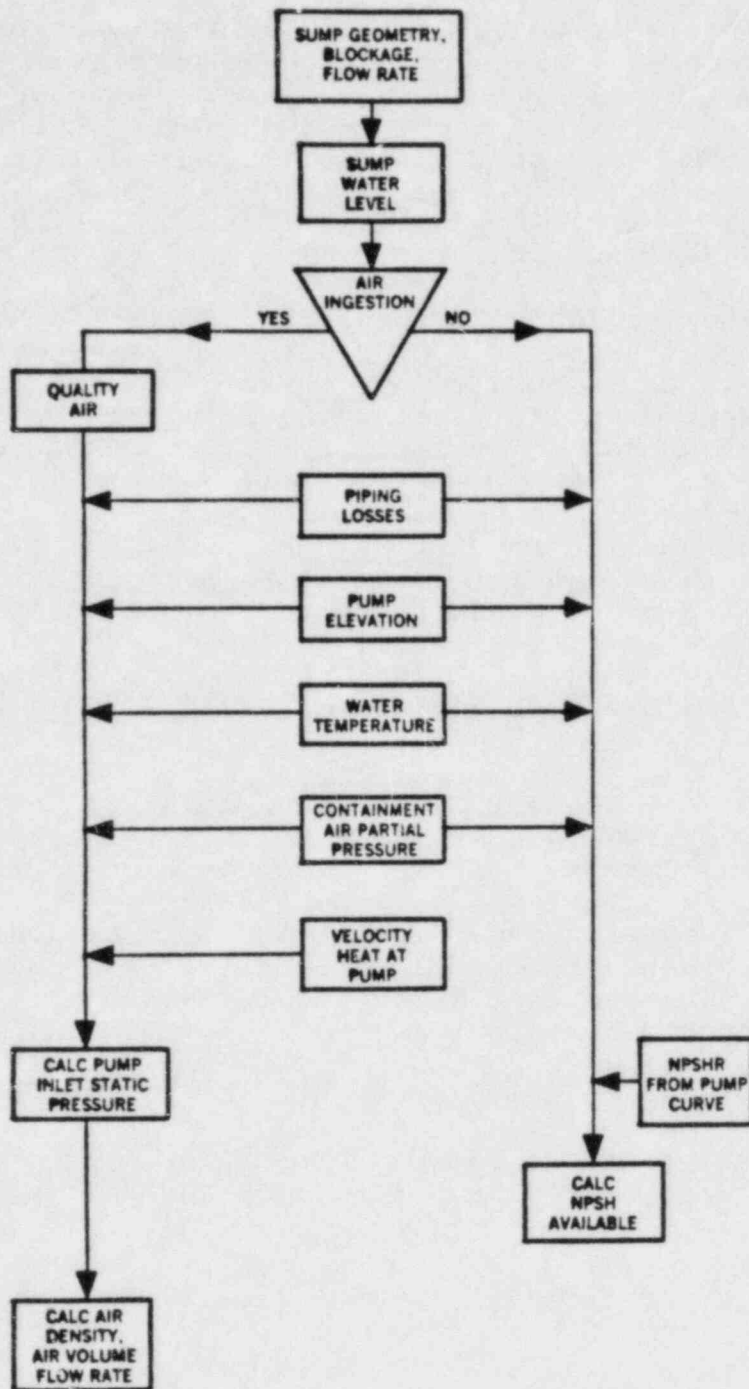


Figure 5.2. Flowchart for Calculation of Pump Inlet Conditions

1. Determine the static water pressure at the sump suction pipe after debris blockage effects have been evaluated. (See Section 5.3.) Note that the water level in the sump should not be so low that a limiting critical water depth occurs at the sump edge such that flow is restricted into the sump.
2. Assess potential level of sump air ingestion using criteria set forth in Section 5.2.
3. Determine pressure losses between sump suction pipe inlet and pump inlet flange for the required RHR and CSS flows. If the pump inlet is located less than 14 pipe diameters from suction pipe inlet, the effect of sump-induced swirl should be evaluated. (See Section 3.2.3 and References 2 and 8).
4. Calculate the static pressure at the pump inlet flange. Static pressure is equal to containment atmospheric pressure plus the hydrostatic pressure due to pump elevation relative to sump surface level less pressure losses and the dynamic pressure due to velocity. (See Section 3.2.3.) Note that no credit is allowed for containment overpressure per SRP Section 6.2.
5. Calculate the air density at the pump inlet, then calculate the air volume flow rate at the pump inlet, incorporating the density difference from sump suction pipe to the pump.
6. If the calculated air ingestion is found to be less than or equal to 2 percent, proceed to Step 7. If the calculated air ingestion is greater than 2 percent, reassess the sump design and operation per Section 5.1.
7. Calculate the net positive suction head (NPSH) available.
8. If air ingestion is indicated, correct the NPSH requirement from the manufacturer's pump curves by the following relationship:

$$\text{NPSH}_{\text{required}}(\text{air/water}) = \text{NPSH}_{\text{required}}(\text{water}) \times \beta$$

where

$$\beta = 1 + 0.50 \alpha_p$$

and  $\alpha_p$  is the air ingestion rate (in percent by volume) at the pump inlet flange.

9. If NPSH available from Step 7 is greater than the NPSH requirement from Step 8, inlet considerations will be satisfied.

If the above review procedure leads to the conclusion that an inadequate NPSH margin exists, further plant specific discussions need to be undertaken with the applicant for resolution of differences, uncertainties in calculations, plant layout details, etc., for resolution of this finding. The lack of credit for containment overpressure should be recognized as a conservatism which should be assessed on a plant specific basis.

#### 5.5 Combined Effects

The findings from Sections 5.2, 5.3 and 5.4 can be combined in the manner shown in Figure 5.3 to determine overall sump performance.

# ECCS SUMP DESIGN

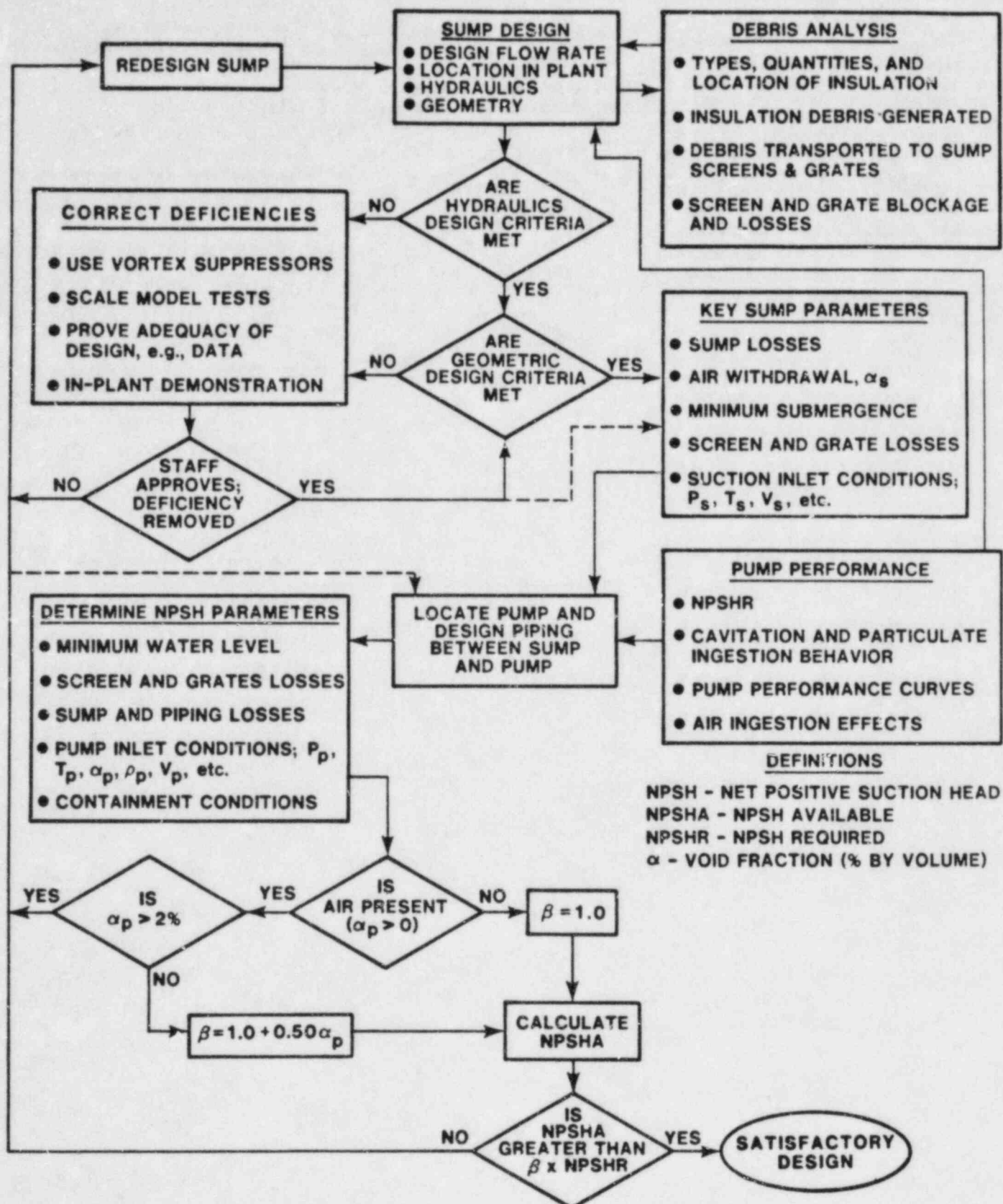


Figure 5.3. Combined Technical Considerations for Sump Performance



## REFERENCES

1. Durgin, W. W., Padmanabhan, M., and Janik, C. R., "The Experimental Facility for Containment Sump Reliability Studies," (Generic Task A-43), ALO-132, Alden Research Laboratory, Worcester Polytechnic Institute, Holden, MA, 1980.
2. Kamath, P., Tantillo, T., and Swift, W., "An Assessment of Residual Heat Removal and Containment Spray System Pumps Performance Under Air and Debris Ingesting Conditions," NUREG/CR-2792, Creare, Inc., Hanover, NH, September 1982.
3. Reyer, R., et. al., "Survey of Insulation Used in Nuclear Power Plants and the Potential for Debris Generation," NUREG/CR-2403, Burns and Roe, Inc., Oradell, NJ, 1981.
4. Kolbe, R. and Gahan, E., "Survey of Insulation Used in Nuclear Power Plants and the Potential for Debris Generation," NUREG/CR-2403, Supplement I, Burns and Roe, Inc., Oradell, NJ, May, 1982.
5. Wysocki, J. J., et. al., "Methodology for Evaluation of Insulation Debris Effects," NUREG/CR-2791, Burns and Roe, Inc., Oradell, NJ, (In revision).
6. Durgin, W. W. and Noreika, J., "The Susceptibility of Fibrous Insulation Pillows to Debris Formation Under Exposure to Energetic Jet Flows," SAND83-7008/NUREG/CR-3170, Alden Research Laboratory, Holden, MA, January 1983.
7. Brocard, D. N., "Buoyancy, Transport, and Head Loss of Fibrous Reactor Insulation," SAND82-7205/NUREG/CR-2982, Alden Research Laboratory, Holden, MA, November 1982.
8. Weigand, G. G. and Thompson, S. L., "Break Flow and Two-Phase Jet Load Model," Sandia National Laboratories, Albuquerque, NM, Presented at International Meeting on Thermal Reactor Safety, Chicago, IL, August, 1982.
9. Weigand, G. G., et. al., "A Parametric Study of Containment Emergency Sump Performance," SAND82-0624/NUREG/CR-2758, Sandia National Laboratories, Albuquerque, NM, July 1982.
10. Hydraulic Institute Standards for Centrifugal, Rotary and Reciprocating Pumps, 13th Edition, Hydraulic Institute, Cleveland, OH, 1975.

11. Merry, H., "Effects of Two-Phase Liquid/Gas Flow on the Performance of Centrifugal Pumps," NEL C130/76, 1976.
12. Murakami, M. and Minemura, K., "Flow of Air Bubbles in Centrifugal Impellers and Its Effect on Pump Performance," 6th Australian Hydraulics and Fluid Mechanics Conference, Adelaide, Australia, December 5-9, 1977.
13. Florjancic, D., "Influence of Gas and Air Admission on the Behavior of Single- and Multi-Stage Pumps," Sulzer Research Number 1970, 1970.
14. "Loviisa Emergency Cooling System Model Tests;" no author given, no publication date given; Translated from Finnish, Sandia National Laboratories, Report No. RS3140/81/191, printed December, 1981.
15. Tuokkola, Y., "Model Test of the Screen Meshes of the Emergency Cooling System," April 25, 1980; Translated from Finnish, Sandia National Laboratories, Report No. RS3140/81/192, printed December, 1981.
16. Niyogi, K. K. and Lunt, R., "Corrosion of Aluminum and Zinc in Containment Following a LOCA and Potential for Precipitation of Corrosion Products in the Sump," United Engineers and Constructors, Inc., Philadelphia, PA, September, 1981.
17. Moody, F. J., "Fluid Reaction and Impingement Loads," Specialty Conference on Structural Design of Nuclear Plant Facilities, Vol. 1, Chicago, IL, December, 1973.
18. Weigand, G. G., Thompson, S. L., and Tomasko, D., "A Two-Phase Jet Model for Pipe Breaks," Proceedings of the Structural Mechanics in Reactor Technology (SMRT) Conference, Paris, France, August, 1981.
19. Thompson, S. L., "Thermal/Hydraulic Analysis Research Program Quarterly Report, January-March 1981," NUREG/CR-2338, Sandia National Laboratories, Albuquerque, NM, October 1981.
20. Padmanabhan, M., "Containment Sump Reliability Studies (Generic Task A-43) - Interim Report on Test Results," Alden Research Laboratory Report No. 59-1, Alden Research Laboratory, Worcester Polytechnic Institute, Holden, MA, June 1981.
21. "Results of Vertical Outlet Sump Tests," Joint ARL/Sandia Report, ARL47-82/SAND82-1286/NUREG/CR-2759, September 1982.

22. Padmanabhan, M. and Hecker, G. E., "Assessment of Scale Effects on Vortexing, Swirl, and Inlet Losses in Large Scale Sump Models," NUREG/CR-2760, Alden Research Laboratory, Worcester Polytechnic Institute, Holden, MA, June 1982.
23. Padmanabhan, M., "Results of Vortex Suppressor Tests, Single Outlet Sump Tests, and Miscellaneous Sensitivity Tests," (Generic Task A-43), Alden Research Laboratory, Worcester Polytechnic Institute, Holden, MA, September 1982.
24. Weigand, G. G., Thompson, S. L., and Tomasko, D., Two-Phase Jet Loads, NUREG/CR-2913, SAND82-1435, prepared for the U.S. Nuclear Regulatory Commission, prepared by Sandia National Laboratories, Albuquerque, NM, 1983.

APPENDIX A

PLANT SUMP DESIGNS  
AND CONTAINMENT LAYOUTS



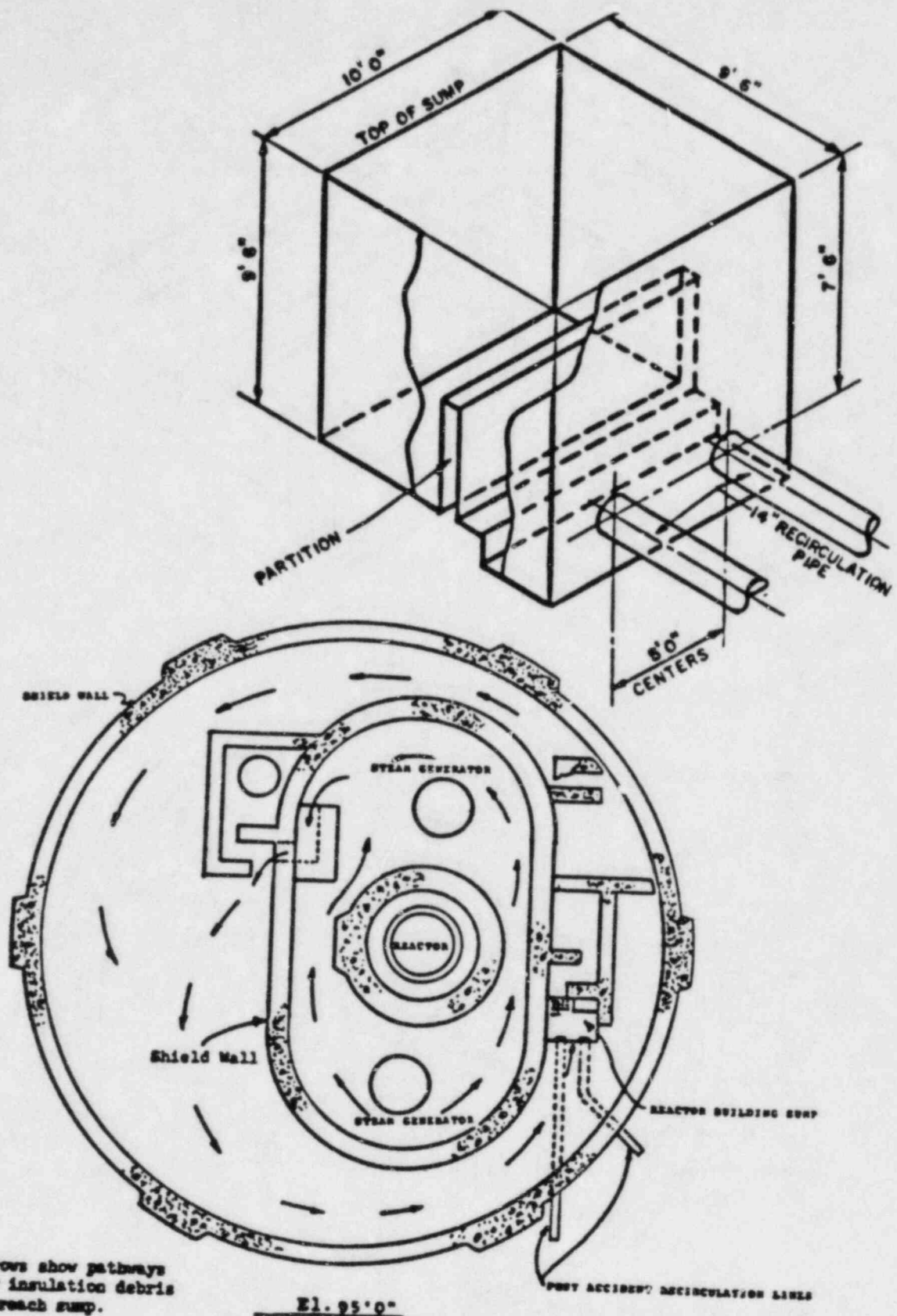
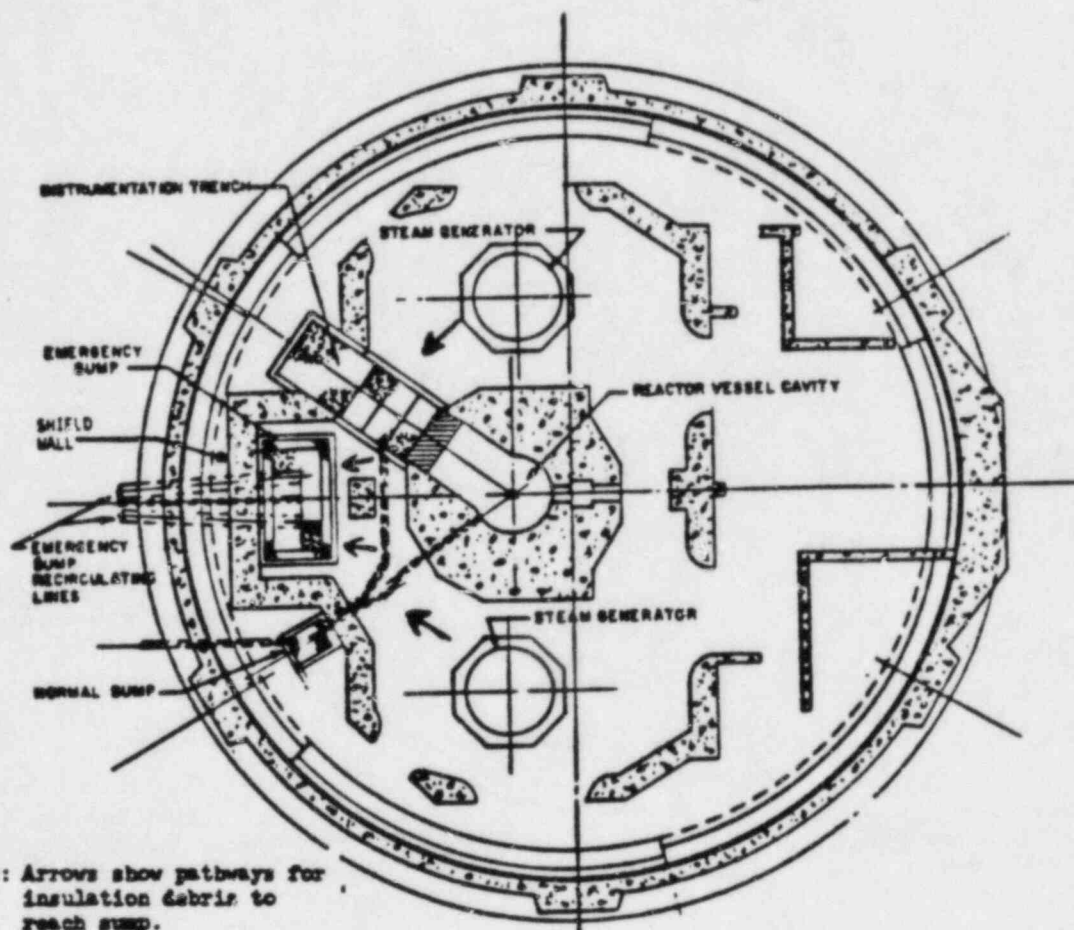
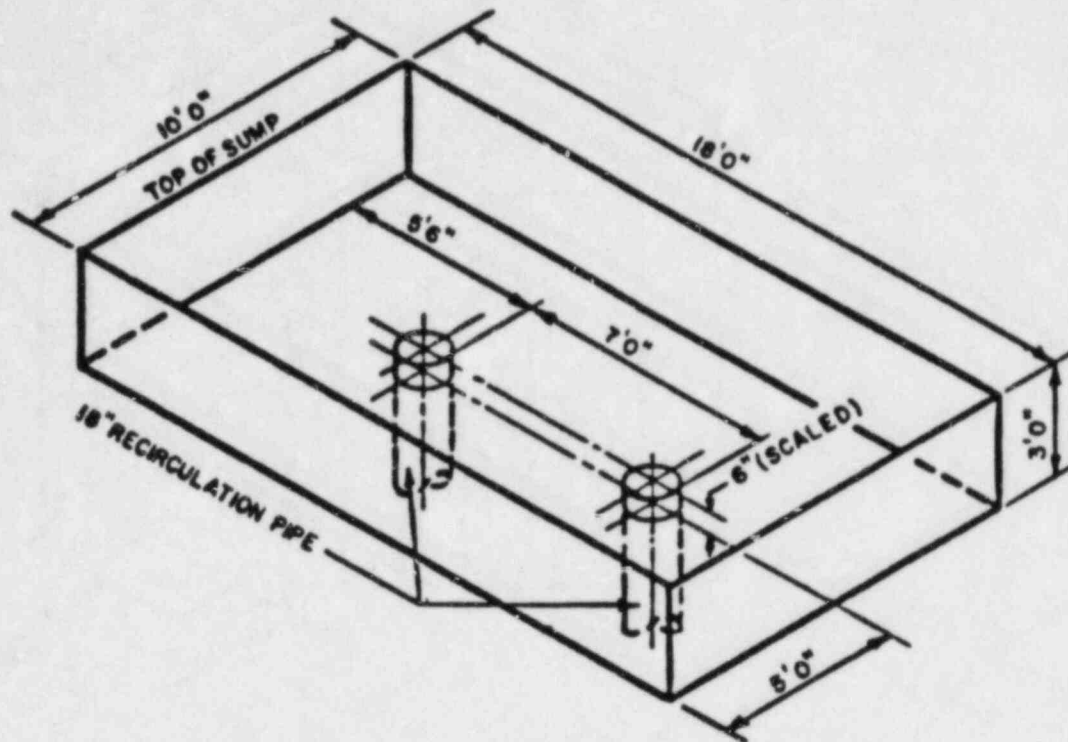
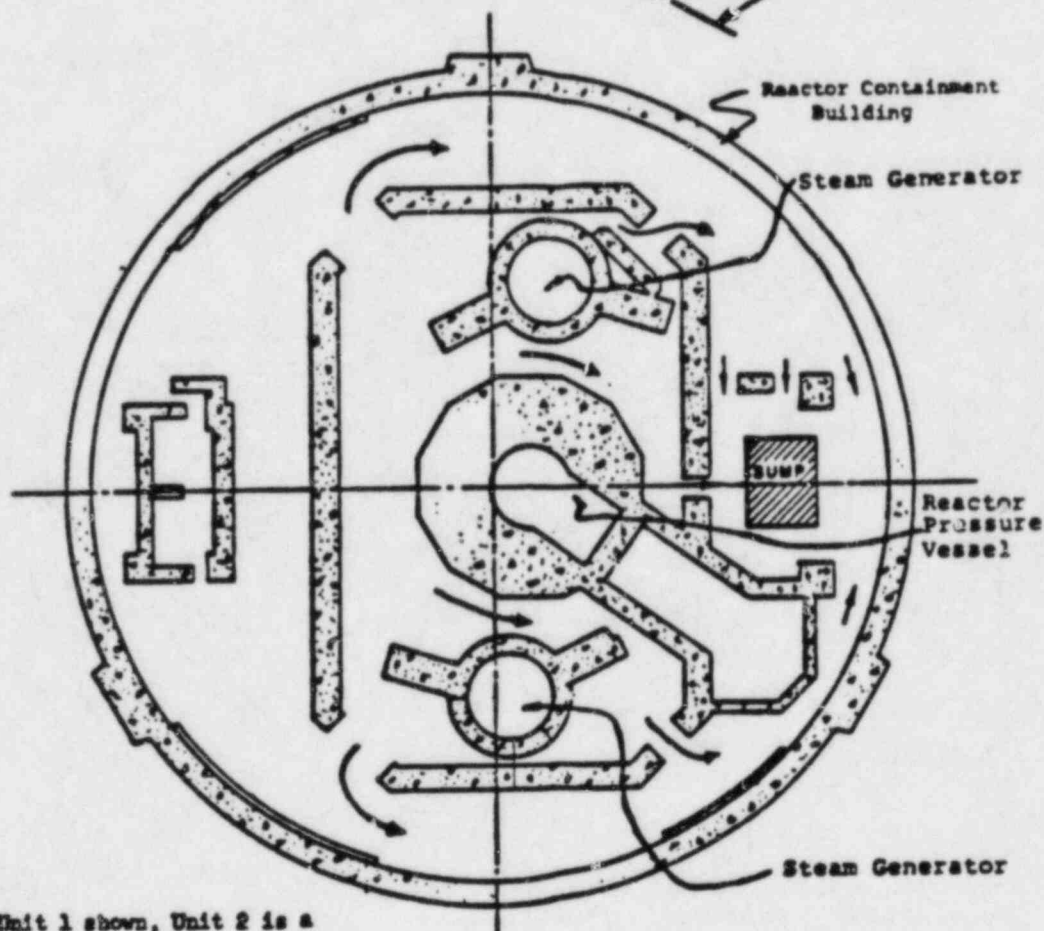
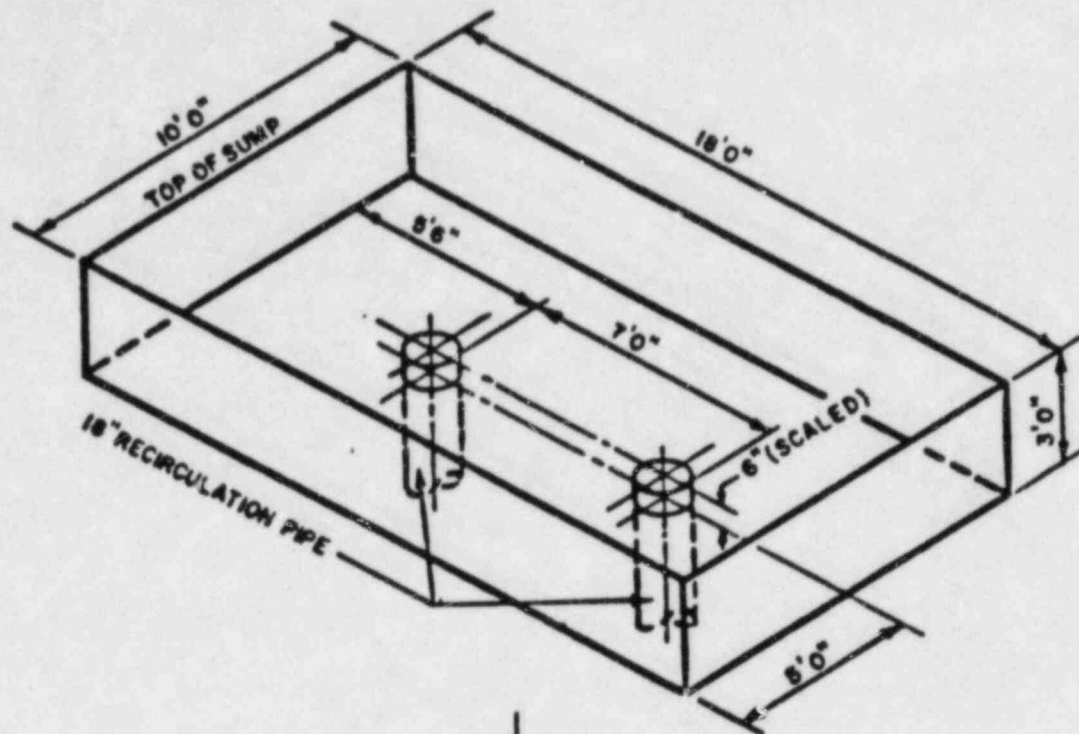


Figure A-1. ECCS Sump and Containment Building Layout, Crystal River Unit 3



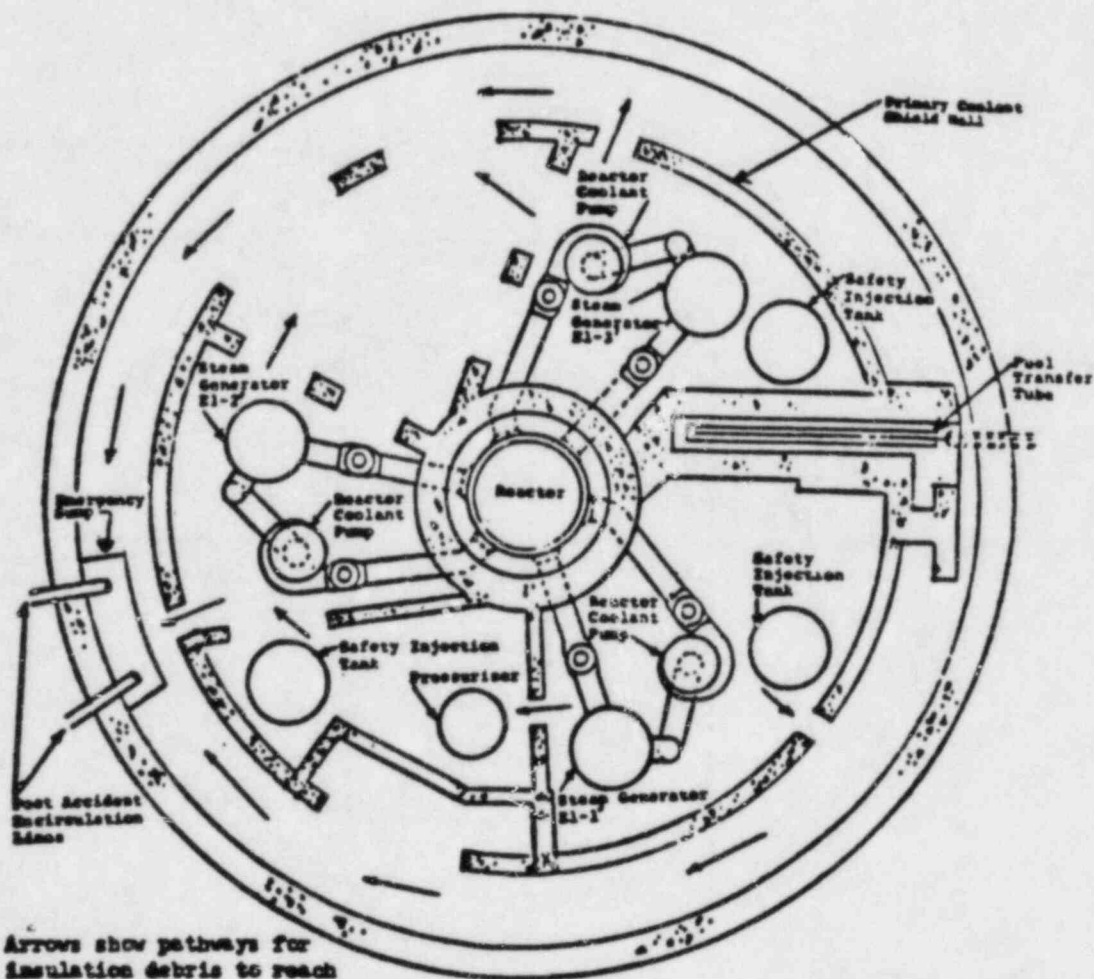
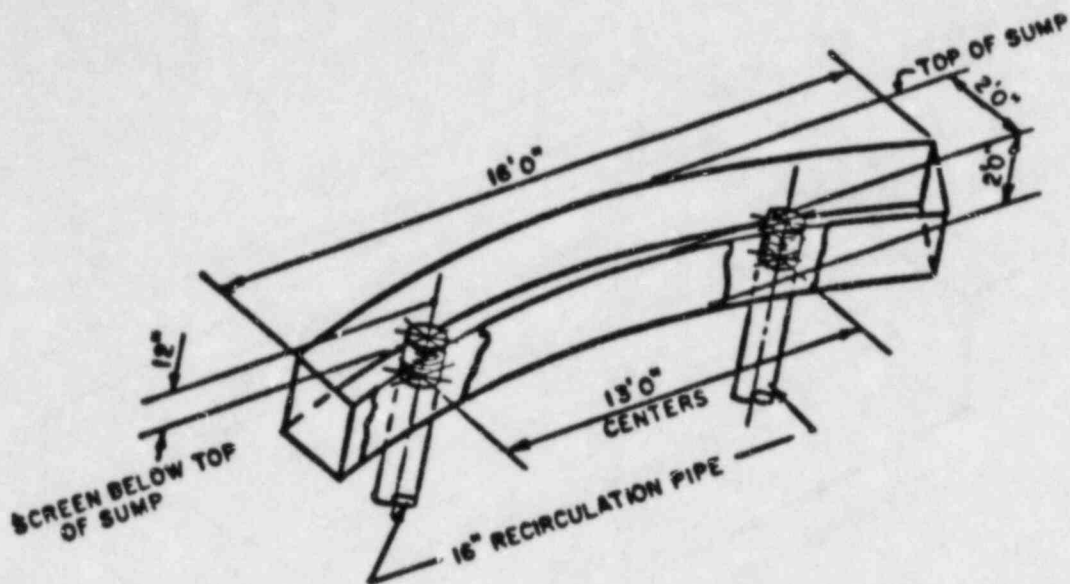
Note: Arrows show pathways for insulation debris to reach sump.

Figure A-2. ECCS Sump and Containment Building Layout, Oconee Unit 3



Note: Unit 1 shown, Unit 2 is a mirror image. Arrows show pathways for insulation debris to reach sump

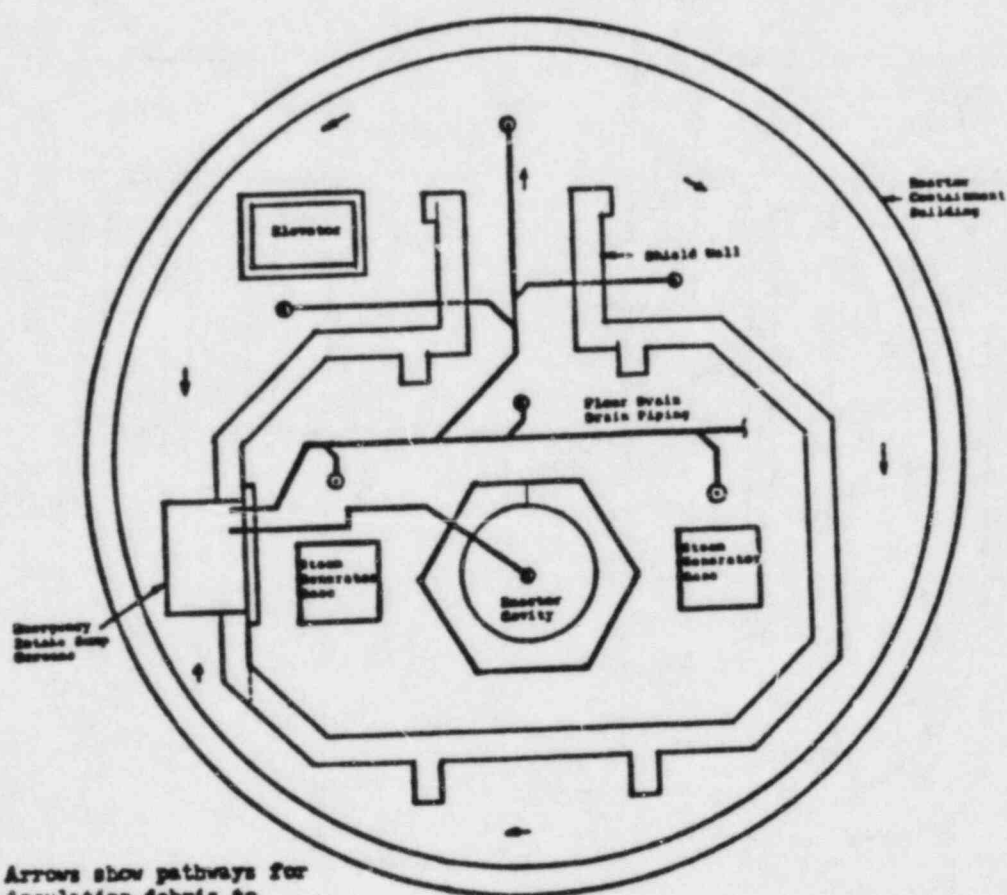
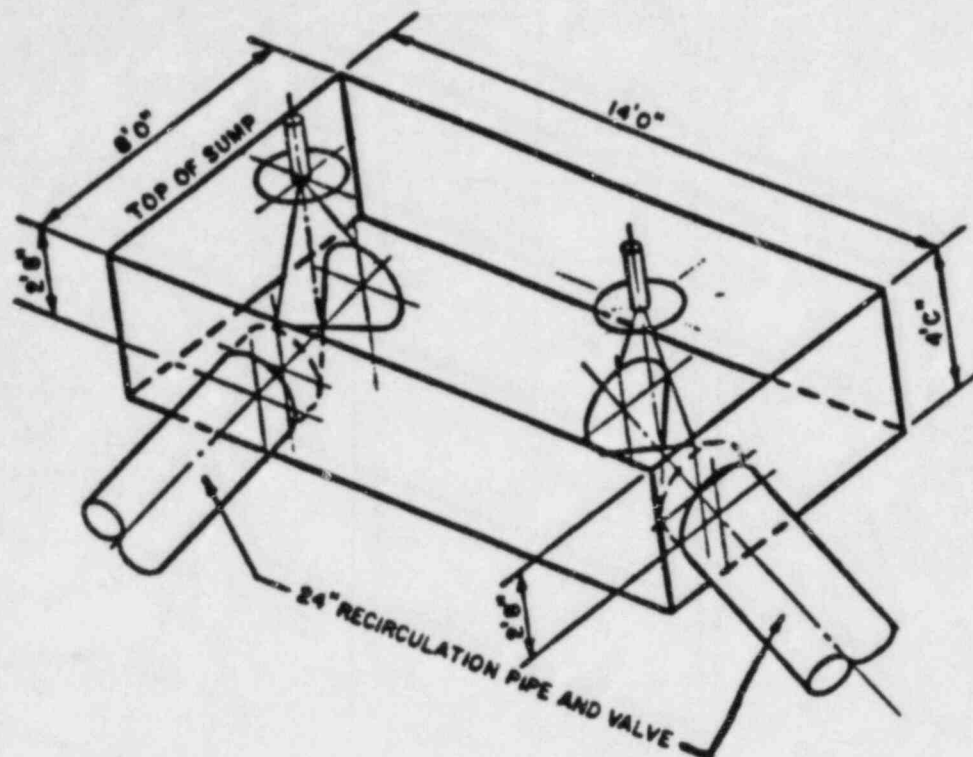
Figure A-3. ECCS Sump and Containment Building Layout, Midland Unit 2



El.-2' 0"

Figure A-4. ECCS Sump and Containment Building Layout, Maine Yankee





Note: Arrows show pathways for insulation debris to reach sump.

Figure A-5. ECCS Sump and Containment Building Layout, Arkansas Unit 2

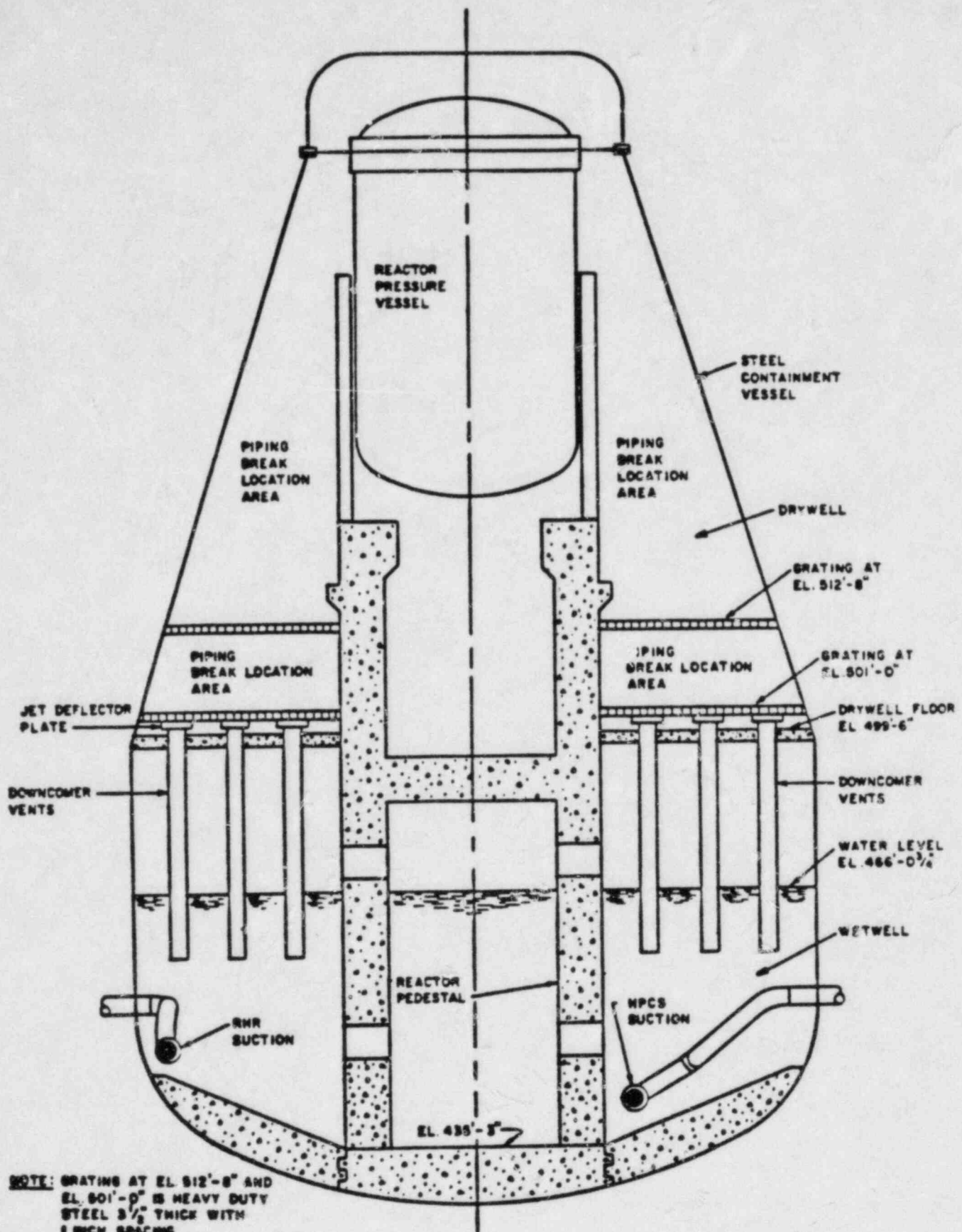


Figure A-6. Primary Containment Vessel, WPPSS Unit 2-

## APPENDIX B

### Estimating Debris Generation, Transport, and Sump Screen Blockage Potential

Generic evaluations regarding insulation debris generation (due to LOCA effects), debris transport, sump screen in Section 3.3 of this report and detailed blockage potential and plant layout dependence are summarized in Reference B-1. Follow-up experimental studies which investigated debris buoyancy characteristics, transport, blocked screen head loss characteristics and jet load damage effects are reported in References B-2 and B-3. These later studies provide data which can be used to bound some of the assumptions in Reference B-1, and also to develop a simplified set of screening evaluations to determine if sump screen blockage can occur. The purpose of this appendix is to provide guidance in using results obtained from the above.

The first step in assessing screen blockage is to determine if the types of insulations employed can: a) be transported to the screen (e.g., by recirculation velocities estimated within containment) and b) if such insulation can be deposited on the screen. Table B-1 presents a first round assessment for screen blockage potential and sets forth three criteria under which debris transport due to fluid velocities will be negligible, or non-existent. Use of Table B-1 thus permits a quick determination of lack of screen blockage. It also should be clearly noted that Table B-1 does not deal with fibrous insulation effects.

Table B-1 sets forth three criteria to assess debris transport potential for the intermediate recirculation velocity ranges excluded in Table B-1, and performs a limiting blocked screen head loss calculation based on three key factors; those being: a) that the total volume of the respective insulations transports to the sump screen (if the recirculation flow velocities are high enough), b) that the head losses for the blocked sump screen are calculated from experimentally determined head loss characteristics, and c) that loss of 50% of the NPSH margin can be tolerated for the plant in question. In particular, Table B-2 provides a rapid means to calculate the equivalent volume of fibrous insulation ( $\bar{V}_{fb}$ ) which could be utilized (and assumed transported in total to the sump screen) and for which the screen blockage effects would not exceed 50% of the NPSH margin required ( $\Delta P_m$ ).

If Tables B-1 and B-2 do not result in acceptable (or non-existent) sump blockage conditions, then the procedure outlined in Figure B-1 (which is derived from the methodology reported in Reference B-1) should be employed for the plant under review.

Figure B-1 outlines and provides guidance for following the methods reported in Reference B-1 for evaluating insulation debris effects. The step-wise procedure described below provides a logical order for performing the calculational methods in Reference B-1. (It is recommended that References B-1, B-2, and B-3 be thoroughly read before attempting debris and screen loss calculations.)

1. Pipe break locations and orientations are determined for possible LOCA's in containment (Box 1 of figure).
2. Three mechanisms for debris generation are considered: pipe whip (Box 2), pipe impact (Box 3) and jet impingement (Box 4). Of these, the mechanism that produces the preponderance of debris is jet impingement.
3. The containment volume intercepted by the jet is determined (conical jet volume) (Box 5).
4. A large break jet can shred insulation at pressures of 20 psig and above (Reference B-2). This is approximately equivalent to an axial distance along the jet centerline of 7 L/D's from the jet origin (Reference B-4, based upon a stagnation pressure of 15 MPa and 35°C subcooled liquid). The volumes of insulation contained within this part of the conical jet volume are to be calculated (Box 6).
5. At points within the conical jet volume where the distance measured along the centerline of the jet is greater than 7 L/D's but is less than the downstream point on the centerline where the average stagnation pressure of the jet is 0.5 psig, insulation is assumed to be dislodged in an as-fabricated form. The outer boundary of the cone, corresponding to a stagnation pressure of 0.5 psig, was established from information in Reference B-1 concerning a lower pressure limit for insulation damage. The volumes of insulation contained within this part of the conical jet volume are to be calculated (Box 7).

Note: The results obtained from this calculation will be used to determine the volume of as-fabricated insulation dislodged; the calculational procedure then proceeds to Box 17.

6. Within the conical jet volume extending from the jet origin to 7 L/D's ( $\sim$  20 psig) downstream, determine if encapsulated or nonencapsulated fibrous insulation is present (Box 8).
7. If the fibrous insulation described in 6 is present within the volume intercepted by the jet, determine its volume from the as-fabricated dimensions (Box 10). Fibrous insulation located in the conical jet volume between the jet origin and 7 L/D's is shredded.



8. Determine the volumes of insulation removed by pipe whip, PW, pipe impact, PI and jet impingement (within 7 L/D boundary), JI. This fibrous portion is to be treated as shredded fibrous debris. Volumes are to be determined from as-fabricated dimensions (Box 9).
  9. Determine those volume fractions of shredded fibrous debris that are promptly transported by pipe whip,  $\alpha_{PW}$ , pipe impact,  $\alpha_{PI}$ , and by jet impingement,  $\alpha_{JI}$ , to the sump screen (Box 11).
  10. Calculate the maximum flow velocity that exists in containment under recirculation conditions using the methods provided in Reference B-1. Determine whether this flow velocity is sufficient to allow the sunken shredded fibrous debris to migrate to the sump using the transport information given in Table B-3 (Box 12).
  11. If the flow velocity calculated from 10, above, is sufficient to cause migration, all the shredded fibrous insulation generated ( $V_{PW} + V_{PI} + V_{JI}$ ) is assumed to migrate to the sump screen (Box 13).
  12. If the flow velocity calculated from 10, above, is not large enough to cause migration, prompt transport is the only mechanism for shredded insulation to reach the screen. The volume of this material at the screen is  $\alpha_{PW} V_{PW} + \alpha_{PI} V_{PI} + \alpha_{JI} V_{JI}$  (Box 14).
  13. When the volume of shredded debris that reaches the sump screen (either 11 or 12 above apply), the equivalent thickness,  $t$ , of shredded debris forming a mat on the sump can be calculated:  $t = V/A_e$ , where  $V$  is the combined debris volume and  $A_e$  is the effective unblocked area of the sump screen (area available for flow) (Box 15).
- Note: Before proceeding to the following step, calculations provided in Boxes 17 through 22 are required.
14. After completing item 5 above, determine the total reflective metallic panel area,  $A_m$ , contained within the entire conical jet volume out to an average stagnation pressure of 0.5 psig on the jet centerline and determine the as-fabricated panel area  $A_f$  of fibrous or other sinkable insulation between  $L/D = 7$  and an average stagnation pressure of 0.5 psig on the jet centerline (Box 17).
  15. The maximum containment flow velocity calculated in item 10, above, is referred to, as are the flow requirements to allow debris migration (Table B-1) (Box 12).

16. If the maximum containment flow velocity is not large enough to allow debris to migrate, as-fabricated debris (either fibrous or reflective metallic) does not reach the sump (Box 18).
17. If the maximum containment flow velocity is large enough to allow the migration of fibrous as-fabricated insulation or both fibrous and reflective metallic insulations, it is assumed that such insulation(s) become aligned along the sump screen face to a height corresponding to the maximum as-fabricated insulation dimension,  $H_I$  (see Reference B-3) (Box 19).
18. If only as-fabricated fibrous material migrates to the screen, determine if its equivalent length,  $A_f/H_I$ , is greater than the sump perimeter,  $P$ . If only as-fabricated reflective metallic can migrate to the screen, calculate the equivalent length,  $A_m/H_I$ . If both species can migrate, calculate the equivalent length of both,  $(A_f + A_m)/H_I$  (Box 20).
19. If the equivalent lengths determined in item 18 above are less than the equivalent perimeter of the sump screen,  $P$ , the area not blocked by as-fabricated insulation is  $A - A_f$ , or  $A - A_m$ , or  $A - (A_f + A_m)$ , where  $A$  is the screen area of the sump (Box 21).
20. If the equivalent lengths calculated in 18 above are greater than the equivalent perimeter of the sump screen,  $P$ , the amount of screen blocked by as-fabricated debris can be no more than the area composed of the perimeter,  $P$ , multiplied by the maximum as-fabricated height,  $H_I$ , of the insulation (see Reference B-3). The area not blocked by as-fabricated insulation is thus calculated to be  $A - HP$ , where  $A$  is the screen area of the sump (Box 22).
21. Using the equivalent shredded fibrous insulation thickness,  $t$ , obtained from 13 above, and the unblocked screen area, obtained from 19 or 20 above, determine the head loss through the debris mat using the head loss relations provided in Reference B-3 (Box 16).
22. The head loss calculated in Step 16 serves as debris analysis input to the requirements for sump design, as shown in Figure 5.4 and discussed under Combined Effects in Section 5.5 of this report.

#### References to Appendix B

- B-1 Wysocki, J. J. et al., "Methodology for Evaluation of Insulation Debris Effects," NUREG/CR-2791, U.S. Nuclear Regulatory Commission, prepared by Burns and Roe, Inc., Oradell, NJ, September 1982.
- B-2 Durgin, W. W. and Noreika, J. F., "The Susceptibility of Fibrous Insulation Blankets to Debris Formation Under Exposure to Energetic Jet Flows," NUREG/CR-3170, U. S. Nuclear Regulatory Commission, prepared by Alden Research Laboratory, Worcester Polytechnic Institute, Holden, MA, 1983.
- B-3 Brocard, D. N., "Buoyancy, Transport and Head Loss of Fibrous Reactor Insulation," NUREG/CR-2982, U.S. Nuclear Regulatory Commission, prepared by Alden Research Laboratory, Worcester Polytechnic Institute, Holden, MA, November 1982.
- B-4 Weigand, G. G., Thompson, S. L., and Tomasko, D. "Two-Phase Jet Loads," NUREG/CR-2913, SAND82-1935, Sandia National Laboratories, Albuquerque, NM, January 1983.

TABLE B-1. First Round Assessment of Screen Blockage Potential

Criteria for "Zero" Potential for Screen Blockage			
	Criteria 1	Criteria 2	Criteria 3
$V_{fb}$	0	0	$> 0$
$V_{rm}$	0	$> 0$	any value
$V_{cc}$	any value	any value	any value
$V_{hg}$	0	0	0
$U_f$	any value	$\leq 2.0$ ft/sec	$\leq 0.15$ ft/sec
$H_w$	$\geq H_s$	$\geq H_s$	$\geq H_s$

$V_{fb}$  = volume of fibrous insulation employed  
 $V_{rm}$  = volume of reflective metallic insulation employed  
 $V_{cc}$  = volume of closed cell insulation with a specific gravity less than 1.0 (for  $H_w \geq H_s$ ) this insulation will float on water surface above the sump.  
 $V_{hg}$  = volume of hygroscopic insulation employed  
 $H_w$  = water level at sump screen  
 $H_s$  = sump screen height  
 $U_f$  = flow velocity at the screen based upon the smaller of (1) the screen area that is shielded from prompt transport of insulation and below the minimum water level or (2) the smallest immediate, total approach-flow-area to the screens/grates below the minimum water level.



TABLE B-2. Short Form Procedure For Determining Levels Of Acceptable Screen Blockage When Fluid Transport Of Insulation Debris Is Possible.

Criteria for an Acceptable Potential for Screen Blockage		
Criteria 1	Criteria 2	Criteria 3
$V_{fb} = 0$ $V_{rm} > 0$ $V_{cc} = \text{any value}$ $V_{hg} = 0$	$V_{fb} > 0$ $V_{rm} > 0$ $V_{cc} = \text{any value}$ $V_{hg} = 0$	$V_{fb} > 0$ $V_{rm} = \text{any value}$ $V_{cc} = 0$ $V_{hg} = 0$
$U_f > 2.0$	$U_f > 2.0$	$0.15 < U_f \leq 2.0$
$H_w \geq H_s$	$H_w \geq H_s$	$H_w \geq H_s$
$A_m = (L_m \times P_s) \leq 0.75 A'_s$	$A_m = (L_m \times P_s) \leq 0.75 A'_s$	$A_m = 0$
$A_e = A'_s - A_m$ $U_e = Q/A_e$		$A_e = A'_s$ $U_e = Q/A_e$
$\left\{ \Delta P = C_o t^m U_e^n \right\}^*$ $\bar{V}_{fb} = A_e \left( \frac{0.5 \Delta P_{pm}}{C_o U_e^n} \right)^{\frac{1}{m}}$		$\left\{ \Delta P = C_o t^m U_e^n \right\}^*$ $\bar{V}_{fb} = A_e \left( \frac{0.5 \Delta P_{pm}}{C_o U_e^n} \right)^{\frac{1}{m}}$
$V_{fb} \leq \bar{V}_{fb}$		$V_{fb} \leq \bar{V}_{fb}$

$V_{fb}$ ,  $V_{rm}$ ,  $V_{cc}$ ,  $V_{hg}$ ,  $H_w$ ,  $H_s$ ,  $U_f$  (see Table B-1)

$A_m$  - screen area blocked by metallic insulation

$A_e$  - effective unblocked screen area (area available to flow,  $Q$ )

$A'_s$  - screen area shielded from prompt transport of insulation and below the minimum water level

$U_e$  - effective flow velocity

$Q$  - volume flow rate

$L_m$  - largest linear dimension for reflective metallic insulation

$P_s$  - sump screen perimeter or its equivalent

$t$  - nominal thickness of shredded insulation on sump screen,  $t$  is the volume of as-fabricated fibrous insulation dislodged and shredded divided by the effective unblocked screen area

$\Delta P_{pm}$  - Net Positive Suction Head Margin, difference between the net-positive suction head available and the net positive suction head required

$V_{fb}$  - volume of fibrous insulation that leads to a head loss of  $0.5 \Delta P_{pm}$

$\Delta P = C_o t^m U_e^n$  - head loss, ( $\Delta P$ ), equation for shredded insulation with nominal thickness  $t$ ,  $\Delta P = \{ft\}$ ,  $t = \{ft\}$ ,  $U_e = \{ft/sec\}$

fiberglass:  $C_o = 1080$ ,  $m = 1.3$ ,  $n = 2.3$

mineral wool:  $C_o = 230$ ,  $m = 1.4$ ,  $n = 2.0$

\* This head loss equation was suggested by the results of experiments reported in Reference B-3. Other expressions developed from properly conducted experiments can be used.

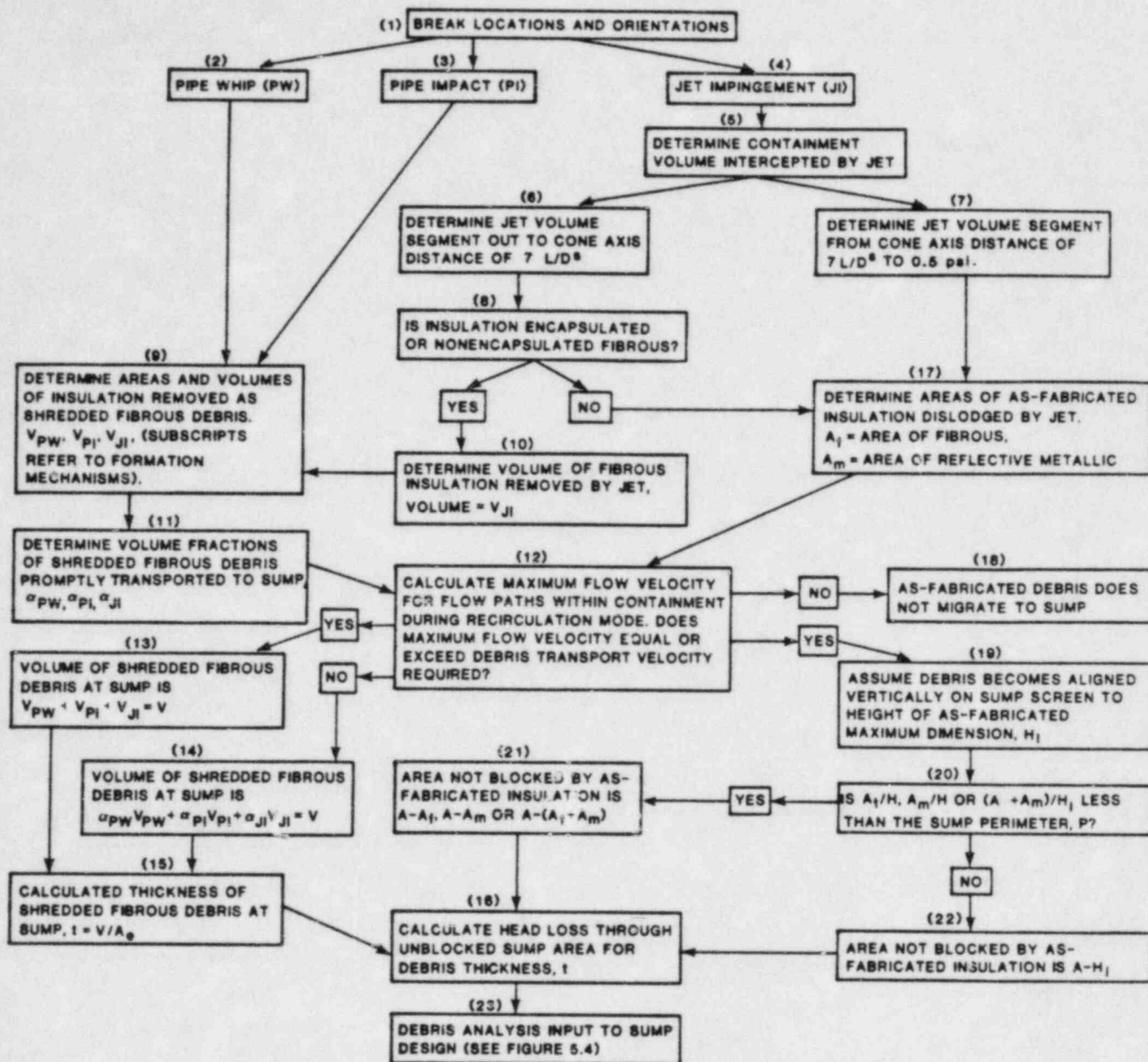
TABLE B-3  
Transportation Tests Results  
From Reference B-3

Condition	Pillow Type	$V_i$ (ft/sec)	$V_s$ (ft/sec)	$V_v$ (ft/sec)	$\Delta H$ (ft)	$\frac{\Delta H}{V^2/2g}$	Comments
Floating whole pillows	1	N/A	N/A	> 2.3			Never flipped
	2	N/A	N/A	N/A			Sunk while against screen; flipped vertical
	3	N/A	N/A	N/A			Sunk while against screen; flipped vertical
Sunken whole pillows	1	1.1	1.1	1.1	0.13		Only one pillow tested
		0.9	1.1	1.1	0.07		
	2	1.2	1.8	2.0	0.44	7.1	Only one pillow tested folded in half on screen
		1.4	1.6	2.4			
	3	1.5	1.7	2.0	0.60	9.4	Pillows on screens overlap by 2 inches
		1.1	1.6	1.6	0.33	8.3	
Sunken pillows with covers removed but included and separated insulation layers	1	1.1	1.1	1.1	0.67	36.0	Not all pieces vertical
		0.9	1.5		0.96	27.5	
	2 or 3	1.1	1.6	1.2	0.71	32.0	
Sunken pillows with covers and insulation layers in 5 pieces (see Figure 2.6)	1	1.0	1.9		1.4	25.0	Not all pieces vertical
		1.1	2.0		1.6	26.0	
	2 or 3	1.0	1.4	1.6	0.54	14.0	Significant overlap of pieces on screen

Table B-3  
(continued)

Condition	Pillow Type	$V_i$ (ft/sec)	$V_S$ (ft/sec)	$V_V$ (ft/sec)	$\Delta H$ (ft)	$\frac{\Delta H}{V^2/2g}$	Comments
Sunken pillows in 4" x 4" x 1" fragments. Covers not included.	1	0.4	1.4	1.6	1.35	34.0	Fragments collect on bottom 1 ft of screen
		0.6	1.3	1.4	2.45	80.0	With turbulence generators. Fragments collect on bottom 3 ft of screen
	2 or 3	1.0	> 1.6				Not all pieces reached the screen. Collected near screen bottom, Figure 4.6
		1.0	> 1.6		0.72	18.1	With turbulence generators. Only about half the pieces on screen. Some pieces at mid-height.
Sunken pillows in shreds. Covers not included.	2 or 3	0.4	> 1.3	N/A	3.7 for 1.0 fps	240	Not all pieces on screen. Screen entirely but not uniformly covered.
Sunken single fragments 4"x4"x1"	1 2 or 3	0.6 0.7					Tests conducted in 1 ft wide flume with 7 inch water depth
4"x1"x1"	1 2 or 3	0.3 0.5					
Shreds	1 2 or 3	0.3 0.2					
Metallic reflective sample	N/A	2.6 2.0	2.6 2.3				

NOTATIONS:  $V_i$  = velocity needed to initiate motion of at least one piece of insulation (not including covers when separated from pillows)  
 $V_S$  = velocity needed to bring all material on screen  
 $V_V$  = velocity needed to flip all pieces vertically on screen  
 $\Delta H$  = head loss at  $V_V$  (or  $V_S$  if  $V_V$  not given)



$V_{PW}$  - VOLUME OF SHREDDED FIBROUS INSULATION REMOVED BY PIPE WHIP. (FT<sup>3</sup>)  
 $V_{PI}$  - VOLUME OF SHREDDED FIBROUS INSULATION REMOVED BY PIPE IMPACT. (FT<sup>3</sup>)  
 $V_{JI}$  - VOLUME OF SHREDDED FIBROUS INSULATION REMOVED BY JET IMPINGEMENT. (FT<sup>3</sup>)  
 $\alpha_{PW}$  - FRACTION OF VOLUME OF SHREDDED INSULATION CAUSED BY PIPE WHIP PROMPTLY TRANSPORTED TO SUMP.  
 $\alpha_{PI}$  - FRACTION OF VOLUME OF SHREDDED INSULATION CAUSED BY PIPE IMPACT PROMPTLY TRANSPORTED TO SUMP.  
 $\alpha_{JI}$  - FRACTION OF VOLUME OF SHREDDED INSULATION CAUSED BY JET IMPINGEMENT PROMPTLY TRANSPORTED TO SUMP.  
 $L/D$  - RATIO OF PIPE LENGTH TO PIPE DIAMETER.  
 $V$  - TOTAL VOLUME OF SHREDDED DEBRIS TRANSPORTED TO SUMP SCREEN (FT<sup>3</sup>)  
 $A_i$  - AREA OF AS-FABRICATED FIBROUS INSULATION DISLODGED BY JET. (FT<sup>2</sup>)  
 $A_m$  - AREA OF AS-FABRICATED REFLECTIVE METALLIC INSULATION DISLODGED BY JET. (FT<sup>2</sup>)  
 $A$  - EFFECTIVE AREA OF SUMP SCREEN (FT<sup>2</sup>)  
 $A_u$  - EFFECTIVE UNBLOCKED SUMP SCREEN AREA (AREA AVAILABLE FOR FLOW) (FT<sup>2</sup>)  
 $H_i$  - MAXIMUM LINEAR DIMENSION OF AS-FABRICATED INSULATION (FT)  
 $P$  - PERIMETER OF EFFECTIVE SUMP SCREEN (FT)  
 $t$  - CALCULATED THICKNESS OF SHREDDED DEBRIS MAT ON SUMP SCREEN (IN)

Figure B-1 Flowchart for the Determination of Insulation Debris Effects



## APPENDIX C

### Insulation Debris Formation as a Result of Two-Phase Jet Impingement

Experiments have been carried out to determine the onset of failure of as-fabricated fibrous insulation due to jet impingement. These experiments were conducted using water jets at ambient temperature, at various stagnation pressures, and at two angles of jet impingement: normal to the insulation surface and 45° to the insulation surface (Reference C-1).

Table C-1 shows the key experimental results from the tests conducted in Reference C-1; the table presents the damage and failure pressure data. The insulation that was the most susceptible to failure was the Type 1 insulating pillows. Visible damage occurred at stagnation pressures of about 10 psig (90° impact) and 15 psig (45° impact); failure of the pillow occurred at stagnation pressures of about 35 psig (90° impact) and 30 psig (45° impact). Visible damage was defined as the pressure at which the first signs of structural failure occurred, e.g., fraying of the fibers in the covering, etc. Failure of the insulation pillow was defined as the pressure where there was a release of fibrous insulation from the as-fabricated insulation panel. In both instances the insulation panel was subjected for a period of five minutes to an impact from a two inch diameter, incompressible water jet at a constant stagnation pressure,  $P_0$ . The stagnation pressure for fibrous insulation panel failure, referred to in this appendix as the failure pressure, will be set at 20 psig. This is the recommended value for incipient failure given in Reference C-1.

#### Two Phase Jets

The flow field for two-phase jets impinging on targets is extremely complicated. Reference C-5 has reported the centerline behavior of two-phase jets and has reported the radial loading for axisymmetric impinging two-phase jets.

In the jet flow field there are three natural divisions of the field. There is a nozzle (or break) region where the flow chokes. In this region there is a core at choked flow thermodynamic properties that projects a distance downstream of the nozzle depending upon the degree of subcooling. Downstream of this region there is the free jet region. Here the jet expands almost as a free, isentropic expansion. The flow is supersonic throughout this entire region. The free jet region terminates at a stationary shock wave near the target. This shock wave arises because of the need for the target to propagate pressure waves upstream and, thus produce a pressure gradient that will direct the fluid around the target. Downstream of the

Table C-1 Experimental Results from Reference C-1 for the  
Stagnation Pressure for Incipient Damage and Failure\*

Insulating Pillow Type	90° Impingement Angle (Pressure, psig) Damage/Failure	45° Impingement Angle (Pressure, psig) Damage/Failure
1	10/35	15/30
2	40/>65	30/>65
3	60/65	45/50

Type 1: 4" mineral wool or refractory mineral fiber core material (6 lb. density) covered with Uniroyal #6555 asbestos cloth coated with 1/2 mil. Mylar.

Type 2: 4" Burlglass 1200, or 4 layers of 1" thick Filomat D (fiberglass) core material, inner covering of knitted stainless steel mesh, outer covering of Alpha Maritex silicone aluminum cloth, product #2619.

Type 3: Same insulation core materials as Type 2. Inner and outer covering of 18 ounce Alpha Maritex cloth, product #7371.

\*For comments about failure modes during the experiments see Reference C-1.

shock is the target region where the local flow field imposes a pressure loading on the target. Depending upon the upstream flow conditions and the L/D of the target there may be a substantial total pressure loss across the shock wave. This loss arises because of the irreversible physics that characterize the shock.

As indicated above, methods for calculating the centerline behavior of impinging two phase jets were developed in Reference C-5. Figures C-1 and C-2 have been taken from Reference C-5 and show the centerline total pressure behavior for vessel (break) stagnation conditions of 15 MPa and 8 MPa at various saturated and subcooled states and for various L/D's. Radial target-pressure distributions were also given in Reference C-5. Figures C-3 and C-4 show target pressure contours. These figures display, in an approximate fashion, the radial target pressure distribution as a function of the axial position of the target and the vessel (or break) stagnation conditions. Figure C-3 is for stagnation conditions of  $P_0 = 150$  bars (15.0 MPa) and  $\Delta T_0 = 35^\circ\text{C}$ , where  $P_0$  is the stagnation pressure and  $\Delta T_0$  denotes the degrees of subcooling. Figure C-4 is for  $P_0 = 80$  bars (8.0 MPa) and  $\Delta T_0 = 0^\circ\text{C}$ . Both of these figures show that the region targeted by an impinging two-phase jet is highly dependent upon the thermodynamic conditions at the break.

#### Fibrous Insulation Debris Model

Test data have indicated that there can be substantial differences in the pressure loss between shredded and as-fabricated insulations for equal volumes blocking a flow stream; the shredded insulations lead to larger losses. Currently, methods do not exist, other than statistical, for evaluating the amount of fibrous insulation that is removed in an accident and becomes shredded as a result of hydrodynamic forces. There is a clear need for such a model because of the large impact sump screen pressure loss can have on the net positive suction head (NPSH) available. At the same time there exist very little data or analyses upon which to base modeling. The next few paragraphs show a model for evaluating the fractions, by volume, of shredded and as-fabricated panels that result; the model is based principally upon two studies recently funded by the NRC. They are provided in References C-1 and C-5. It should be understood that the approach used in developing this model was to make assumptions that always resulted in substantial conservatism in arriving at the amount of shredded fibrous insulation; this was done because shredded fibrous insulation poses the greatest potential threat to NPSH available.

The model consists of defining two regions within the two-phase jet volume defined in Reference C-6. The first region is a circular cone with total included angle of  $90^\circ$  extending from the jet origin to 7 L/D's downstream (see Figure C-5); all of the fibrous insulation within this volume is assumed to be shredded. The second region is the frustum of a circular cone

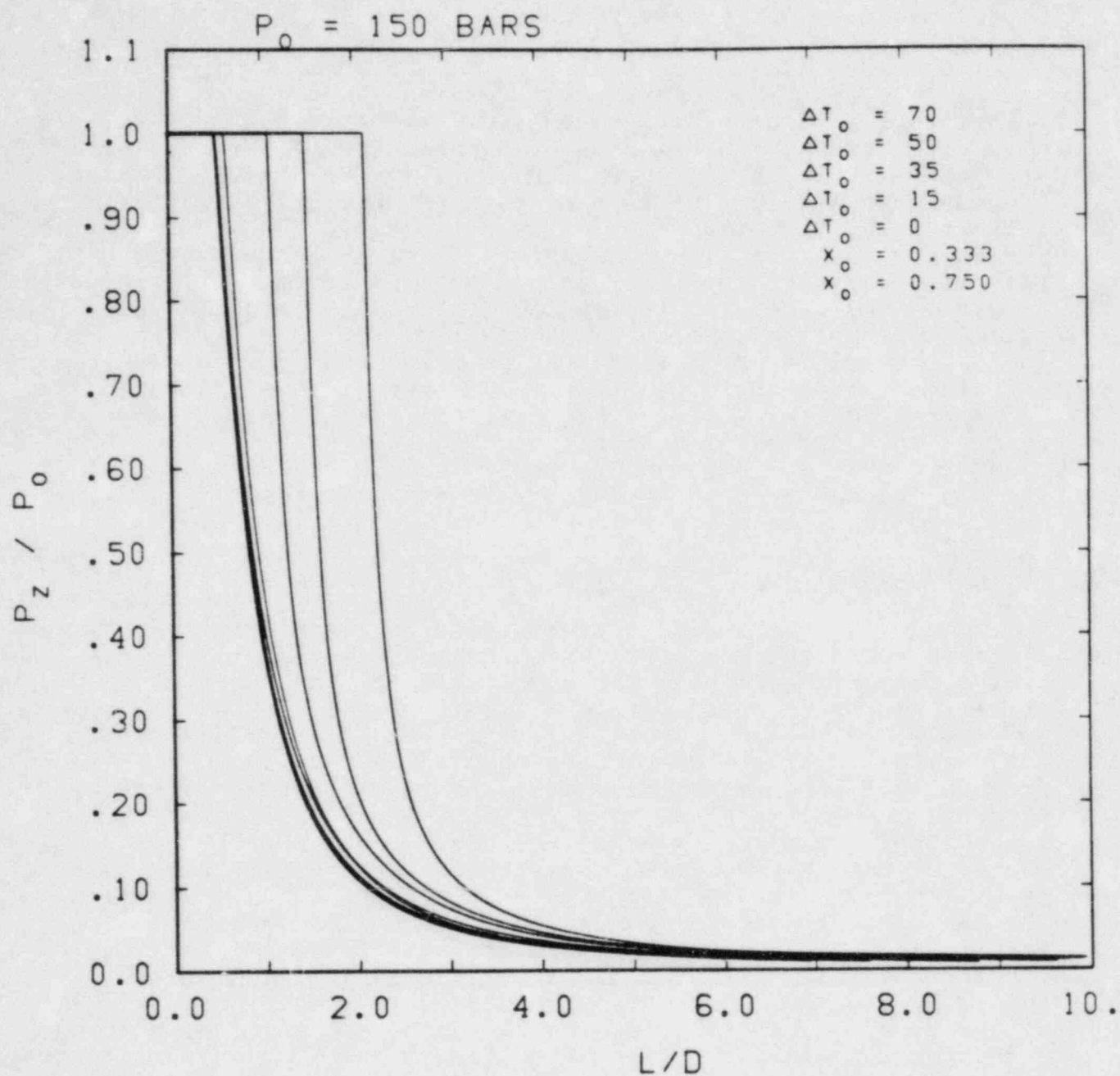


Figure C-1 Centerline target pressure as a function of axial target position ( $L/D$ ) for break stagnation conditions of 150 bars and various subcoolings and qualities.  $L$  is the target position,  $D$  is the pipe diameter  $P_z$  is the centerline pressure, and  $P_0$  is the stagnation pressure at the break.



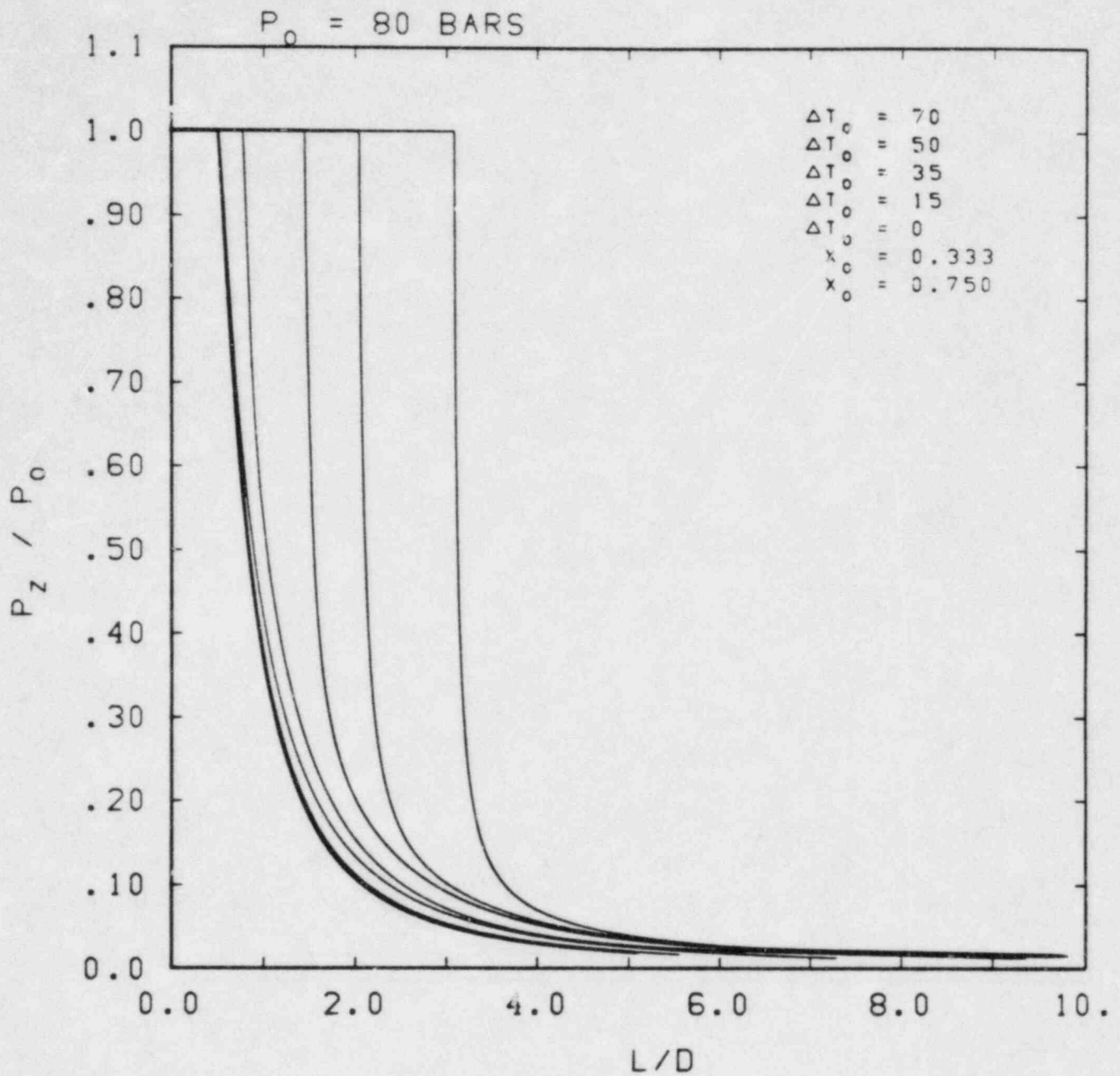


Figure C-2 Centerline target pressure as a function of axial position ( $L/D$ ) for break stagnation conditions of 80 bars and various subcoolings and qualities.  $L$  is the target position,  $D$  is the pipe diameter,  $P_z$  is the centerline pressure, and  $P_0$  is the stagnation pressure at the break.

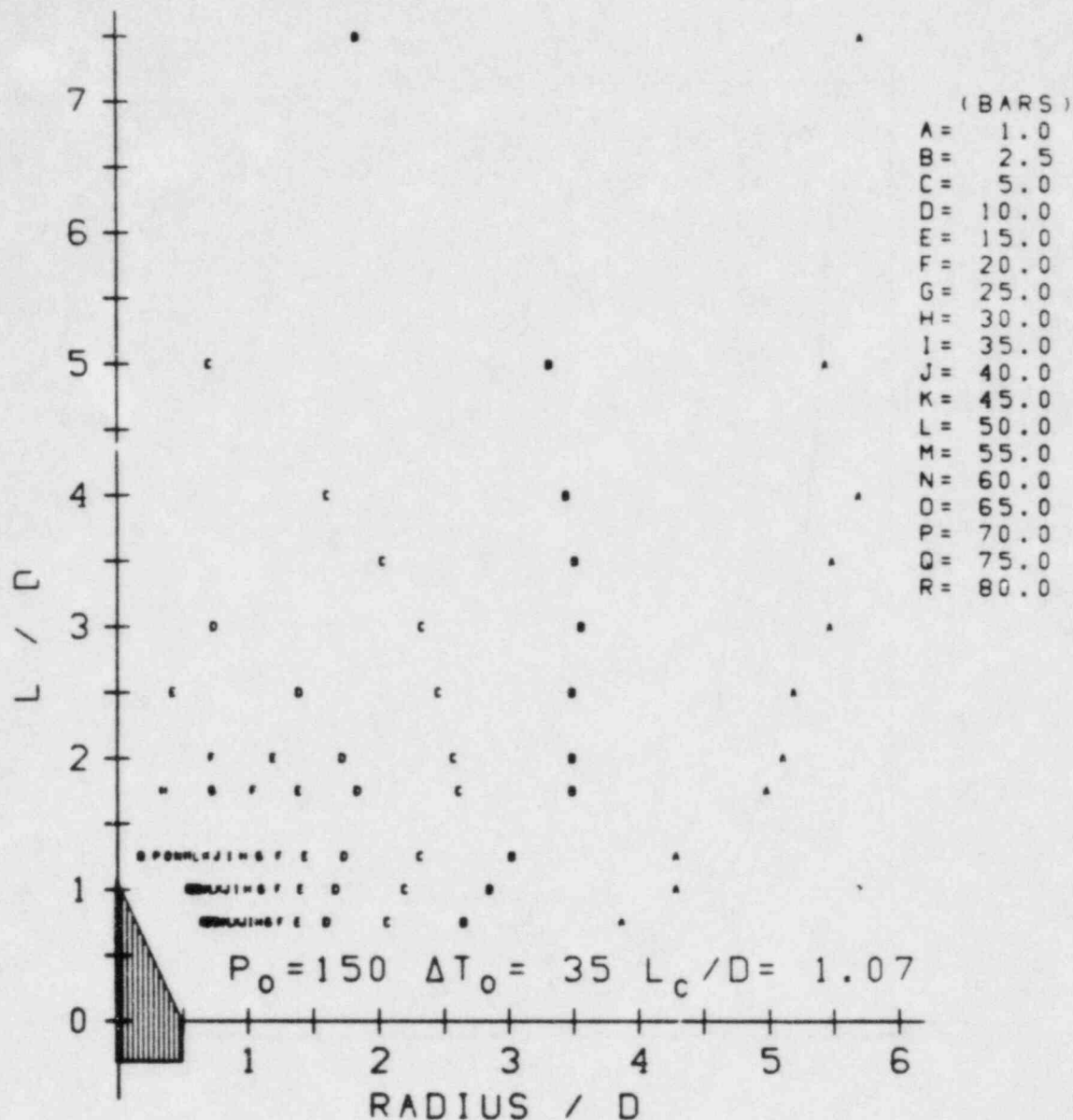


Figure C-3 Composite target pressure contours as a function of target  $L/D$  and target  $RADIUS/D$  for stagnation conditions of  $P_0 = 150$  bars and 35 degrees of subcooling. Smooth lines connecting like alphabetic letters form an approximate pressure contour corresponding, in bars, to the pressure versus alphabetic letter key. This contour is approximate and is only informational.

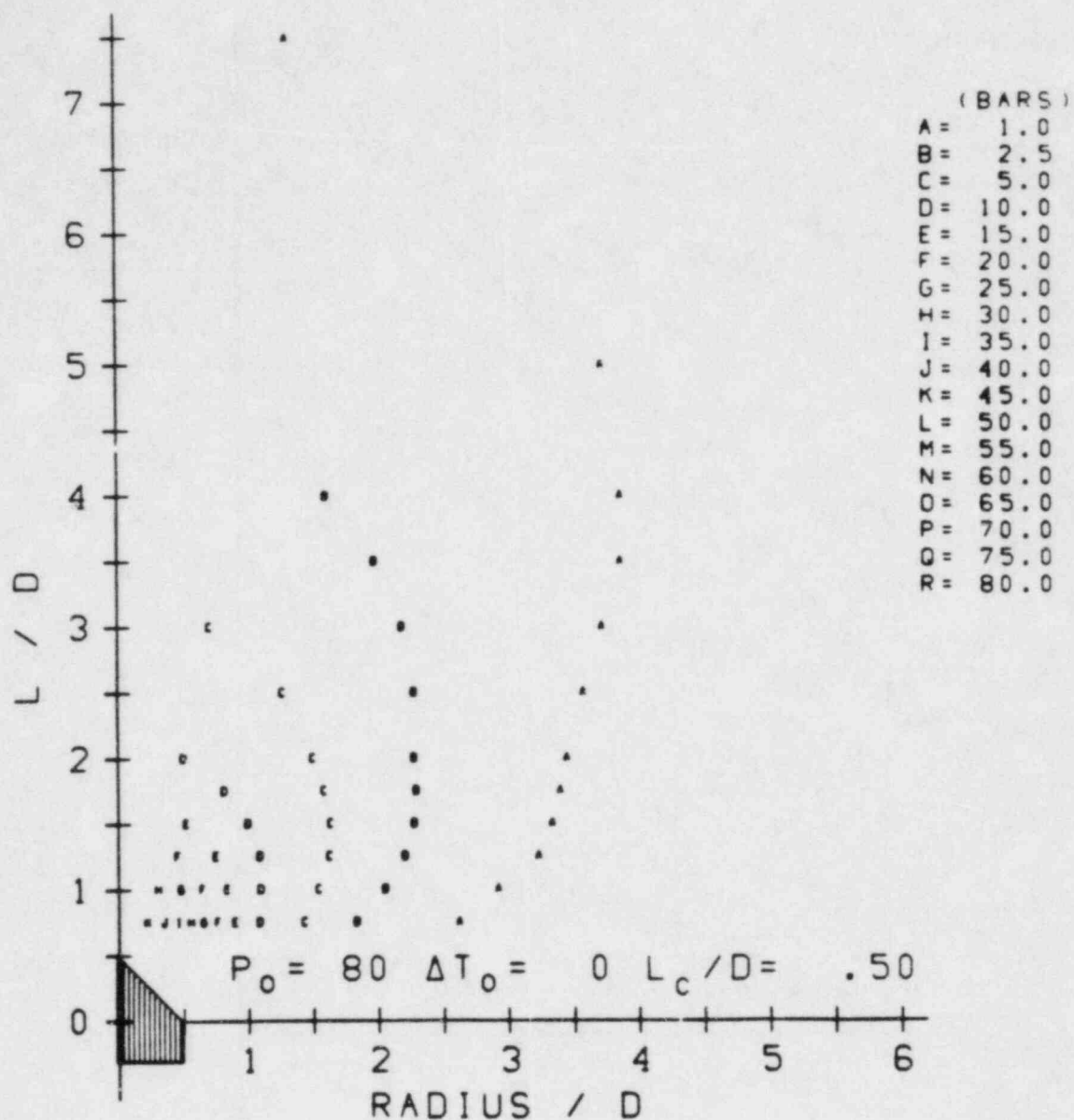


Figure C-4 Composite target pressure contours as a function of target  $L/D$  and  $RADIUS/D$  for stagnation conditions of  $P_0 = 80$  bars and saturated liquid. Smooth lines connecting like alphabetic letters form an approximate pressure contour corresponding, in bars, to the pressure versus alphabetic letter key. This contour is approximate and is only informational.

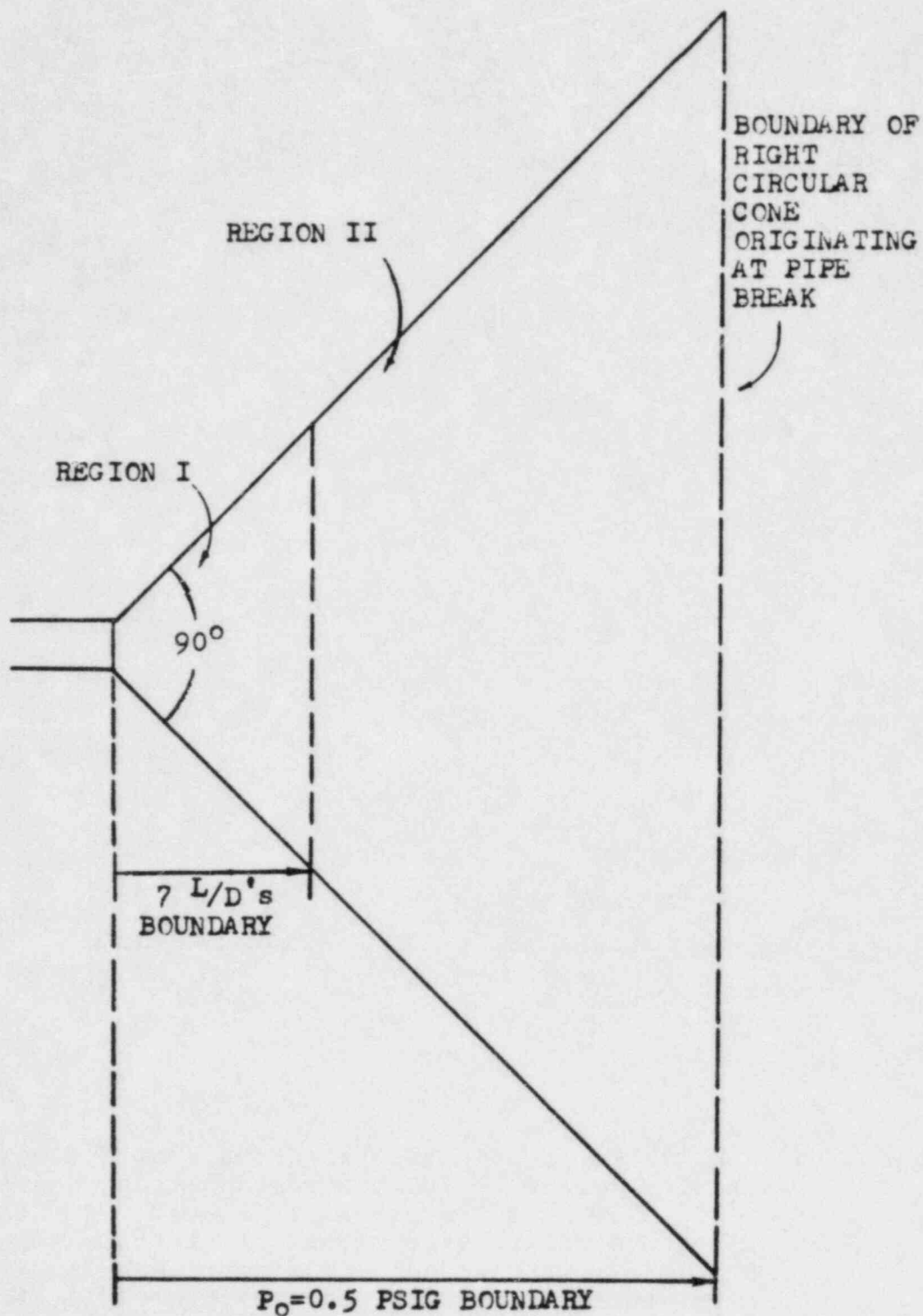


FIGURE C-5. ILLUSTRATION SHOWING THE TWO REGIONS  
FOR THE INSULATION DEBRIS MODEL



with total included angle of  $90^\circ$  that extends from 7 L/D's to the point where the average stagnation pressure becomes 0.5 psig; in this region all of the fibrous insulation is assumed to be dislodged as as-fabricated panels.

The size of the first volume was established using insulation integrity data from Reference C-1 and using two-phase jet expansion models from Reference C-5. In Reference C-1, as noted above, data indicated that the onset of insulation failure damage can occur at stagnation pressures as low as 20 psig. The assumption that is made for the purposes of this model is that fibrous insulation shreds at stagnation pressures greater than or equal to the failure pressure, 20 psig. Referring to Figures C-1 and C-2 the value of 20 psig occurs approximately 7 L/D's downstream of the jet origin along the centerline of the jet.

Choosing the failure threshold for fibrous insulations as 20 psig requires the extrapolation of data taken using a two inch diameter, incompressible water jet to a loss-of-coolant accident (LOCA) situation that may involve large, high energy, and compressible two-phase jets. The uncertainties present in such an extrapolation must, therefore, be recognized. The principal area of concern is the implicit assumption that a two-phase LOCA jet is analogous to a 2 inch diameter incompressible water jet. This concern stems from (1) differences in loading mechanisms and (2) the region affected by the jet (cone-of-influence). Damage to insulation from a two-phase jet could result from normal surface loading, loading resulting from shear forces acting tangential to the surface and from loading that could result from pressure imbalances due to distortions of the insulation surface. Although this extrapolation is disturbing, every effort has been made to mitigate any effects due to scale or different phenomena by choosing conservative failure criteria and affected volume.

The size of the second volume was established using the Moody jet analysis as modified in Reference C-6. This volume begins at  $L/D = 7$  and extends to a plane in the jet where the jet thrust (as calculated by Moody) divided by the jet area is equal to 0.5 psi. This is the plane where the average distributed pressure (force per unit area) on a flat axisymmetric target would be equal to 0.5 psig. (The outer boundary for dislodging insulation by jet forces, 0.5 psig boundary, was established in Reference C-6.) The Moody type jet model was selected for establishing the outer boundary of region II because it always resulted in a larger L/D value for the boundary than the two-phase jet analysis in Reference C-5, thus assuring that the effects of modeling uncertainties are mitigated by a conservative boundary selection. Moreover, the above boundary does not change the jet volume defined in Reference C-6. Finally, note that all other forms of insulation (reflective metallic, closed cell, etc.) that are in the jet volume (volumes I and II above) are assumed to be dislodged by the jet in as-fabricated panels.

### Other Discussion

The experiments referenced here (Reference C-1) were conducted with a single phase fluid (water) at ambient temperature. Under these conditions, the principal mode of failure that was observed (i.e., rips or tears occurring in the insulation covering near the periphery of the area impacted by the jet) supports the above modeling, which assumes that the damage to the insulation is due principally to stress occurring under normal pressure loadings.

However, under two-phase jet flow conditions, other phenomena can become important in influencing the mode of failure of insulation coverings.

A significant effect of the impact of a two-phase jet onto a surface normal to the jet axis is the migration of fluid at high velocities parallel to the surface. The forces associated with such flow could result in shear stresses in the fabric sufficient to fail the covering. Were such a failure mechanism to become the principal failure mode, the above failure-pressure criterion for insulation failure may not remain valid.

An additional consideration to take into account is the effect of temperature on the strength of materials used for insulation coverings. Under LOCA conditions, insulation coverings would be subject to higher temperatures than the temperatures that existed in the incompressible water jet experiments. For those insulation covers, however, made up of fiberglass or similar refractory material, no significant change in strength of the materials will occur as a result of such temperature differences. In fact, as long as fiberglass remains solid, its strength increases with increasing temperature (Reference C-2). Furthermore, the types of fiberglass used for insulation covers, e.g., lime-aluminum borosilicate glass, can be used for continuous duty up to about 600°F (Reference C-3) and has a softening temperature range of between 1350°F and 1560°F (Reference C-4).

Finally, within several pipe diameters of the pipe break, analysis (Reference C-5) indicates that the angle subtended by the exiting jet may be significantly greater than 90°. In that volume, a greater amount of insulation debris (e.g., shredded insulation debris) would be generated than under the 90° included angle assumption used here and in Reference C-6. It is expected, however, that the assumption that insulation disintegration occurs (i.e., insulation shreds or fibers form the resultant debris) within an included angle of 90° from the jet origin to a distance at which the stagnation pressure reduces to 20 psig is sufficiently conservative to provide an overall conservative result.

The assumption is made that a stagnation pressure of 0.5 psig represents the lower limit to which insulation damage (intact insulation dislodged) can occur. The value of 0.5 psig was given in Reference C-6 and is considered to be conservative.

A number of the assumptions presented regarding fibrous debris generation have evolved from analytical studies (References C-5 and C-6) and experimental work (Reference C-1) and are considered to be conservative for the following reasons:

1. Complete insulation disintegration (i.e., the rendering of as-fabricated insulation into shreds or fibers) is assumed within jet volumes where stagnation pressures equal or exceed 20 psig. Such stagnation pressures (20 psig) have been observed to be those for the threshold of damage to the covers of the most damage susceptible as-fabricated insulations. Inasmuch as no detailed study has been made on the disintegration or dislodgement of insulations, the most severe damage (compatible with existing knowledge) to insulation from the standpoint of potential sump blockage has been assumed.
2. The duration of jet impingement during jet damage experiments lasted approximately twice that required for large LOCA blowdown (i.e., 5 min. versus approximately 2 min.).
3. The outer boundary of volume I where the fibrous insulation is shredded was fixed on the basis of the occurrence of a stagnation pressure of 20 psig along the centerline of the jet. The pressure, in fact, falls off in a radial direction from the jet axis.
4. Insulation, in as-fabricated form, is assumed to be dislodged at stagnation pressures between 20 psig (7 L/Ds) and 0.5 psig.

Consideration must be given, however, to other phenomena related to two phase jet flow. These could result in insulation covering failure under conditions less rigorous than those assumed in this development. They include:

1. A major failure mechanism, under two-phase jet conditions, may be shear force failure or imbalanced pressure force failure as opposed to normal pressure force loading.
2. For some target situations (subcooled flows on close-in targets) the 90° cone of influence assumption may not be sufficient to target all affected insulation.



## References to Appendix C

- C-1 Durgin, W. W. and Noreika, J. F., "The Susceptibility of Fibrous Insulation Pillows to Debris Formation Under Exposure to Energetic Jet Flows," NUREG/CR-3170, U.S. Nuclear Regulatory Commission, Prepared by Alden Research Laboratory, Worcester Polytechnic Institute, Holden, MA, 1983.
- C-2 Handbook of Tables for Applied Engineering Science; Second Edition; Polz, R.E., Tuve, G.L., editors; CRC Press; Cleveland, OH, 1983.
- C-3 The Encyclopedia of Engineering Materials and Processes; Clauser, H.R. editor-in-chief; Reinhard Publishing Corporation; New York, NY, 1963.
- C-4 Handbook of Plastics and Elastomers; Harper, C.A., editor-in-chief; McGraw-Hill Book Company; New York, NY, 1975.
- C-5 Weigand, G. G. and Thompson, S. L. "Break Flow and Two-Phase Jet Load Model," Sandia National Laboratories, Albuquerque, NM. Presented at International Meeting on Thermal Reactor Safety, Chicago, IL August 1982.
- C-6 Wysocki, J. J., et al., "Methodology for Evaluation of Insulation Debris," NUREG/CR-2791, Burns and Roe, Inc., Oradell, NJ, September 1982.



<b>NRC FORM 335</b> (7-77)		<b>U.S. NUCLEAR REGULATORY COMMISSION</b> <b>BIBLIOGRAPHIC DATA SHEET</b>		1. REPORT NUMBER (Assigned by DDC) NUREG-0897 "For Comment"	
4. TITLE AND SUBTITLE (Add Volume No., if appropriate) Containment Emergency Sump Performance Technical Findings Related to Unresolved Safety Issue A-43				2. (Leave blank)	
7. AUTHOR(S) A. W. Serkiz				3. RECIPIENT'S ACCESSION NO.	
9. PERFORMING ORGANIZATION NAME AND MAILING ADDRESS (Include Zip Code) Division of Safety Technology Office of Nuclear Reactor Regulation U.S. Nuclear Regulatory Commission Washington, DC 20555				5. DATE REPORT COMPLETED MONTH March YEAR 1983	
12. SPONSORING ORGANIZATION NAME AND MAILING ADDRESS (Include Zip Code) Same as 9, above.				DATE REPORT ISSUED MONTH April YEAR 1983	
13. TYPE OF REPORT Final Staff Report				6. (Leave blank)	
15. SUPPLEMENTARY NOTES				8. (Leave blank)	
16. ABSTRACT (200 words or less) This report summarizes key technical findings related to the Unresolved Safety Issue (USI) A-43, Containment Emergency Sump Performance. The technical issues can be subdivided into: sump hydraulic performance, LOCA generated debris effects and recirculation pump performance under post-LOCA conditions. The technical findings presented in this report provide a means to address these sump design and performance aspects and provide the technical basis for the proposed changes to NRC's Standard Review Plan, Section 6.2.2 and Regulatory Guide 1.82.				10. PROJECT/TASK/WORK UNIT NO. USI A-43	
17. KEY WORDS AND DOCUMENT ANALYSIS Containment Emergency Sump Performance USI A-43				11. CONTRACT NO.	
17b. IDENTIFIERS/OPEN-ENDED TERMS				14. (Leave blank)	
18. AVAILABILITY STATEMENT Unlimited Availability		19. SECURITY CLASS (This report) Unclassified		21. NO. OF PAGES	
		20. SECURITY CLASS (This page) Unclassified		22. PRICE \$	

UNITED STATES  
NUCLEAR REGULATORY COMMISSION  
WASHINGTON, D.C. 20555

OFFICIAL BUSINESS  
PENALTY FOR PRIVATE USE, \$300

FIRST CLASS MAIL  
POSTAGE & FEES PAID  
USNRC  
WASH D C  
PERMIT No. 562

120555078877 1 C00796  
US NRC  
ADM DIV OF TIDC  
POLICY & PUB MGT BR-PDR NUREG  
W-501  
WASHINGTON DC 20555